Temperature impact on yeast metabolism
- Insights from experimental and modeling approaches-

Proefschrift

ter verkrijging van de graad van doctor
aan de Technische Universiteit Delft,
op gezag van de Rector Magnificus, prof. ir. K.C.A.M. Luyben,
voorzitter van het College voor Promoties,
in het openbaar te verdedigen op maandag 15 juli 2013 om 15.00 uur

door

Ana Luísa BRAGA DA CRUZ

Mestre em Engenharia Biológica,
Instituto Superior Técnico, Portugal,
geboren te S. Julião do Tojal, Portugal

Dit proefschrift is goedgekeurd door de promotor:
Prof. dr. Ir. J.J. Heijnen

Copromotor: Dr. W.M. van Gulik

Samenstelling promotiecommissie:

Rector Magnificus	voorzitter
Prof. dr. ir. J.J. Heijnen	Technische Universiteit Delft, promotor
Dr. W.M. van Gulik	Technische Universiteit Delft, copromotor
Prof. dr. J.T. Pronk	Technische Universiteit Delft
Prof. dr. M.J. Teixeira de Mattos	Universiteit van Amsterdam
Prof. dr. ir. V.A.P. Martins dos Santos	Wageningen UR
Prof. dr. ir. M. Reuss	Universität Stuttgart, Duitsland
Dr. ir. H. Bloemen	Heineken
Prof. dr. ir. H. Noorman	Technische Universiteit Delft, reservelid

The research presented in this thesis was performed at the Cell Systems Engineering group, Department of Biotechnology, Faculty of Applied Sciences, Delft University of Technology (The Netherlands).

This project was carried out within the research programs of the Kluyver Centre for Genomics of Industrial Fermentation and the Netherlands Consortium for Systems Biology, which are both sponsored by the Netherlands Genomics Initiative.

Thesis published by: Uitgeverij BOXPress, ‘s-Hertogenbosch
ISBN: 978-90-8891-660-1

O mar tem fim, o céu talvez o tenha,
Mas não a ânsia da Coisa indefinida
Que o ser indefinida faz tamanha.

Fernando Pessoa

Table of Contents

Summary

Temperature is an environmental parameter that greatly affects the growth of microorganisms, due to its impact on the activity of all enzymes in the network. This is particularly relevant in habitats where there are large temperature changes, either daily or seasonal. Understanding how organisms have adapted to cope with these temperature-cycles can provide valuable insight for the development and optimization of strains used in industrial processes where sub- or supraoptimal temperatures are required. Some examples are brewing and wine production where low temperatures are preferred to preserve the flavors produced during yeast fermentation and facilitate downstream processing by accelerating biomass sedimentation. The yeast *Saccharomyces cerevisiae* is used in many fermentation processes and, therefore, it is considered as a good model to study the impact of temperature on metabolism. Besides being widely applied in industry and the large number of analytical and genetic tools available to study it, this yeast is also exposed to broad ranges of temperatures in its natural environment.

The first step to evaluate the impact of temperature on growth is to study it in conditions where there is no other limiting factor, such as the substrate concentration. By performing sequential-batch fermentations at mild suboptimal temperatures (12, 18, 24 and 30 °C) it was possible to obtain relations for the temperature dependency of the main (CO_2, ethanol, biomass, glycerol) and minor production rates (acetate, lactate, succinate and pyruvate) during growth under anaerobic-glucose-excess conditions. It was observed that the yields of the main products on substrate are temperature-independent, meaning that there are no major changes in growth stoichiometry during temperature changes at mild suboptimal temperatures. The temperature impact on the consumption and production rates was quantified using an empirical equation from literature (the Ratkowsky equation), allowing the construction of a black-box model that describes the temperature dependency of growth and (by)product formation in *S. cerevisiae* in glucose-excess conditions.

To assess if the obtained black-box model could be extrapolated to other conditions, the black-box model was extended to glucose-limiting regimes. The parameterization and validation of the model was done by performing different temperature perturbations to anaerobic glucose-limited chemostat

cultures at 12 and 30 °C. It was confirmed that the growth stoichiometry is temperature independent also for glucose-limited conditions.

However, acetate production and storage carbohydrate metabolism were strongly affected by changes in the residual substrate concentration, which increased at lower temperatures as a consequence of the lower specific activity of the glucose transporters. A comparison between the kinetic parameters from the 12 °C and 30 °C chemostats allowed concluding that different hexose transporters must have been expressed in the two cultivations. However, because the kinetic parameters obtained from the temperature shift experiments carried out in the 12 °C chemostat were the same as the ones describing the effect of temperature under glucose-excess conditions (batch), it was concluded that the expression of different hexose transporters is most likely a consequence of the very different residual glucose concentration and not temperature itself.

A strong metabolic regulation by the extracellular substrate concentration was also observed when extending the study to intracellular metabolism. Plotting the level of each glycolytic metabolite against the residual glucose concentration from batch cultivations at different temperatures and during different temperature shifts applied to glucose-limited chemostats, resulted in unique saturation curves. Each metabolite concentration increased with increasing residual glucose level, reaching a stable level at non-limiting glucose concentrations. For each metabolite, all measurements of its intracellular level versus residual glucose concentration appeared to fall on the same curve, irrespective of the cultivation temperature and conditions applied (dynamic temperature shift, steady-state chemostat or batch). It is shown that, for the mild suboptimal temperature range (12 – 30 °C), the enzyme levels, equilibrium and affinity constants can be considered as temperature independent, while the cultivation temperature significantly affects the specific catalytic activity. An important finding, obtained from theoretical considerations and mathematical modeling of these experiments, was that the observed unique relation between intracellular metabolite level and extracellular glucose concentration for each metabolite indicates that the temperature impact on the catalytic capacity is the same, or at least very similar, for all glycolytic enzymes of *S. cerevisiae*. It is also shown that this property results in minimal changes in intracellular metabolite levels during temperature perturbations, and thus reduces the need for energy-costly

changes in enzyme levels to maintain the metabolite homeostasis during such perturbations.

From this research it became clear that the metabolic response to temperature changes during growth under glucose-limiting conditions is a consequence of simultaneous changes in the residual substrate concentration and the catalytic capacities of the enzymes. Nonetheless, there are still very few kinetic models that can describe the impact of the residual substrate concentration on the kinetics of anaerobic growth and on the regulation of central carbon metabolism in *S. cerevisiae*. This was addressed by developing a kinetic model of anaerobic yeast glycolysis. It was possible to minimize the number of parameters used by applying a thermodynamic classification of the reactions in the network based on data gathered from anaerobic chemostat cultivations at different growth rates (from 0.025 to 0.27 h^{-1}). The resulting kinetic model required only a few complex mechanistic rate equations, while the remaining kinetic functions could be simplified without compromising the performance of the model.

From *in vitro* enzyme activity measurements and estimation of the protein content in the cell it was possible to calculate the enzyme production rates. It was found that, except for hexokinase, the residual glucose concentration also regulates the production of each glycolytic enzyme according to a Hill function that is valid for both aerobic and anaerobic conditions. By including the kinetics of enzyme production together with the *in vivo* parameters estimated for the different enzymatic reactions, the kinetic model could describe the glycolytic fluxes, metabolite levels and changes in enzyme concentrations for the considered range of growth rates and residual glucose concentration. Also it was shown that the model can easily be extended to describe dynamic conditions such as mild temperature shifts.

Besides the relevant findings regarding temperature impact on yeast metabolism, this thesis presents a framework to study the impact of temperature and residual glucose concentration on the metabolism of organisms. It is critical to make rational decisions on the experimental setup applied since different temperatures may trigger changes in other important metabolic regulators such as substrate concentration. The models and experimental approaches presented here can directly be applied to other organisms or to study more extreme temperature conditions.

Samenvatting

Temperatuur is een omgevingsparameter die grote invloed heeft op de groei van micro-organismen, door het effect op de activiteit van alle enzymen in de cel. Dit geldt met name in een omgeving waar er grote temperatuurverschillen bestaan, dagelijks of seizoensgebonden. Kennis over hoe organismen zich hebben aangepast aan deze temperatuur-cycli kan waardevol inzicht geven voor de ontwikkeling en optimalisatie van stammen die worden gebruikt in industriële processen waarbij sub- of supraoptimale temperaturen vereist zijn. Enkele voorbeelden hiervan zijn het brouwen van bier en de productie van wijn, waar lage temperaturen de voorkeur hebben om de smaken te behouden en de opwerking te vergemakkelijken door het versnellen van biomassa sedimentatie. De gist *Saccharomyces cerevisiae* wordt in vele fermentatieprocessen gebruikt en kan derhalve als een goed model worden beschouwd voor de studie van de invloed van temperatuur op het metabolisme. Bovendien wordt deze gist reeds op grote schaal toegepast in de industrie, zijn er een groot aantal analytische methoden en genetische beschikbaar om deze gist te kunnen bestuderen en wordt deze ook in het natuurlijke leefmilieu aan een breed bereik van temperaturen blootgesteld.

De eerste stap om het effect van temperatuur op de groei te evalueren is deze te bestuderen in omstandigheden waarin geen andere beperkende factor is, zoals bijvoorbeeld de substraatconcentratie. Door het uitvoeren van series van opeenvolgende batch fermentaties bij verschillende temperaturen (12, 18, 24 en 30 °C) kon de relatie tussen de kweektemperatuur en de vormingssnelheid van de belangrijkste producten (CO_2, ethanol, biomassa en glycerol) maar ook van producten die in mindere mate worden gevormd (acetaat, lactaat, succinaat en pyruvaat) worden verkregen tijdens de groei onder anaerobe omstandigheden en een overmaat aan substraat (glucose). Er werd waargenomen dat de opbrengsten van de belangrijkste producten onafhankelijk zijn van de temperatuur, hetgeen betekent dat er geen significante wijzigingen in de stoichiometrie zijn tijdens groei bij milde suboptimale temperaturen (12 – 30 °C). Het effect van de temperatuur op de snelheden van substraat consumptie, groei en (bij)productvorming kon worden gekwantificeerd met behulp van een empirische vergelijking uit literatuur (het Ratkowsky model), waarmee het mogelijk was een black-box model te construeren dat de temperatuurafhankelijkheid van groei en productvorming in *S. cerevisiae* beschrijft. Maar omdat in de uitgevoerde

experimenten de afhankelijkheid van temperatuur samen met de stoichiometrische en kinetische parameters tijdens groei bij een overmaat aan glucose werden verkregen, was het nodig om het model te evalueren onder glucose gelimiteerde omstandigheden, in een kweeksysteem met een ingestelde toevoersnelheid van glucose die lager is dan nodig voor maximale groei (d.w.z. een chemostaat).

De parameterschatting en validatie van het model voor deze condities werd gedaan door het uitvoeren van verschillende temperatuur perturbaties in anaerobe chemostaat culturen bij 12 en 30 °C. Bevestigd werd dat de groei stoichiometrie ook temperatuur onafhankelijk is bij glucose-limiterende omstandigheden. Echter, acetaat productie en koolhydraatmetabolisme bleken sterk te worden beïnvloed door veranderingen in de substraat concentratie, die stijgt bij dalende temperatuur, als gevolg van de lagere capaciteit van de glucose transporters (die zorgen voor de opname van glucose uit het medium door de cellen) bij lagere temperaturen. Een vergelijking tussen de kinetische parameters voor glucose transport bepaald voor chemostaat cultures uitgevoerd bij 12 °C en 30 °C leidde tot de conclusie dat verschillende glucose transporters tot expressie moeten zijn gebracht bij deze verschillende temperaturen. Maar aangezien de kinetische parameters bepaald voor de 12 °C chemostaat dezelfde waren als die verkregen zijn uit het effect van temperatuur onder batch omstandigheden, kan er worden geconcludeerd dat de expressie van verschillende glucose transporters waarschijnlijk een gevolg is van de residuele glucoseconcentratie en niet van de temperatuur.

Een sterke invloed van de extracellulaire substraatconcentratie werd ook waargenomen bij het bestuderen van het intracellulaire metabolisme. Het uitzetten van de intracellulaire concentratie van elke glycolytische metaboliet tegen de extracellulaire glucose concentratie tijdens batch cultivatie en tijdens verschillende temperatuur perturbaties uitgevoerd in glucose-gelimiteerde chemostaten, resulteerde in unieke relaties voor elke metaboliet, waarbij bij toenemende glucose concentratie de metaboliet concentratie asymptotisch een maximum bereikt. Hierbij gold dat de temperatuur waarbij de intracellulaire metaboliet concentratie en de extracellulaire glucose concentratie waren gemeten niet van belang was. Alle metingen bleken op dezelfde curve te vallen. Hetzelfde gold voor de kweek condities (dynamische temperatuurverschuiving, steady-state chemostaat of batch). Er werd aangetoond dat voor de milde suboptimale temperaturen

(12-30 °C) zowel de enzym niveaus als de evenwicht en affiniteitsconstanten als temperatuur onafhankelijk kunnen worden beschouwd, terwijl de kweektemperatuur bepalend is voor de specifieke katalytische activiteit van het enzym. Een belangrijke conclusie, die zowel uit de theoretische beschouwingen en mathematische modellen kon worden getrokken, was dat de waargenomen unieke relatie tussen intracellulaire metaboliet niveaus en extracellulaire glucose concentratie aangeeft dat het effect van de temperatuur op de katalytische capaciteit hetzelfde, of althans zeer vergelijkbaar is voor alle glycolytische enzymen van *S. cerevisiae*. Voorts kon worden aangetoond dat deze eigenschap leidt tot minimale veranderingen in intracellulaire metabolietconcentraties gedurende temperatuur veranderingen, waardoor het aanpassen van enzym activiteiten, om de metaboliet homeostase bij dergelijke perturbaties te handhaven, middels energie verbruikende cycli van enzym afbraak en synthese, tot een minimum kan worden beperkt.

Uit dit onderzoek bleek dat de veranderingen van metaboliet concentraties tijdens temperatuurveranderingen bij groei onder glucose-limiterende omstandigheden het gevolg is van gelijktijdige verandering in de resterende substraat concentratie en de katalytische capaciteit van de enzymen. Toch zijn er nog maar weinig kinetische modellen die de invloed van de resterende substraat concentratie op de kinetiek van intracellulair metabolisme tijdens de anaerobe groei van *S. cerevisiae* kunnen beschrijven. Daarom werd tijdens dit onderzoek een kinetisch model ontwikkeld voor de anaerobe glycolyse in gist. Het bleek mogelijk om het aantal parameters in dit model te minimaliseren door een thermodynamische indeling van de reacties in het netwerk, op grond van gegevens uit anaerobe chemostaat cultivaties uitgevoerd in een breed groeisnelheid gebied (0.025 tot 0.27 h^{-1}). Voor dit kinetische model bleken slechts een paar mechanistisch complexe snelheidsvergelijkingen nodig te zijn, terwijl de resterende kinetische functies vereenvoudigd konden worden zonder de prestaties van het model geweld aan te doen. Van uitgevoerde *in vitro* enzymactiviteit metingen en schattingen van het eiwitgehalte in de cel kon de enzymproductie snelheid berekend worden. Behalve voor hexokinase, kon worden afgeleid dat de productiesnelheid van ieder glycolytisch enzym volgens een Hill functie afhankelijk zijn van de residuele glucose concentratie, wat gold voor zowel aerobe als anaerobe omstandigheden. Door het toevoegen van deze kinetiek van enzymproductie samen met de *in vivo* parameters geschat voor verschillende enzymatische reacties aan het model, kan het kinetische model

een beschrijving geven van zowel de glycolytische fluxen als veranderingen in metaboliet concentraties en enzymconcentraties voor de toegepaste experimentele condities (groeisnelheden, temperaturen en residuele glucose concentraties). Ook werd aangetoond dat het model gemakkelijk kan worden uitgebreid om dynamische omstandigheden zoals als gevolg van plotselinge temperatuur veranderingen te beschrijven.

De resultaten van dit proefschrift vormen een raamwerk om de impact van de temperatuur en residuele substraat concentratie op het metabolisme van organismen te bestuderen. Het is van cruciaal belang om rationele beslissingen te kunnen nemen over de toegepaste experimentele omstandigheden, aangezien verschillende temperaturen kunnen leiden tot veranderingen in andere belangrijke metabolische regulatoren, zoals substraat concentratie. De gepresenteerde modellen en experimentele benaderingen kunnen rechtstreeks worden toegepast om temperatuur effecten op andere organismen en/of de effecten van meer extreme temperaturen bestuderen.

1. General Introduction

Temperature: its environmental and biotechnological relevance

Temperature is one of the physical properties that largely influences the functioning of all organisms. To be able to survive, they need to be adapted not only to the average temperature of their habitat, but in many cases also need to withstand temperature oscillations, such as diurnal temperature cycles (day and night conditions) and seasonal shifts (summer and winter). Because diurnal cycles and seasonal shifts occur within significantly different time scales (hours versus months), the way organisms respond can be different for the two situations. The mechanisms employed by organisms to respond to fast temperature changes (less than 12h) is commonly known as temperature adaptation, while acclimation is usually employed to describe physiological adjustments organisms go through during long-term temperature changes.

The temperature profiles can be quite different between different places on the globe (**Figure 1.1**). For instance, despite the fact that temperatures in Oslo (Norway) are lower than in Lisbon (Portugal), the difference between highest and lowest daily temperatures is similar for both cities (6 °C during Winter and 10 °C during Summer time). Other cities, like Tete in Mozambique, experience larger daily temperature shifts (average 11.3 °C) than seasonal modifications in the maximum or minimum temperatures throughout the year (average 7.3 °C). The opposite is seen for desert locations such as Timimoun (Algeria) where annual temperatures can change within a 39.5 °C range. Such differences in daily and seasonal temperature profiles must have had a big impact on evolution and survival of organisms in natural habitats. But the same should hold true for organisms in an artificial environment, such as in industrial fermentation processes. Many microorganisms are currently used for the production of a variety of

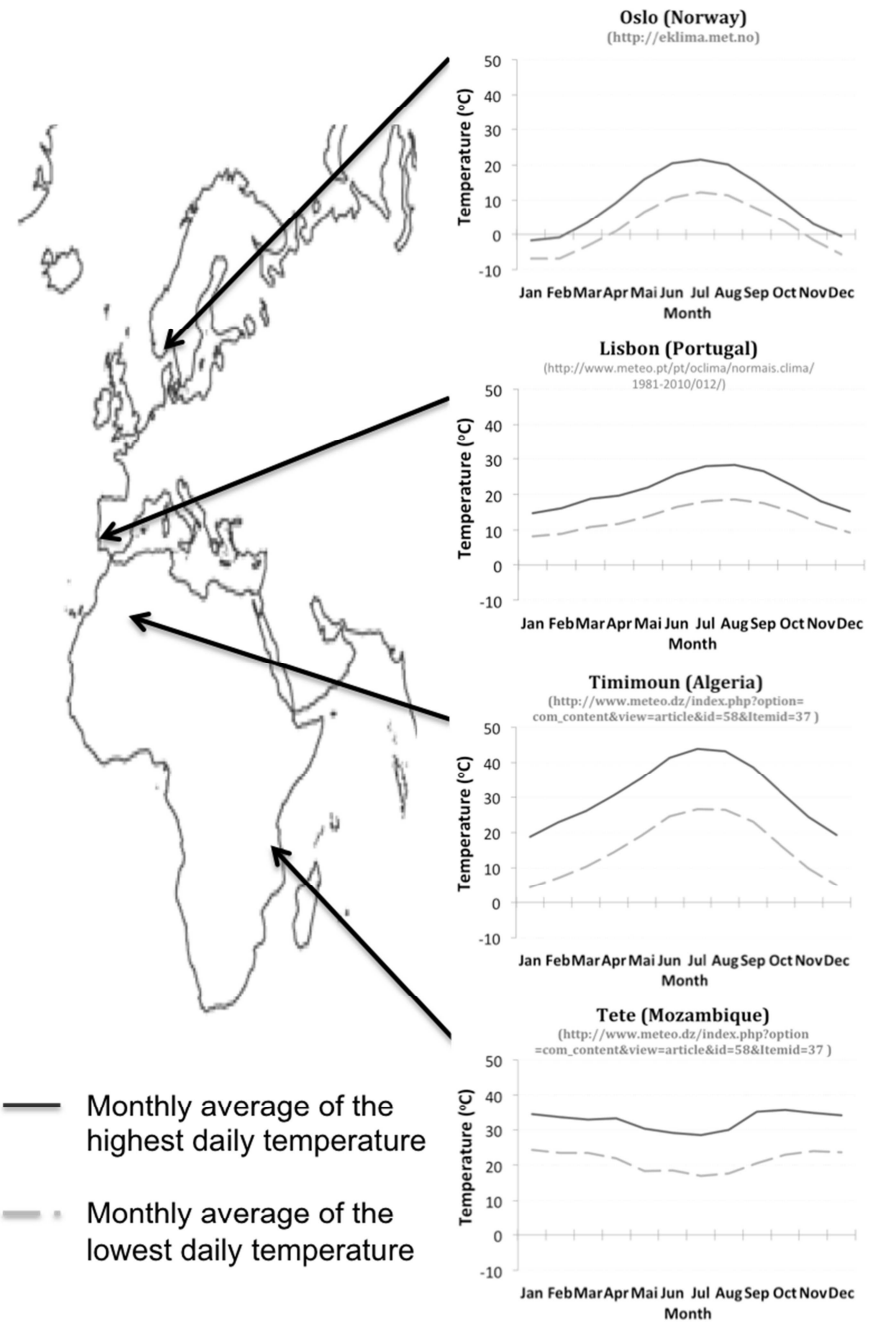

Figure 1.1: *Annual temperature profiles in Oslo, Lisbon, Timimoun and Tete. The data were retrieved from the official website of meteorological institutes of the respective country (references given in the plots, last accessed on the 29th October 2012).*

biochemicals, such as pharmaceutical compounds, flavors and nutritional ingredients for the food industry. Traditionally, the organisms are selected based on the product yield, i.e. the maximum amount of product of interest they can produce from the feedstock used. However, the temperature for which the maximum yield is achieved might not be compatible to the one applied in the industrial process. For instance, if the optimal temperature for production of a compound of interest is lower than the environmental temperature, operational costs will be increased due to the need to cool down the fermentation vessel. To be able to manipulate the metabolism of organisms such that they produce optimally at cost-effective temperatures would be very valuable to current biotechnological practices. But before being able to do so it is essential to understand how temperature influences the growth and product formation of microorganisms and which mechanisms are used by cells to respond to temperature changes.

Temperature impact on microbial metabolism

The temperature for which the growth rate is maximal (also called optimal growth temperature or T_{opt}) can be quite different between species. Organisms that have evolved in cold habitats achieve their maximum growth rates at relatively low temperatures while the opposite happens to organisms from hot environments (**Figure 1.2**). This makes the notion of hot and cold extremely context dependent. For a matter of simplicity, a classification system has been created to categorize organisms regarding their preferred temperature. Organisms for which the maximum growth rate is obtained at temperatures lower than 10 °C are called psychrophilic, while thermophiles achieve their maximum growth rate at temperatures higher than 40 °C. The term mesophile is applied to organisms that achieve maximum growth rates in the range 10 to 40 °C. Besides with respect to T_{opt}, organisms can also be classified regarding the temperature ranges where, optimally or not, they are able to grow. Eurythermal organisms can withstand broad temperature ranges while stenothermal can only grow at very narrow ranges.

The fact that so many different classifications regarding temperature behavior exist could indicate that the temperature impact on metabolism would be tremendously different between species. However, a few conserved characteristics can be noticed between the different classifications (**Figure 1.2**). For the temperature range immediately below T_{opt} (mild-

suboptimal range), the growth rate of all organisms decreases with decreasing temperature, following the Arrenhius law for chemical reactions. Temperatures higher than T_{opt}, on the other hand, also result in a decrease in growth rate, but the effect is much more severe. This behavior for the entire span of temperature where growth can occur is very similar to the temperature impact on the rate of enzyme-catalyzed reactions, the most abundant type of reactions in an organism.

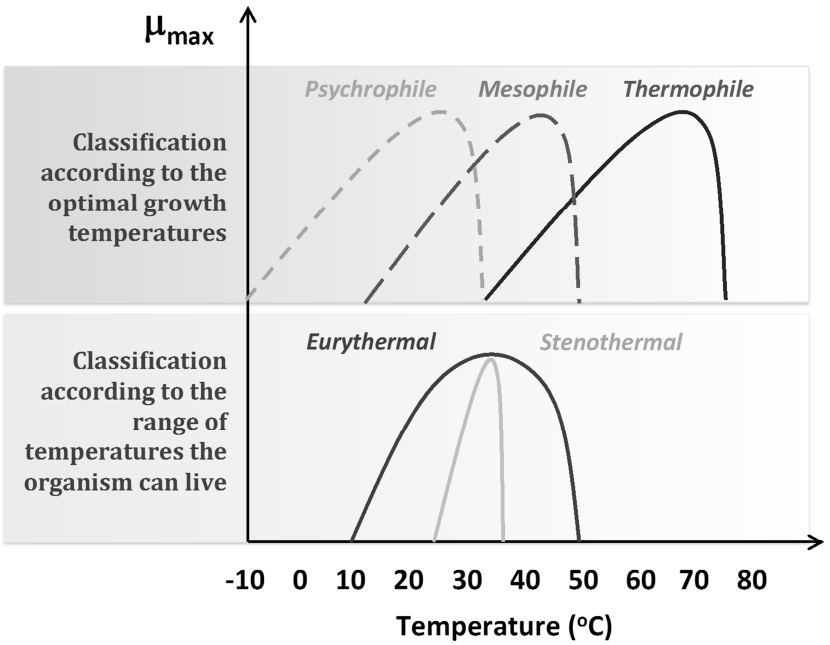

Figure 1.2: *Normalized growth-rate dependencies with temperature for psychrophilic, mesophilic and thermophilic organisms.*

The rate of most chemical reactions increases with increasing temperature due to the higher kinetic energy of the reactants. The same holds true for enzymatic reactions but the conformation of proteins, such as enzymes, is also sensitive to temperature changes. Conditions very far apart from the optimum (both high or low temperatures) can result in enzyme denaturation (structural alterations of the way enzymes are folded), leading to irreversible modifications of the site where substrate and/or products would bind (active site). Under such conditions, the rate of the enzyme-catalyzed reactions will steeply decrease, even at increasing temperature. Because each enzyme has its own unique amino acid composition and

structure, it is generally expected that different enzymes have different temperature sensitivities. Many people have already tried to investigate the temperature impact on purified enzymes via *in vitro* activity measurements (Hazel and Prosser, 1974). One of the goals of such studies was to identify potential reactions that could become rate-controlling steps in a pathway, due to severe loss of the enzyme activity at lower temperatures. However, in many cases the results were not coherent between different laboratories nor could they be directly reconciled with physiological observations, such as growth rate dependency with temperature. The lack of consistency between studies indicates in part that the artificial conditions applied in *in vitro* assays might compromise the observed temperature-relations. In any case, it is improbable that a full comprehension of the temperature impact on the physiology of organisms can come from studies on isolated enzymes. The overall response upon temperature changes is likely to be determined by the combined effect of temperature on all the different enzymes in the organism, together with possible specific genetic-regulation mechanisms triggered to compensate for the decreased specific catalytic activity of the enzyme at lower temperatures.

Mechanisms of temperature compensation in microorganisms

Some pluricellular organisms, such as mammals, are able to cope with temperature fluctuations by maintaining a constant internal temperature. Microorganisms, on the contrary, are poikilotherms, meaning that their internal temperature is intrinsically dependent on the ambient one. Therefore, changes in environmental temperature will immediately have an impact on the metabolism of microorganisms. Because of their small size (μm scale), they cannot simply migrate to spots or habitats with more optimal conditions upon changes in temperature. Also they need to keep the lowest generation time possible (or high growth rate) so they are not outcompeted by other organisms once temperatures are suboptimal. So there must be mechanisms by which microorganisms minimize temperature impact on their metabolism.

Many studies have focused on physiological responses to compensate for suboptimal temperatures, such as cell composition. For instance, Woods (2003) has postulated that cells counteract the decrease in rates of biochemical reactions at low temperature by increasing their protein and RNA contents. This hypothesis came from an extensive analysis of literature

data concerning the total nitrogen (N) and phosphorus (P) contents of organisms exposed to temperature shifts of at least 5 °C. Generally the increase of the cellular P content is related to RNA levels, whereas N relates to the total protein content. Besides the positive effect that a higher protein content (namely higher enzyme levels) has on the rates of biochemical reactions, it can also help to protect cells against intracellular freezing. A high soluble protein content decreases the freezing point of the cytosol, allowing metabolites and other cell components to keep flowing easily inside the cell.

A similar function has been reported to the increase of the intracellular amounts of carbohydrates such as trehalose. Schade *et al.* (2004) have observed that, under carbon-excess conditions, the yeast *Saccharomyces cerevisiae* does not accumulate carbohydrates in response to cold (10 °C) during the first 2h. A reproducible increase of storage carbohydrates (namely trehalose and glycogen) only happened 12h after the cold shock from 30 °C to 10 °C and should therefore be considered as an acclimation response. However there was no decrease in growth rate or viability in mutants that did not accumulate glycogen or/nor trehalose, raising the question if modifications in total carbohydrate content are, in fact, a necessary mechanism of temperature acclimation.

A trait of temperature acclimation for which there is more consensuses are changes in total lipid content or composition during growth at low temperatures. Lower temperatures lead to an increase of the total amount of lipids in mesophilic organisms, together with an elongation of the fatty acids and a higher percentage of unsaturation (Kishimoto, 1994; Suutari and Laakso, 1994). The increase in unsaturation percentage and chain length leads to a decrease of the melting point of the fatty acids, allowing cell membranes at low temperatures to remain in a fluidic state, to ensure proper functioning of membrane-bound proteins.

It is interesting to point out at this stage that the combination of the results mentioned above point towards an increase in the total amounts of all cell components (either protein, lipids, RNA or storage carbohydrates) at lower temperatures. However, this is simply not feasible from a biochemical and mathematical point of view. Because protein production is an energy demanding process, cells usually do not accumulate carbohydrates in conditions where high protein production rates are needed (e.g. high growth rates). Even if the increased protein content comes from a decrease in its

degradation rate at lower temperatures, the average reported increase in protein, total lipid and carbohydrate contents (usually expressed as mass percentage) would in some cases imply a sum of all those fractions higher than 100%.

An interesting study of Brown and Rose (1969) with the mesophilic yeast *Candida utilis* has shown that changes in cell composition are highly connected to the experimental setup used (carbon source and nutrient availability). Similar conclusions were also drawn by Tai *et al.* (2007b) when comparing results from anaerobic glucose-limited and nitrogen-limited chemostat cultivations of *S. cerevisiae*. These condition-specific responses indicate that, except for the alterations in the lipids present in the cellular membrane, changes in cell composition are not the main mechanism of temperature compensation. Temperature specific responses would therefore be likely related to the regulation of activity and expression of particular enzymes.

Similar to what happens with other types of stress (such as pH, nutrients availability…), the optimization of enzymatic rates can be achieved by increasing the amount of the rate-controlling enzymes (vertical regulation) or by modifying intracellular and extracellular concentrations of reactants and co-factors (metabolite regulation).

Vertical regulation can be investigated through measurements of the transcriptome and proteome of the cell at different temperatures. Unfortunately, most results show that genes that are differently expressed at lower temperatures are also dependent on the experimental conditions applied, namely the substrate availability (**Table 1.1**). Moreover, published transcriptome data do not provide any indications for temperature-induced changes in the expression of isoenzymes that could compensate for the loss of catalytic activity at lower temperatures. In addition, most studies show very little correlation between transcript levels and enzyme activities, making it even harder to discriminate between specific mechanisms of temperature regulation. Metabolome data (i.e. measurements of the concentrations of substrates, reactants and co-factors) could probably provide the missing link, but there are a very limited number of studies that have carried out such measurements at different temperatures.

Even if available, it would be very likely that also here the experimental conditions play a role determining the metabolome response to temperature shifts. A way to obtain comprehensive knowledge from the gathered data

Table 1.1: *Family of genes differently regulated in cold-shock and acclimation experiments with the yeast Saccharomyces cerevisiae.*

Reference	Sahara *et al.*, 2002	Schade *et al.*, 2004	Murata *et al.*, 2006	Schade *et al.*, 2004	Tai *et al.*, 2007b
Conditions	Cold shock from 30 to 10 °C	Cold shock from 30 to 10 °C	Cold shock from 25 to 4 °C	Batch acclimation at 10 °C	Chemostat acclimation at 12 °C
Down-Regulated Genes	• Heat-shock proteins.	• Heat-shock proteins.	• Protein synthesis, mainly with binding functions or cofactor requirements; • Protein activity regulation and fate (mostly RPL and RPS and enzymes for tRNA synthesis).	• Protein synthesis (ribosomal protein genes) and modification; • Nucleotide biosynthesis; • Vesicle transport.	• Carbohydrate metabolism; • Response to stimulus; • Transport.
Up-regulated Genes	• RNA polymerase and RNA processing genes; • 4h after cold shock, both genes for production and degradation of glycogen were over expressed; • Genes for trehalose metabolism were down-regulated up to 4h, and after up-regulated;	• Genes related to transport, lipid and aminoacids metabolism and transcription; • RNA helicases, RNA processing and RNA polymerase genes; • Fatty acid desaturases.	• Cell rescue, defense and virulence; • Energy production and metabolism (inc. glycolysis and storage carbohydrates).	• Carbohydrate metabolism and regulation; • Storage carbohydrates metabolism.	• Nuclear export; • Ribosome biogenesis and assembly.

and to be able to unravel the temperature impact on metabolism from the effects of other environmental conditions (such as nutrient availability) is to apply a systems biology approach, thereby combining experimentation under strictly controlled conditions and kinetic modeling.

Incorporation of temperature effects in kinetic metabolic models: a promising tool to obtain interpretable results?

Kinetic models are mathematical representations of the impact different factors have on the activity of the enzymes present in a metabolic pathway. If the assumptions used to build the kinetic model are sufficiently correct, it can be used to describe fluxes and concentrations of effectors (metabolites, enzymes, transcript levels…) for a set of experimental conditions. This *in silico* approach is valuable to test different hypotheses that would otherwise be too complicated to be understood (e.g. the complex relations between different metabolite levels under dynamic conditions) or not yet possible to be experimentally verified (e.g. *in vivo* enzyme activities).

To this date there are only very few kinetic metabolic models in which the effects of temperature-are taken into account, most likely due to the complexity of interactions underneath the microbial response to temperature changes. An *in silico* study from Chaui-Berlinck *et al.* (2004) has led to the conclusion that changes in the flux through a pathway as a consequence of temperature alterations cannot be predicted based on the analysis of the temperature impact on the isolated pathway components (e.g. catalytic activities of each enzyme). More recently, Ruoff *et al.* (2007) have presented several model-driven hypotheses for the strategies by which organisms could maintain fluxes at different temperatures. By taking into account metabolic and hierarchical control analysis, the authors could derive for which network topologies (i.e. reversibility, presence of regulation loops, branching,…) it is possible to have mechanisms that compensate the loss of catalytic activity at lower temperatures. Unfortunately, none of the studies could present experimental evidences that established the *in vivo* mechanisms used by the organisms to compensate for temperature changes, nor which reaction or metabolite pool determines the metabolic flux at different temperatures. Hatakeyama and Kaneko (2012) have recently presented an interesting model that illustrates temperature impact on setting circadian rhythms in cyanobacteria. Although the *in silico* predictions

could already point out which proteins regulate the response to temperature oscillations, the conditions applied in the model were too specific to allow it to be used with other organisms.

Another reason for the small number of kinetic models that include temperature-dependency is the scarceness of experimental data available to build it or to establish the initial hypotheses. Frequently the mathematical functions used to describe the rate of an enzymatic reaction are very complex and with a high number of parameters. If the experimental data used to estimate such parameters do not cover a wide range of fluxes and concentrations, it might happen that the kinetic parameters will never be identified, compromising the predictive power of the model. It is therefore crucial to couple the development of kinetic models to rational experimental design, aiming at obtaining sufficiently rich datasets that cover a wide range of fluxes and concentrations.

Saccharomyces cerevisiae as an experimental platform

To study mechanisms of temperature compensation it is wise to use an organism known to be able to grow at broad ranges of temperature and that is easy to cultivate under laboratory conditions. This allows setting precise experimental conditions and obtaining data for a wide range of temperatures, fluxes and intracellular metabolite concentrations. For these reasons, the yeast *Saccharomyces cerevisiae* appears to be a suitable candidate to be used as a model organism.

S. cerevisiae is a mesophilic poikilotherm ($T_{opt} \approx$ 36 °C) known to inhabit environments subjected to broad temperature ranges. Moreover, *S. cerevisiae* is used in a variety of industrial processes. These range from ancient practices (such as beer brewing) to more recent processes such as production of heterologous proteins (e.g. insulin precursors) and bioethanol. More interestingly, many of the biotechnological processes that use *S. cerevisiae* need to occur at temperatures not optimal for its growth. Examples are the production of ale beer, where a fermentation step at 20 °C is followed by a temperature drop to 10 °C so cells can quickly settle and be separated from the broth (Scott and Hall, 1970). Also baking industry is quite interested in temperature effect on metabolism due to the need of having yeasts cultures that are inactive but tolerant to low shelf-temperatures (see patents from Baensch *et al.*, 1998; Gysler *et al.*, 1996; Kawasaki *et al.*, 2000).

To understand how *S. cerevisiae* responds to temperature provides valuable information to be used in strain development programs.

The biotechnological relevance of *S. cerevisiae* has led to a large number of studies regarding its metabolism under many different experimental conditions (see, for instance, Hohmann and Mager, 2003; Walker, 1998). Such data might be valuable when dissociating the temperature impact from the effect of other experimental parameters. Also a considerable number of analytical tools to study *S. cerevisiae* is available, including enzyme activity measurements and intracellular metabolite analysis, that allow obtaining relevant *in vivo* data for the development of kinetic models.

Aim and outline of this thesis

The aim of this thesis is to elucidate mechanisms used by *S. cerevisiae* to respond to temperature changes by applying both experimental and modeling approaches. A top-down approach was used, meaning that the temperature impact on substrate uptake and rates of by-products formation was quantified before taking a look at the intracellular behavior. Because temperature extremes strongly affect the structure of proteins, increasing the complexity of the response to temperature, this study only focuses on the mild-suboptimal range (12 to 30 °C). Also this is likely to be the most relevant environmental range since the T_{opt} of most microorganisms is close to the maximum temperature reached in their natural habitat.

The first step taken was to evaluate the temperature impact under glucose-excess conditions, since the fluxes under such settings are maximal and independent of the extracellular substrate concentration (**Chapter 2**). A sequential-batch setup was used to guarantee that inoculum cells were fully adapted to the temperature applied and that there was no interference from carryover of substrates/products from previous cultivation conditions (either pre-culture or previous batch). In this way it was assured that the observed changes in rate and stoichiometry of growth were exclusively a consequence of the fermentation temperature.

To evaluate if the results from glucose-excess conditions are also valid under glucose limitation, a series of experiments were conducted in anaerobic glucose-limited chemostats at a fixed growth rate, while the temperature was changed within the range of 12-30 °C within different timescales, i.e. from 15 minutes to 1.5h (**Chapter 3**). Temperature

perturbations were applied to both 12 °C and 30 °C chemostat cultures to evaluate if the adaptive response would be different in cells acclimated to low temperatures. In other words, if the regulation of the glycolytic flux upon temperature changes could be different between the two steady-state cultures due to the adjustments of enzyme expression levels or cell physiology in acclimated cells. With the data gathered it was possible to develop a black-box model capable of reproducing the changes in fluxes upon temperature perturbations, both in batch and glucose-limited chemostat cultivations. Also the temperature impact on the *in vivo* kinetics of central carbon metabolism could be discriminated from the kinetic effect of limiting glucose concentration.

Although the results obtained from the experiments described above provided already a good indication on how temperature influences the growth and product yields of the main anaerobic by-products, the derived black-box description did not provide indications on which enzymes are the ones controlling the response to temperature changes in a broad range of substrate concentrations. To answer this, two hypotheses on how the activity of the different enzymes in a network should change with temperature in order to sustain the fluxes determined in chapters 2 and 3 were drawn from a theoretical model (**Chapter 4**). According to the results of the theoretical model, the intracellular metabolite levels measured during different temperature-perturbation experiments allows to verify if: (1) all enzymes have similar temperature sensitivity or (2) if there is one enzyme for which the catalytic activity becomes limiting at low temperatures. Intracellular metabolite measurements of cells grown in batch cultivations at different temperatures and in glucose-limited chemostat cultivations subjected to dynamic temperature conditions, allowed validating which of the hypotheses better represents the temperature response of central-carbon metabolism. Surprisingly, the results accentuated the tremendous impact of the extracellular glucose concentration on the regulation of the glycolytic flux. To develop a temperature-dependent kinetic model valid for glucose-limited conditions, it is essential that this dependency is taken into account, forcing the model to be robust and stable for a wide range of both fluxes and metabolite concentrations.

Chapter 5 presents the experimental and theoretical strategies used to construct such a model. A first version of the model was built without taking the effect of temperature into account. To obtain the model parameters,

anaerobic glucose-limited chemostat cultivations were carried out at a large range of different growth rates (0.025 to 0.27 h^{-1}) at 30 °C. The advantage of using steady-state cultivations is that the fluxes can be accurately estimated, in comparison to dynamic conditions such as pulse experiments. This, together with measurements of the enzyme activities and intracellular metabolite levels for the different growth rates, allowed evaluating which kinetic format is the best to reproduce the *in vivo* flux of each individual glycolytic reaction for the measured range of intracellular metabolite levels. Once the kinetic parameters were identified, it was possible to insert the kinetic equations into the steady-state glycolytic model. Subsequently the cultivation temperature was included as an extra variable by incorporating the Ratkowsky equation for each enzymatic reaction (see Chapter 2). This resulted in a kinetic model for anaerobic yeast glycolysis, including the temperature-dependency of rates. This model proved to be valid for different steady-state temperatures as well as for dynamic temperature changes that do not require stress-related responses (e.g. enzyme phosphorylation).

Last but not least, a resume of the major conclusions drawn from this thesis, together with a discussion of its environmental and biotechnological relevance, is provided in **Chapter 6**. Because temperature affects the metabolism of all organisms and this study only focused on *S. cerevisiae* under anaerobic mild-hypothermic temperatures, some thoughts will also be presented regarding the validity of the results and applicability of the approaches followed to study other organisms and/or temperature ranges.

2. Temperature impact on the anaerobic stoichiometry and kinetics of growth under glucose-excess conditions

Abstract

This chapter presents a characterization of the stoichiometry and kinetics of anaerobic batch growth of *Saccharomyces cerevisiae* at cultivation temperatures between 12 and 30 °C. To minimize the influence of the inoculum condition and ensure full adaptation to the cultivation temperature, the experiments were carried out in sequencing batch reactors. It was observed that the growth rate obtained in the first batch performed after each temperature shift was 10 to 30% different compared with the subsequent batches at the same temperature, which were much more reproducible. This indicates that the sequencing batch approach provides accurate and reproducible growth rate data.

Data reconciliation was applied to the measured time patterns of substrate, biomass, carbon dioxide and by-products with the constraint that the elemental conservation relations were satisfied, allowing to obtain consistent best estimates of all uptake and secretion rates. Subsequently it was attempted to obtain an appropriate model description of the temperature dependency of these rates. It was found that the Ratkowsky model provided a better description of the temperature dependency of growth, uptake and secretion rates than the Arrhenius law. Most interesting was to find that most of the biomass specific rates have the same temperature dependency, leading to a near temperature independent batch stoichiometry.

Introduction

Temperature impact on microbial growth is a recurrent topic in biotechnology studies. Its main interest comes from the effect temperature has on the kinetic properties of all organisms and the need to conciliate fermentation temperature and cost-effective industrial production. In the brewing and wine industries, for example, low temperatures are favorable for the preservation of flavors, but detrimental for growth and ethanol production rates of the yeast strains used.

It is known that temperature influences all biochemical reaction rates but, on the other hand, it should be realized that the amounts of compounds being produced are intrinsically related to the amounts of substrates consumed. This relation is in such a way that all the balances to the elements (for instance carbon, nitrogen, oxygen,…) should be satisfied. Therefore, a change in one of the metabolic rates will certainly have an impact at some other point of the metabolic network. So, to obtain a proper characterization of a biological system, it is important to consider all quantifiable uptake and secretion fluxes. Previous attempts to describe the temperature dependency of microbial metabolism have been limited to modeling the impact of the temperature on the growth rate or on the kinetic parameters of a single product of interest (Boulton, 1980; Kovarova *et al.*, 1996). Thereby other relevant conversion rates, such as production of glycerol and CO_2, have often not been taken into account. There is therefore a lack of consistent data that allows obtaining a description of the temperature impact on microbial central metabolism as a whole.

To undertake such studies it is essential to have accurate and reliable data. The use of batch cultivations in shake flasks, under non-well defined conditions, may lead to unreliable and incomplete results, due to lack of dissolved oxygen control, off-gas readings and pH control. From thus obtained data it is not possible to verify whether the observed changes have been caused exclusively by temperature differences. In addition, attention must be given to the influence of the pre-culture composition and population heterogeneity on the obtained batch culture results. If cultures are directly inoculated from a working cell stock or from a pre-culture carried out under conditions different from the ones used in the main fermentation, there can be carryover of compounds that interfere with the growth of the organism. It is also important to realize that the presence of subpopulations in the

inoculum can influence the overall response to the cultivation conditions applied (Den Besten *et al.*, 2007; Van Derlinden *et al.*, 2008).

Furthermore, a study from Shaw (1967) on the effect of abrupt temperature shifts on the growth of several yeast strains, has shown that there is a transient state where the observed growth rate is different from the one reached after adaptation to the new temperature. If the shift is performed to temperatures lower than the optimum, a lag phase might be observed, of which the duration depends on the absolute value of the temperature shift. These are strong indications that one should be careful when using results from single batch experiments.

Sequencing batch reactors (SBR) have been extensively used in research on waste water treatment processes (Wilderer *et al.*, 2001) and have lately shown an increased application as an evolutionary engineering tool (Sauer, 2001). Basically, an SBR consists of a fill-and-draw system, where part of the broth from the previous batch cultivation is used as inoculum for the subsequent one. It has recently been shown that the use of an SBR setup significantly improved the reproducibility of batch cultivations of *S. cerevisiae* (Abbott *et al.*, 2009). Therefore we have chosen to apply SBR cultivation to investigate the temperature dependencies of growth, substrate uptake and formation of all main (by)products of *Saccharomyces cerevisiae* during anaerobic batch growth at 12, 18, 24 and 30 °C. Based on the obtained data the temperature dependency of the kinetics and stoichiometry of the growth of *S. cerevisiae* under these conditions is thoroughly evaluated. A comparison is made between applicability of two of the most widely used models to describe the temperature impact on mesophilic growth: the Arrhenius law and the model of Ratkowsky *et al.* (1982).

Proper relations are this way obtained between all relevant production and consumption rates for a temperature range relevant for industrial applications. Also the estimated parameters might be further use to develop more detailed kinetic models as, for instance, the temperature impact on glycolysis.

Materials and Methods

Strain and growth conditions

Saccharomyces cerevisiae strain CEN.PK113-7D Mat**a** (Entian and Kötter, 2007) was initially grown in a shake flask at 30 °C, as described by Van den Brink *et al.* (2008). This strain is adapted to mild temperatures (15 to 40 °C) and grows optimally at temperatures close to 35 °C (Postmus *et al.*, 2008). When cells reached mid-exponential phase ($OD_{660nm} \approx 2.0$), 100 mL of culture were used to inoculate a 1L fermentor (Applikon, Schiedam, The Netherlands) with 650 mL of medium containing 0.3 $g.L^{-1}$ $(NH_4)_2SO_4$, 0.3 $g.L^{-1}$ $K_2H_2PO_4$, 3.0 $g.L^{-1}$ $(NH_4)_2H_2PO_4$, 0.5 $g.L^{-1}$ $MgSO_4.7H_2O$, 0.4 $g.L^{-1}$ of Tween 80, 10 $mg.L^{-1}$ ergosterol and 25 $g.L^{-1}$ glucose. Furthermore 1 $ml.L^{-1}$ of vitamin and 1 $ml.L^{-1}$ trace-elements solution with compositions as described by Postma *et al.* (1989) were added together with 0.15 $g.L^{-1}$ of antifoam (Antifoam C, Sigma Aldrich, Saint Louis, USA).

The pH of the fermentor was continuously measured and controlled at 5.0 by automatic addition of 2M H_2SO_4 or 2M KOH, by means of a Biostat B plus controller (Sartorius BBI systems, Melsungen, Germany). The culture temperature was measured continuously using a temperature sensor inside the fermentor and was controlled via the thermocirculator of the Biostat B plus. Fully anaerobic conditions were obtained by continuous sparging both the fermentor and medium vessel with nitrogen gas (0.69 mol. $h^{-1} \approx 0.26$ $L.min^{-1}$) via a Brooks 5850 TR mass flow controller (Hatfield, PA, USA). This guarantied that the medium used to refill the fermentor would not contain oxygen. The fermentations were performed at an overpressure of 0.2 bar and at a stirrer speed of 600 rpm.

The progression of all batches was monitored online by both measuring the concentration of CO_2 in the exhaust gas (NGA 2000 gas analyzer, Rosemount, Minnesota, USA) and the total amount of base added. When base addition stopped for a pre-defined amount of time, the broth volume was decreased to 100 mL and refilled with fresh medium to start a new batch. After 3 sequential batches were carried out at a certain temperature set-point (30, 24, 18 or 12 °C), the temperature of the setup was changed during the fermentor refilling. Two runs of at least 15 sequential batches were performed following this approach. To evaluate whether genetic and/or physiological changes had occurred after the series of sequential batch

cultivations, the last 3 batches were carried out at the same temperature as the first series (30 °C).

To make sure that the cultures were fully adapted, two initial batches were run at each cultivation temperature, before samples were taken. At least 5 samples for optical density (OD_{660}) and extracellular metabolites were taken during each batch culture.

Measurements of both dry weight and OD_{660} were performed in batches at all temperatures studied to obtain the OD_{660} to dry weight calibration line.

Analytical methods

Rapid sampling of culture filtrate for extracellular metabolite analysis was performed with the cold steel beads method (Mashego *et al.*, 2003). The amount of beads was adjusted, depending on the cultivation temperature, to prevent freezing of the sample. The filtrate samples were stored at –20 °C until analysis. Samples were analyzed in duplicate using high-performance liquid chromatography (HPLC) with a Bio-Rad Aminex column at a temperature of 60 °C. The mobile phase was 5.0 mM phosphoric acid of which the flow rate was set to 0.6 $ml.min^{-1}$. Glucose, ethanol and glycerol were measured using a Waters 2410 refractive index detector, while a Waters 2487 dual-wavelength absorbance detector at 214 nm was used for acetate and lactate quantification.

The amounts of succinate and pyruvate were measured by GC-MS analysis following the protocol of Cipollina *et al.* (2009), using ^{13}C-labelled-cell-extract as internal standard.

Estimation of rates, temperature-parameters and data reconciliation

During unlimited growth in batch culture, all biomass specific net conversion rates can be assumed constant and maximal. The change in time of the amounts of all compounds ($N_i(t)$), which are consumed and produced by the organism, is then described by

$$\frac{dN_i}{dt} = q_{\max,i} N_X(t), \tag{2.1}$$

where i is one of the eleven compounds involved: the substrate glucose (S), biomass (X), ethanol (Eth), glycerol (Gly), carbon dioxide (CO_2), acetate

(Ace), succinate (Suc), pyruvate (Pyr), lactate (Lac), water (H_2O) and ammonia (NH_4^+). Integration of equation (2.1) for biomass (X) and the definition of growth rate, $\mu_{max}=q_{max,X}$, yields the exponential growth equation:

$$N_X(t) = N_X(0)e^{\mu_{\max}.t}. \tag{2.2}$$

The CO_2 production rate, F_{CO2}, can be calculated from the measured concentration of CO_2 in the off-gas and the N_2 gassing rate. It suffices to substitute equation (2.2) into equation (2.1) to obtain the equation for the exponential increase of the CO_2 production rate during unlimited batch growth:

$$F_{CO_2} = \frac{dN_{CO_2}}{dt} = q_{\max,CO_2} N_X(0)e^{\mu_{\max}.t}. \tag{2.3}$$

By combining equations (2.1) and (2.2) and subsequent integration, a relation is obtained describing the exponential change of the amounts of the consumed and produced compounds in the fermentation broth as a function of time,

$$N_i(t) = N_i(0) + q_{\max,i}\frac{N_X(0)}{\mu_{\max}}\left(e^{\mu_{\max}.t} - 1\right). \tag{2.4}$$

A correction had to be made for ethanol, as evaporation significantly influences the result. Therefore a term accounting for evaporation ($-k_{evap}N_{Etoh}(t)$) was included in the compound balance (equation (2.1)). After integration, the result describing the amount of ethanol in the broth as a function of time is:

$$N_{eth}(t) = \left(N_{eth}(0) - q_{\max,i}\frac{N_X(0)}{\mu_{\max}+k_{evap}}\right)e^{-k_{evap}.t} + q_{\max,i}\frac{N_X(0)}{\mu_{\max}+k_{evap}}e^{\mu_{\max}.t} \tag{2.5}$$

The evaporation constant, k_{evap}, for the bioreactor was determined for different temperatures in separate experiments (data not shown) and found to be $k_{evap}(T)=2.63\text{x}10^5.\exp(-4670/T)$, where T is the temperature in K.

As the above mentioned set of 11 reactants represent all significant compounds converted, the elemental conservation relations (i.e. for C, H, O and N) can be used as constraints for the reconciliation of the measurement data. The elemental conservation relations have the form

$$\sum_{i=1}^{11} n_i q_{\max,i} = 0, \tag{2.6}$$

where n_i are the relevant stoichiometric coefficients for each relation.

To estimate the maximum biomass specific conversion rates at each temperature ($\mu_{max}(T)$ and $q_{max,i}(T)$) and the initial amounts, $N_i(0)$, an optimization routine was applied where the weighted residual sum of squares between the nine experimental measurements (for i=S, X, Eth, Gly, CO_2, Ace, Suc, Pyr and Lac) and amounts predicted by equations (2.2) – (2.5) was minimized under the constraint that the four elemental conservation relations were satisfied. As the complete system contains eleven net conversion rates, the four constraints between them dictate that only seven conversion rates have to be determined to obtain the complete set of rates. If measurements are available for nine compounds, the complete system is two times over determined, allowing data reconciliation and gross error detection (Verheijen, 2003).

With the obtained estimates of $q_{max,i}$ it is possible to express each rate relative to the substrate uptake rate (further on called yield on substrate) for each temperature,

$$Y_{iS} = q_{\max,i} / q_{\max,S}. \tag{2.7}$$

In order to analyze whether these ratios are temperature dependent, a model was tested wherein the ratios between all net conversion rates were fixed, independent of the cultivation temperature. This was achieved by incorporating these yields (equation (2.7)) in equation (2.4):

$$N_i(t) = N_i(0) + Y_{is} q_{\max,S} \frac{N_X(0)}{\mu_{\max}} \left(e^{\mu_{\max} \cdot t} - 1 \right). \tag{2.8}$$

By doing so, the initial problem was reduced from 36 unknown rates ($q_{max,i}$ of the 9 carbon containing components for the 4 different temperatures studied), to 12 (4 $q_{max,S}$ values for the 4 different temperatures and 8 Y_{iS} values).

The same optimization approach was used to test the validity of the two temperature models: the Arrhenius law and the model of Ratkowsky *et al.* (1982) (respectively equations (2.9) and (2.10)).

$$q_{\max,i} = A_i . e^{-\frac{Ea_i}{R.T}} \quad (2.9)$$

$$q_{\max,i} = b_i^* . (T - T_{\min,i})^2 \quad (2.10)$$

To this end, equation (2.9) or (2.10) was substituted in equation (2.4) and either the pre-exponential parameter and activation energy of the Arrhenius law (respectively A_i and Ea_i), and the empirical parameters from the Ratkowsky model (b^*_i and $T_{min,i}$) were estimated.

Statistical analysis of the estimated parameters

Chi-squared tests were used to determine the adequacy of the models with respect to the experimental errors while F-tests were applied to evaluate the statistical consistency of model reduction. The reasoning behind the choice of these tests can be found in Verheijen (2003). For all cases, a significance level of 0.05 was used. At least two rounds of iterations were run for each step to ensure that the solution was not a local minimum. A detailed description of the applied statistical procedures can be found in the appendix (page 45).

Results and Discussion

Performance of the sequential-batch setup

Two identical runs of sequential-batch-fermentations were performed, whereby the cultivation temperature was subsequently decreased from 30 to 24, 18, 12 °C and increased back to the initial temperature of 30 °C. At least 3 successive fermentations were carried out at each temperature (see **Figure 2.1**). Examples of the obtained exponential curves of cumulative CO_2 production for the four different cultivation temperatures are presented in **Figure 2.2**.

Fitting of equation (2.4) to the obtained CO_2 curves provides μ_{max} values for each cultivation. The good reproduction of the experimental data, including the initial measurements at time zero, indicated that a lag phase was either very short or absent. This can be explained by the fact that subsequent batches were initiated directly at the end of the exponential

phase of the previous one, and that the amount of inoculum used was relatively high (13 % w/w).

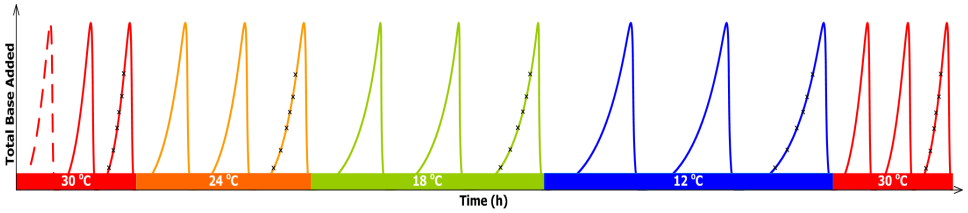

Figure 2.1: *Description of the sequential batch experiment used to investigate the impact of temperature on the net conversion rates. Each run of sequential-batch-fermentations consisted of 5 series of 3 batch cultivations carried out at 30, 24, 18 and 12 ℃. (x) indicate the times at which samples were taken for extracellular metabolite analysis.*

When plotting the obtained growth rates as a function of the number of fermentations (1, 2 or 3), it was observed that the growth rate of the first batch of each series was, in most cases, significantly different from the subsequent ones (**Figure 2.3**). The difference was largest (24%) for the first batch of the entire run of sequential fermentations. This was not unexpected because of the physiological changes that the inoculum, grown aerobically in shake flasks, has to go through, to adapt to the fully anaerobic conditions of the SBR. These adaptations include adjustments of enzyme levels to compensate for the loss of respiratory capacity, as was observed by Larsson *et al.* (1997).

The deviations observed for the first batches at different temperatures are also in accordance with the transient-growth theory developed by Shaw (1967) who reports that temperature shifts performed in a moderate range close to the optimum growth temperature cause a fast adaptation to the new temperature. For larger shifts, a transient period is generally observed where the growth rate is different than after adaptation to the new temperature. The temperature range where the transient state can be observed depends on the physiology of the organism (Shaw, 1967). In the present study it was seen that the differences between growth rates determined for the 24 °C batches are smaller when compared to the ones performed at 18 and 12 °C. This indicates that temperatures between 24 and 30 °C are within the moderate range, while for temperatures of 18 °C or lower this strain can no longer immediately adapt to the new temperature,

causing a transient state of growth. These overall results indicate that even considering the milder shifts, such as a 6 °C step in temperature, the cells are not able to fully adapt in one single batch.

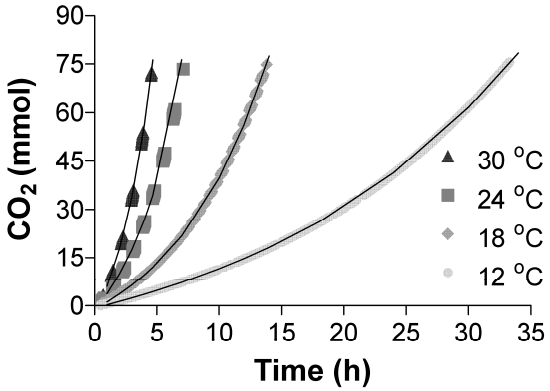

Figure 2.2: *Time profiles of the cumulative amounts of carbon dioxide produced during batches at 30 ℃, 24 ℃, 18 ℃ and 12 ℃. The data shown refer to batch number 2 of each temperature. The dots represent the experimental data, while the lines represent the fitted exponential equations.*

As an example, in a previous study with the same strain and medium conditions, the growth rate obtained with single batch fermentations at 30 °C was 0.34 ±0.01 h^{-1} (Tai *et al.*, 2007a). As can be seen in **Figure 2.3** this value is significantly different from the one obtained in the third batch using the sequential batch setup (0.28 ±0.01 h^{-1}). This points out that sampling during the first four generations can lead to unreliable results concerning physiological properties and kinetic parameters such as $\mu_{max}(T)$.

Estimates of the biomass specific conversion rates and temperature (in)dependency of growth stoichiometry

From the measured time profiles of substrate, biomass, CO_2 and excreted products the respective biomass specific net conversion rates were obtained for each cultivation temperature, following the parameter estimation and data reconciliation procedure outlined in the materials and methods section. With this procedure the complete dataset of nine time profiles was used to obtain a consistent estimation of all biomass specific net conversion rates at different cultivation temperatures, with minimized experimental error in the

estimated rates, thus obtaining a reliable set of parameters for further modeling steps.

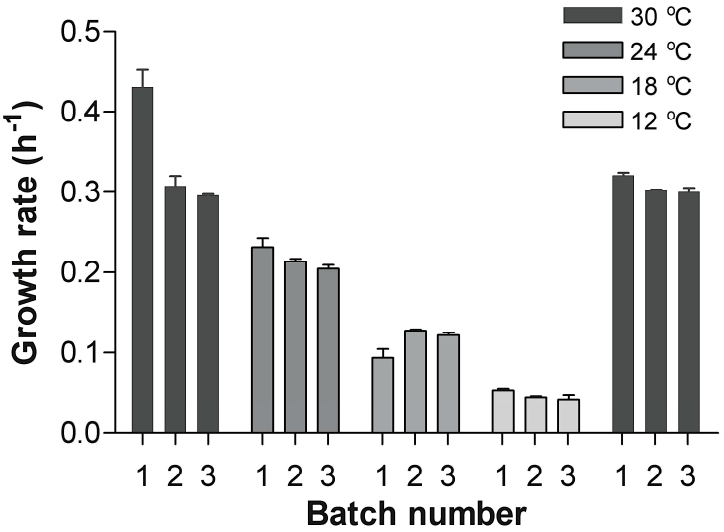

Figure 2.3: *Growth rates obtained from the time profiles of cumulative CO_2 production. The error bars indicate the standard error obtained from the average of two different runs of sequential-batch experiments.*

It was observed for all temperatures that an optimal solution could only be obtained when data points were used until two biomass-doubling-times. Taking data into account beyond two doubling times resulted in increasing deviations from the exponential functions (equations (2.2) to (2.5)). This observation is most likely associated with the residual glucose concentration at that time point (approximately 40 mM) which is close to the affinity constant determined for the mid exponential phase in cells grown from similar initial glucose concentrations (Maier *et al.*, 2002). Due to that, the glucose uptake rate at that stage becomes notably lower than the $q_{S,max}$. Therefore, including measurements done at later time points will result in underestimation of the maximum uptake and secretion rates.

As can be seen from **Figure 2.3**, the measured metabolite profiles could be satisfactory described using the fitted parameters. From the reconciled rates (**Table 2.1**) it was possible to calculate the yields of consumed and produced compounds on substrate for each temperature studied.

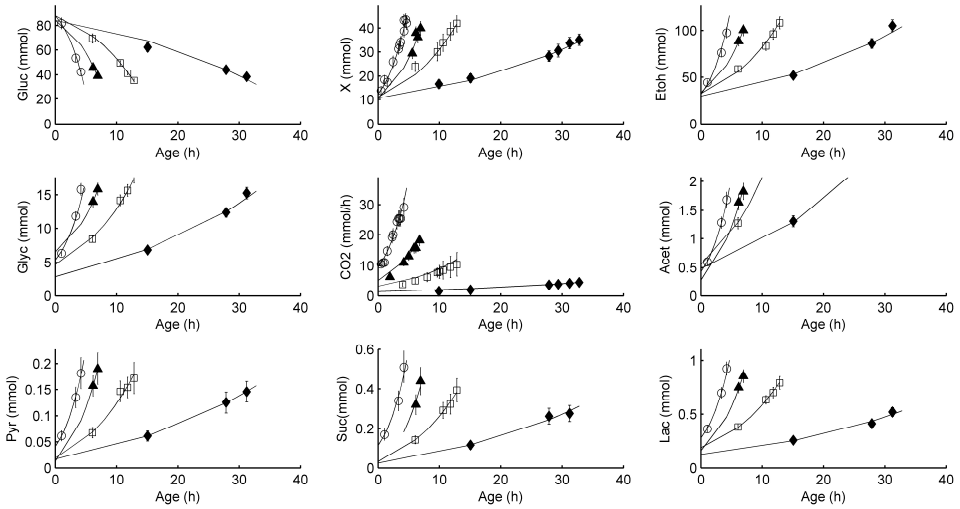

Figure 2.4: *Time patterns of the amounts of metabolites measured during sequential batch cultivations at 30 °C (○), 24 °C (▲), 18 °C (□) and 12 °C (◆). The points represent the experimental data, while the lines represent the best estimates from the data reconciliation routine. The error bars refer to the standard deviations of at least two measurements.*

As presented in **Figure 2.4**, the thus obtained yields appear in most cases to be temperature independent, implying that the stoichiometry of growth did not change significantly with temperature. To evaluate this hypothesis, the data reconciliation procedure was applied to the complete dataset whereby, one at a time, the rate of each compound was replaced by a yield on substrate, according to equation (2.8). Secondly, a similar procedure was applied whereby the yields of all components were fixed at the same time.

For all cases tested, the model could still successfully describe the experimental data (p values of the chi-square test between 0.191 and 0.999). However, the results from the F-test suggested that the goodness of fit was significantly less when fixing the yields of ethanol (p=0.013), glycerol (p=0.004) and/or acetate ($p=1x10^{-5}$). Clearly, the inferior fit after fixing the acetate yield is caused by the fact that acetate production was strongly influenced by the cultivation temperature, as can be seen from the changing yield coefficient in ***Figure 2.5.*** An explanation for this change in stoichiometry could be the increased glycerol production at lower temperatures. It has been shown that glycerol is an important component for thermotolerance and, for that reason, *S. cerevisiae* accumulates glycerol when transferred

from 30 to 12 °C (Panadero *et al.*, 2006). An increase in glycerol production results in an overproduction of NAD^+ that, under anaerobic conditions, can only be compensated by the production of a more oxidized compound than ethanol, e.g. acetate, so the redox balance in the cell can be maintained.

Even though in ***Figure 2.5*** there seems to be a change in the yield coefficients for lactate and succinate, this observation could not be statistically supported (p values were higher than 0.7). This might be a consequence of the relatively large measurement errors for succinate and lactate (in average 15%) that result from the low accuracy of the analytical platform used for the low concentrations range of these metabolites.

Nevertheless, since even for the lower temperature studied the carbon involved in acetate production is only 1.6% of the total carbon flowing in the cell, it is possible to assume that for the main glycolytic pathway the stoichiometry is temperature independent. This means that the glucose consumed per mol of catabolic products formed remains practically the same, independently of the temperature.

Table 2.1: *Biomass specific conversion rates obtained from batch cultivations carried out at different temperatures. The values presented are the average from two different runs of sequential batch fermentations of the third batch at each temperature.*

Fluxes	**Cultivation Temperature**			
(mmol.g_{DW}^{-1}.h^{-1})	**30 °C**	**24 °C**	**18 °C**	**12 °C**
($-q_S$)	18.00 ±0.58	11.50 ±0.29	6.85 ±0.25	2.99 ±0.13
μ (h^{-1})	0.279 ±0.012	0.194 ±0.007	0.104 ±0.006	0.036 ±0.002
q_{CO2}	29.59 ±1.01	18.52 ±0.49	11.01 ±0.44	4.91 ±0.22
q_{Eth}	27.69 ±0.98	17.24 ±0.47	10.12 ±0.43	4.52 ±0.21
q_{Glyc}	3.41 ±0.24	2.29 ±0.11	1.62 ±0.08	0.724 ±0.060
q_{Ace} [(a)]	467 ±34	401 ±19	299 ±21	144 ±16
q_{Lac} [(a)]	232 ±20	176.7 ±7.7	78.3 ±3.0	23.3 ±2.1
q_{Pyr} [(a)]	138 ±20	103.1 ±7.3	45.2 ±4.5	16.4 ±2.9
q_{Suc} [(a)]	53.1 ±8.9	44.1 ±0.9	20.7 ±1.1	8.1 ±0.8
q_{H2O}	2.362 ±0.202	1.691 ±0.115	0.705 ±0.098	0.161 ±0.049
($-q_{NH4+}$)	1.563 ±0.070	1.087 ±0.042	0.583 ±0.035	0.201 ±0.013

[(a)] *Fluxes expressed in* $\mu mol.g_{DW}^{-1}.h^{-1}$.

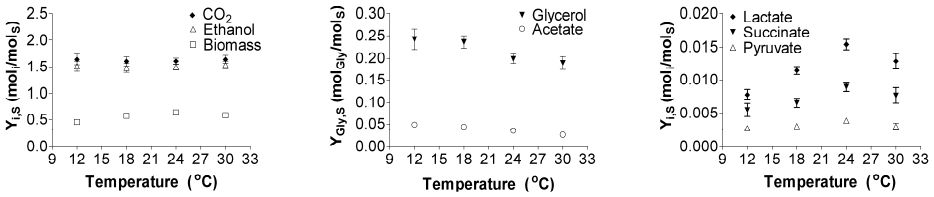

Figure 2.5: *Yields on substrate as a function of temperature. The values were calculated from the reconciled net conversion rates. The error bars refer to the standard errors.*

Temperature dependency of the net conversion rates: Arrhenius versus Ratkowsky

Apart from the stoichiometric coefficients, also the kinetic parameters that determine the temperature impact on growth, substrate uptake and product secretion rates are crucial to obtain a proper mathematical model for the temperature dependency of growth. To this end, both the Arrhenius law (equation (2.9)) and the Ratkowsky model (equation (2.10)) were tested. None of the yields were fixed during these modeling steps so it would be possible to independently estimate the temperature-parameters for all the individual compounds.

As can be seen from **Figure 2.6**, the Ratkowsky model provided a better fit to the data than the Arrhenius law (p value of 0.182 for the Ratkowsky model and 0.013 for the Arrhenius law). However, one should keep in mind that the theory underneath the Arrhenius law comes from single reaction rate constants while the rates in biological systems (substrates taken up and products excreted) are a result of a sequence of metabolic reactions, each with potentially different temperature coefficients. On the other hand, the Ratkowsky formula was found to describe especially the growth processes adequately over a considerable range and for several microorganisms (Ratkowsky *et al.*, 1982).

Nevertheless, both models studied provided an indication for the temperature independency of stoichiometry. It was observed that the T_{min} parameter from Ratkowsky and Ea_i from Arrhenius was the same for all uptake and secretion rates (respectively 273.37 ±273.61 K and 73.1±2.1 kJ.mol^{-1}). If we then consider equations (2.9) and (2.10), this means that the only way to satisfy the elemental balances is to have constant yields. It should also be mentioned that a large error was obtained for the T_{min} in all

the optimizations performed, even when testing the hypothesis of different T_{min} for the different metabolites (data not shown). This observation has been previously discussed by Bernaerts *et al.* (2002) and is a consequence of the lack of accurate growth rate data at near-freezing temperatures, which hampers a precise estimation of this parameter.

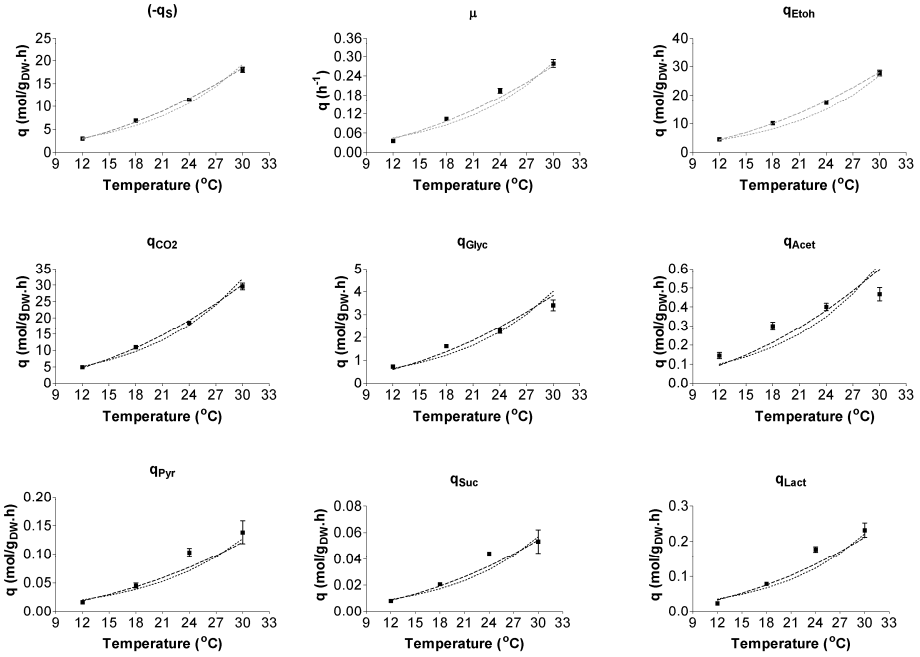

Figure 2.6: *Biomass specific fluxes calculated from the experimental data reconciliation (■), the Arrhenius law (……) and the Ratkowsky model (-----).*

Conclusions

This study investigated the global impact of mild hypothermic temperatures on the anaerobic growth of *S. cerevisiae*.

It was demonstrated that by using a sequencing batch approach, the influence of inoculum composition and presence of transient states for the prediction of growth rates could be eliminated. It also became clear that using data obtained during the first 4 generations after a 6 °C shift might lead to wrong μ_{max} predictions. In general, this strengthens that scientists need to

take into account the physiological adaptation of the organism to the culture conditions applied and its impact on the results obtained.

Our complete set of measurements (biomass, substrate, CO_2, ethanol, glycerol, acetate, lactate, succinate and pyruvate) allowed obtaining a consistent set of $q_{max,i}$ values for each temperature tested that satisfied the elemental balances. An analysis of the $q_{max,i}$ rates allowed concluding that the stoichiometry of anaerobic growth of *S. cerevisiae* is not changing with temperature for the major carbon fluxes, meaning that the yields on glucose can be considered temperature independent for the range tested. All other $q_{max,i}$ rates can therefore be easily calculated from the temperature dependent $q_{max,S}$ and the temperature-independent yield coefficients, excluding the need for temperature-dependent rate equations for the majority of the metabolites.

Appendices

Nomenclature

A	Pre-exponential parameter of the Arrhenius model (mmol.C-mol$_X^{-1}$.h^{-1})
b_i^*	Parameter adapted from Ratkowsky *et al.* (1982) (mmol.C-mol$_X^{-1}$.h^{-1}.K^{-2})
Ea_i	Activation energy from the Arrhenius model (J.mol^{-1})
F_i	Flow of compound *i* (mmol.h^{-1})
$N_i(t)$	Amount of component *i* (mol)
n_i	Stoichiometric coefficient of compound *i*
OD_{660}	Optical density measured at 660 nm
$q_{max,i}$	Biomass specific production rate of component *i* (mmol.C-mol$_X^{-1}$.h^{-1})
R	Gas constant (kJ.K^{-1}.mol^{-1})
t	Time (h)
T	Temperature (K)
T_{min}	Parameter of the model from Ratkowsky *et al.* (1982) (K)
Y_{ij}	Macroscopic yield of compound *j* into compound *i* (mol$_i$.mol$_j^{-1}$)
μ	Specific growth rate (h^{-1})

Subindexes

Ace	Acetate
CO_2	Carbon dioxide
Eth	Ethanol
Gly	Glycerol
Lac	Lactate
Pyr	Pyruvate
S	Carbon source (glucose)
Suc	Succinate
X	Biomass
i	Index for metabolite compounds
j	Index for different observation times
k	Index for different temperatures

Formal description of the estimation routines applied for data reconciliation and temperature modeling

To estimate the rates at each temperature ($q_{max,i}$, μ_{max}) and the initial amounts of all the components ($N_i(0)$), an optimization routine was applied to each temperature data set, where the overall residual sum of squares between experimental measurements, N_{ij} for component i at $t = t_j$, and the amounts predicted by equation (2.4) ($\tilde{N}(t_j)$) was minimized:

$$\left\{\hat{N}_i(0), \hat{q}_{\max,i}, \hat{\mu}_{\max}\right\} = \arg \min_{\substack{N_i(0), q_{\max,i}, \mu_{\max} \\ s.t. \sum_i n_i q_{\max,i} = 0}} \sum_i \sum_{t_j}^{t_j < t_f} \left(\frac{N_{ij} - \hat{N}_i(t_j, N_i(0), q_{\max,i}, \mu_{\max})}{\sigma_{ij}} \right)^2 \qquad (2.11)$$

As explained before, it was further imposed as constraint that the elemental conservation relations should be satisfied. Therefore, the sum of the product between the stoichiometric coefficients n_i and the respective rate had to balance, and are introduced above as constraint for the optimization.

This procedure provides the best estimates of the initial concentrations and rates for all the considered metabolites, and for each individual temperature.

To model the temperature impact on the biomass specific rates $q_{max,i}(T)$, the rates in balance (2.4) were replaced by the Arrhenius and Ratkowsky equations, leading to best estimates of the parameters of the temperature models:

$$\left\{\hat{N}_i(0,T_k),\hat{A}_i,\hat{Ea}_i\right\}=\arg\min_{\substack{N_i(0,T_k),A_i,Ea_i \\ s.t.\sum_i n_i q_{\max,i}=0 \quad \forall T_k}} \sum_{T_k}\sum_{i}\sum_{t_j}^{t_j<t_f}\left(\frac{N_{ijk}-\hat{N}_i(t_j,T_k,N_i(0,T_k),A_i,Ea_i)}{\sigma_{ijk}}\right)^2 \tag{2.12}$$

$$\left\{\hat{N}_i(0,T_k),\hat{b}_i^*,\hat{T}_{\min}\right\}=\arg\min_{\substack{N_i(0,T_k),b_i^*,T_{\min} \\ s.t.\sum_i n_i q_{\max,i}=0 \quad \forall T_k}} \sum_{T_k}\sum_{i}\sum_{t_j}^{t_j<t_f}\left(\frac{N_{ijk}-\hat{N}_i(t_j,T_k,N_i(0,T_k),b_i^*,T_{\min})}{\sigma_{ijk}}\right)^2 \tag{2.13}$$

Finally, in order to investigate if the stoichiometry of growth was temperature independent, a model was tested where $q_{max,i}$ was replaced by its correlation with the yield on substrate (Y_{iS}):

$$\left\{\hat{N}_i(0,T_k),\hat{q}_{\max,S}(T_k),\hat{Y}_{iS}\right\}=\arg\min_{\substack{N_i(0,T_k),q_{\max,S}(T_k),Y_{iS} \\ s.t.\sum_i n_i q_{\max,i}=0 \quad \forall T_k}} \sum_{T_k}\sum_{i}\sum_{t_j}^{t_j<t_f}\left(\frac{N_{ijk}-\hat{N}_i(t_j,N_i(0,T_k),q_{\max,S}(T_k),Y_{iS})}{\sigma_{ijk}}\right)^2 \tag{2.14}$$

3. Discriminating between temperature and substrate dependencies of yeast metabolic rates using dynamic temperature conditions

Abstract

Many kinetic models that describe the impact of temperature on metabolism have been derived from batch culture studies. Because in such cultivations all nutrients are in excess, changes in the growth and other biomass specific rates will be uniquely a consequence of the different temperatures applied. However, such models have limited value for substrate-limited conditions, which are often applied in industrial fermentation processes. To develop a model capable of describing the temperature dependency of growth under glucose-limiting conditions, it is necessary to apply experimental design strategies where, by perturbing the temperature of the cultivation, both the substrate uptake rate and its residual concentration will change over a wide range.

Four temperature shifts have been designed and applied to anaerobic glucose-limited chemostat cultivations of *Saccharomyces cerevisiae*. From the gathered data it was possible to build a temperature-dependent black-box model that covers the anaerobic glucose-uptake rate and production of carbon dioxide, ethanol, biomass, glycerol, acetate, succinate, pyruvate and lactate. Results from experiments with different initial steady-state temperature and rates of temperature perturbation were compared. It was found that the yield on glucose for most extracellular compounds is independent of temperature and residual glucose concentration. The exceptions were the acetate yield and storage carbohydrate metabolism, where there is a strong impact of the extracellular glucose concentration but

not temperature. Only the kinetics of glucose uptake was different between temperature shifts applied to 30 °C and 12 °C chemostat cultivations. This appeared to be related to the expression of different glucose transporters in chemostats at different steady-state temperatures, as a consequence of the higher residual glucose concentration at lower temperatures.

Introduction

Temperature receives more and more emphasis in microbiology studies, where focus is being given to understand the regulation mechanisms below the optimal temperature for growth. This knowledge can ultimately help to select or improve the strains that are more productive at a temperature of the industrial process that is otherwise suboptimal to growth. To perform this sort of studies it is necessary to cultivate the organisms at different temperatures. However, depending on the experimental setup chosen, drawing clear conclusions regarding the impact of temperature on metabolism might be hindered by the effect of co-varying variables, such as substrate concentration or growth rate.

Shake-flasks and batch cultivations are still the preferred setups to study the effect of temperature on the physiology of microorganisms. An example is the previous chapter where, by performing anaerobic sequential-batch fermentations at different temperatures, it was found that there are no significant changes in the yields on glucose of the major catabolic products of *Saccharomyces cerevisiae* between 12 and 30 °C. Information on the effect of the temperature on the stoichiometry and the consumption and production rates of the relevant metabolites is crucial for constructing black-box kinetic models that quantify the temperature impact on uptake and secretion fluxes. In batch fermentations the substrate concentration is in excess and plays no kinetic role. As a consequence, the growth rate is always maximal and a change in temperature results in a change of (maximum) growth rate. This implies that observations obtained from substrate-excess conditions reflect the combined action of temperature and growth rate on the regulation of fluxes. Experiments in glucose-limited conditions with the same growth rate and different temperatures can be run to avoid the effect of varying growth rate. The question then rises whether models developed from batch data can be extrapolated to describe glucose-limited processes were the growth rate of the cells is controlled by the substrate feed rate and whereby the residual

substrate concentration, besides temperature, plays a role in regulating the kinetics of growth and product formation. Because it is known that residual substrate also plays a role as signal molecule and/or regulator (Gancedo, 2008) it is important to take its concentration into account when investigating temperature effects under substrate limited cultivation conditions.

A way to investigate this could be to perform glucose-limited chemostat cultivations at different temperatures and growth rates. If in chemostat cultures the outflow rate, and thus the specific growth rate, is set to be the same for lower temperatures, the residual glucose concentration, and possibly enzyme levels, would change as a way to compensate for the decrease of their catalytic activities at lower temperatures. However, to gather from steady-state chemostat cultivations at different temperatures a relevant range of fluxes and residual substrate concentrations, required to obtain a sufficiently rich dataset to allow proper parameter estimation, involves extensive and time-demanding laboratory work. Also the fact that, during prolonged cultivations, enzyme levels could have adapted to the different conditions (temperature and growth rate) would hamper the separation of the impact of residual substrate concentration and temperature in the kinetic response to temperature shifts (Mashego *et al.*, 2005).

Rapid perturbation experiments have been widely used to investigate metabolic regulation and *in vivo* enzyme kinetics (Taymaz-Nikerel *et al.*, 2011; Theobald *et al.*, 1997; Oldiges and Takors, 2005). The advantage of such type of experiments is that the time of the perturbation can be kept short enough to avoid significant changes in enzyme levels, avoiding an impact on the overall metabolism. Changes in fluxes will then be a direct consequence of the perturbation applied. By applying rapid temperature shifts to steady-state chemostat cultivations, it is possible to perturb the fluxes in a controlled way by setting the rate of the temperature shift. For instance, fast temperature shifts in glucose-limited chemostats will initially impose large changes in the glycolytic flux at a relatively narrow range of extracellular glucose concentrations. This means that a small number of different temperature perturbations would be sufficient to obtain a wide range of fluxes and residual substrate concentrations at different temperatures without massive changes in enzyme levels.

In this study we explore the use of different temperature perturbations to model the dependence of uptake and secretion rates on temperature in anaerobic cultivations of *Saccharomyces cerevisiae* where the substrate concentration is growth limiting. A black-box model to describe the temperature dependency of growth and (by)product formation was constructed, using parameters obtained from both batch fermentations (Chapter 2) and steady-state chemostat cultures at 12 and 30 °C. The model was further validated and optimized with data from linear-temperature-shifts performed to the same chemostat cultures. This approach allowed distinguishing between the impact of temperature and the impact of residual glucose concentration on changes in the substrate uptake and production rates of (by)products in glucose-limiting cultivations.

Materials and Methods

Cultivation procedures

Strain and Media

Saccharomyces cerevisiae CEN.PK113-7D (Mat**a**) (Entian and Kötter, 2007; Nijkamp *et al.*, 2012) was used in all experiments.

The pre-culture medium contained 5.0 $g.L^{-1}$ $(NH_4)_2SO_4$, 3.0 $g.L^{-1}$ KH_2PO_4, 0.5 $g.L^{-1}$ $MgSO_4.7H_2O$, 18 $g.L^{-1}$ glucose and 1.0 $ml.L^{-1}$ of a trace element solution and 1.0 $ml.L^{-1}$ of a vitamin solution. The compositions of the trace element and vitamin solutions were the same as described by (Verduyn *et al.*, 1990).

The synthetic medium used for the chemostat cultivations contained 0.3 $g.L^{-1}$ $(NH_4)_2SO_4$, 0.3 $g.L^{-1}$ $K_2H_2PO_4$, 3.0 $g.L^{-1}$ $NH_4H_2PO_4$, 0.5 $g.L^{-1}$ $MgSO_4.7H_2O$, 0.4 $g.L^{-1}$ of Tween 80, 10 $mg.L^{-1}$ ergosterol, 25 $g.L^{-1}$ glucose, 1.0 $ml.L^{-1}$ of trace element solution and 1.0 $ml.L^{-1}$ of vitamin solution (both solutions with the same compositions as used for preparing the pre-culture medium).

The pre-culture medium and vitamin solution were filter sterilized via a PVDF membrane with 0.2 µm pore diameter (Millipore, Massachusetts, USA). The synthetic medium without glucose and ergosterol was heat-sterilized for 20 min at 120 °C. The glucose solution was heat-sterilized for 20 min at 110 °C before being added to the medium.

Chemostat cultivations

1 ml of a working cell stock of *Saccharomyces cerevisiae* was used to inoculate 100 ml of pre-culture medium in a 500 ml un-baffled shake flask. This pre-culture was grown for 7h at 30 °C and 200 rpm on a gyratory shaker. The whole pre-culture was used to inoculate 900 ml of synthetic medium in a 2.0 L fermentor (Applikon, Schiedam, The Netherlands). Cells were grown under anaerobic glucose-limited conditions at a dilution rate (*D*) of 0.03 h^{-1}. The working volume of the culture was kept at 1.0 liter via an electrical level sensor that controlled the effluent pump. The amount of effluent was monitored with a balance during the entire experiments, so it was possible to calculate the flow out from the fermentor. At the end of each fermentation, the total amount of broth was withdrawn and weighted to obtain the accurate working volume.

The pH was monitored online and maintained at 5.0 by automatic addition of 2.0 M KOH or 2.0 M H_2SO_4 using a Biostat Bplus controller (Sartorius BBI Systems, Melsungen, Germany). The pH sensor (type 465-50-S7, Mettler-Toledo, Urdof, Switzerland) was equipped with automatic temperature compensation. Oxygen diffusion from the environment into the liquid media was avoided by using oxygen impermeable Norprene tubings and butyl septa, as well as by sparging the medium vessel and fermentor with pure nitrogen gas (N_2). The N_2 flow rates for both medium vessel and fermentor were controlled at 0.35 vvm by means of mass flow controllers (Brooks 5850 TR, Hatfield, PA, USA).

The temperature was initially set to either 12 or 30 °C. After 5 residence times (7 days) of constant CO_2 readings and base addition profiles, samples were taken to measure the steady-state concentration of biomass dry weight and extracellular metabolites. Subsequently temperature was linearly changed in time (intervals of 0.25 to 0.5h) between 12 and 30 °C, according to the profiles shown in **Figure 3.1**. Shifts A30, B30 and C30 were applied to 30 °C chemostats, and A12 to a chemostat at 12 °C. The temperature profiles were defined and controlled via the MFCS/ win 2.1 software (Sartorius BBI Systems, Melsungen, Germany).

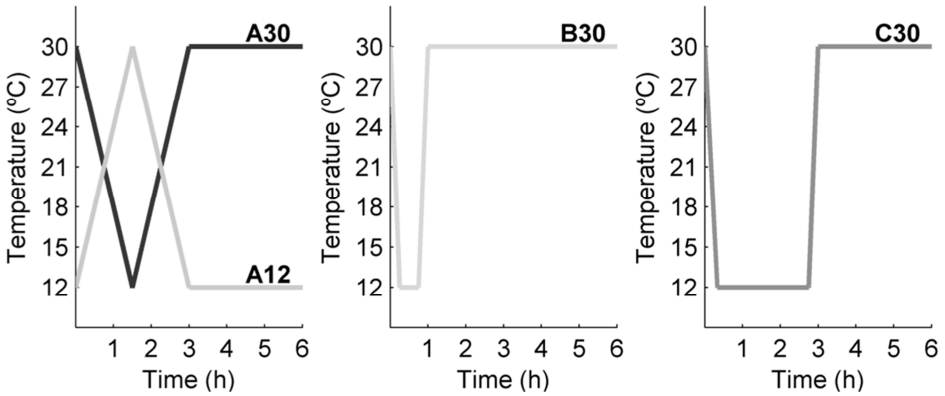

Figure 3.1: *Temperature-perturbation profiles applied to chemostat cultivations (dilution rate of 0.03 h^{-1}). For shifts A12 and A30 the temperature increase/decrease took 1.5h. The temperature decrease in experiments B30 and C30 were performed within 30 minutes. The temperature increase in experiments B30 and C30 took, respectively, 30 and 15 minutes.*

Analytical procedures

Quantification of extracellular metabolite concentrations

For extracellular metabolites and residual substrate, 2.0 ml of broth samples were taken and processed as described by Canelas *et al.* (2008), with exception for the amount of steel beads. The amount of beads at -20 °C required to decrease the temperature of the sampled broth instantly to 1 °C was obtained from the heat balance for the system steel-water, as described by Mashego *et al.* (2003). The residual amounts of glucose in these samples, as well as the concentrations of ethanol, glycerol and acetate, were determined by high-performance liquid chromatography analysis with a Bio-Rad Aminex HPX-87H column at 60 °C. The column was eluted with 5 mM phosphoric acid at a flow rate of 0.6 $ml.min^{-1}$. Acetate was detected with a Waters 2487 dual-wavelength absorbance detector at 214 nm. Glucose, ethanol, and glycerol were detected with a Waters 2410 refractive index detector. The pyruvate and succinate contents were measured by GC-MS using U-^{13}C-labeled cell extract as internal standard (Wu *et al.*, 2005).

The dry weight was measured in duplo, following the method described by Mashego *et al.* (2005).

Off-gas analysis

The CO_2 production was monitored online by measuring its volume fraction in the off-gas. The exhaust gas was cooled with a condenser connected to a cryostat set at 5 °C and dried with a Permapure dryer (Inacom Instruments, Overberg, The Netherlands) before analysis of the CO_2 by a Rosemount NGA 2000 gas analyzer (Minnesota, USA).

Analysis of storage carbohydrate content

The trehalose and glycogen contents were measured by the enzymatic method developed by Parrou and Francois (1997), where trehalose and glycogen are hydrolyzed to glucose by, respectively, trehalase and amyloglucosidase. The glucose concentration in these samples was determined with the enzymatic kit 0716251 from R-Biopharm/Roche (Darmstadt, Germany).

Modeling and statistical procedures

Calculation of biomass-specific rates and data reconciliation

The biomass-specific net conversion rates, i.e., growth rate, glucose consumption rate, and the production rates of carbon dioxide, ethanol, glycerol, acetate, succinate, pyruvate and lactate during the chemostat experiments, were calculated from their steady-state mole balances. The experimentally set gas and liquid inflow rates and the measured concentrations of compounds, including their experimental errors, were used as input data for these calculations. Because with the available set of measurements an over determined system was obtained, data reconciliation and gross error detection could be applied. Under the constraint that the elemental conservation relations should be satisfied, standard data reconciliation techniques were used to obtain the best estimates of the net conversion rates with their standard errors, according to Verheijen (2009).

The reconciliation was considered acceptable if there were no significant measurement deviations at a significance level of 5%, and the weighed sum of squares was lower than the degree of redundancy of the system.

Black-box modeling of temperature dependency

The general mole balance for each compound *i* in the broth can be written as:

$$\frac{dN_i}{dt} = F_{in}C_{in,i} - F_{out}C_{out,i} + q_i C_X V \quad (3.1)$$

wherein N_i represents the amount of compound i in the bioreactor (mmol), F_{in} and F_{out} the feed and effluent flows, ($L.h^{-1}$), $C_{in,i}$ and $C_{out,i}$ the concentrations of compound *i* in the feed and effluent ($mmol.L^{-1}$), q_i the biomass specific conversion rate of compound *i* in the reactor ($mmol.g_{DW}^{-1}.h^{-1}$), C_X the biomass concentration ($g_{DW}.L^{-1}$) and *V* the liquid volume in the reactor (L).

For the mole balance of ethanol, evaporation from the chemostat was also taken into account. The balance then became:

$$\frac{dN_{etoh}}{dt} = F_{in}C_{etoh,in} - (F_{out} + k_{evap}V)C_{etoh,out} + q_{etoh}C_X V \quad (3.2)$$

wherein k_{evap} is the ethanol evaporation rate expressed as mole of ethanol evaporated per mole of ethanol present in the vessel per hour. The rate of ethanol evaporation was experimentally determined for the chemostat cultivation conditions applied and was assumed to change with temperature (*T*) according to the Arrhenius law (Chapter 2):

$$k_{evap} = 5.74\times10^2.e^{\frac{-3510}{T+273.15}} \quad (3.3)$$

For the CO_2 balance, and since the chemostat was run under anaerobic conditions, it was assumed that the off gas was composed only of nitrogen and carbon dioxide. Measurements of the O_2 content in the dried off-gas never showed values above 0.002% (data not shown) indicating that the above assumption is correct. Therefore, the volumetric fraction of N_2 in the off gas ($x_{N_2}^{out}$) could be calculated according to:

$$x_{N_2}^{out} = 1 - x_{CO_2}^{out} \quad (3.4)$$

Because nitrogen is not metabolized under these experimental conditions, the inflow of gaseous nitrogen ($\psi_{N_2}^{in}$ in $L_{N2}.h^{-1}$) will be the same as its outflow from the fermentor:

$$\psi_{N_2}^{in} = \psi_{N_2}^{out} \Leftrightarrow \psi_{gas}^{in}.x_{N_2}^{in} = \psi_{gas}^{out}.x_{N_2}^{out} \quad (3.5)$$

The flux of gas leaving the fermentor (ψ_{gas}^{out}) in L.h^{-1} was calculated from equations (3.4) and (3.5), and taking into account that the inflow gas only contained nitrogen ($x_{N_2}^{in} = 1$) as:

$$\psi_{gas}^{out} = \frac{\psi_{gas}^{in}}{\left(1 - x_{CO_2}^{out}\right)} \quad (3.6)$$

To convert the gas flow from L.h^{-1} to mmol.h^{-1} the ideal gas law was applied to normal gas conditions (273.15 K and 100 kPa). So 1 mmol of gas is equivalent to 0.022473 L of gas. The q_{CO2} was then calculated according to the gas-phase CO_2 balance, where N_{CO2} is the total amount of CO_2 (mmol).

$$\frac{dN_{CO_2}}{dt} = \frac{\psi_g^{out} x_{CO_2}^{out}}{22.473 \times 10^{-3}} + q_{CO_2} C_X V \quad (3.7)$$

The feed rate of the chemostat, in kg.h^{-1}, was calculated from the total mass balance as:

$$F_{in} = F_{out} - F_{base} + \psi_{CO_2} \quad (3.8)$$

F_{out} is the gravimetrically determined effluent flow, ψ_{CO2} is the mass of carbon dioxide leaving the fermentor, F_{base} is the mass flow of base added during the fermentation to maintain pH 5.0. The rates of water and ethanol evaporation were negligible when compared to the other terms of this total mass balance. Therefore, they were not included in this calculation. For conversion of the obtained feed flow from kg.h^{-1} to L.h^{-1} the specific gravity of the feed medium was assumed to be equal to one, using water as the reference fluid.

In the previous chapter it was found that the anaerobic stoichiometry of growth of *S. cerevisiae* in batch cultures did not change significantly with temperature between 12 and 30 °C. Therefore q_S was defined as the only temperature-dependent rate, while all other production rates, including growth rate, were calculated by multiplying its experimental yield (mol$_i$.mol$_S^{-1}$) with the absolute value of the biomass specific glucose consumption rate:

$$q_i = Y_{iS}.\left|q_S\right| \quad (3.9)$$

For q_S, hyperbolic-substrate uptake kinetics was assumed with $q_{S,max}$ as the only temperature-dependent parameter and K_S assumed as temperature independent:

$$q_S\left(T,S\right)=q_{S,\max}(T)\cdot\frac{S}{K_S+S} \tag{3.10}$$

The relation between $q_{S,max}$ and temperature was described by an empirical function (Ratkowsky *et al.*, 1982) as:

$$q_{S,\max}=b^*(T-T_{\min})^2 \tag{3.11}$$

T is temperature in °C and b^* and T_{min} are the empirical parameters from the Ratkowsky model in, respectively $mmol.g_{DW}^{-1}.h^{-1}.°C^{-2}$ and °C. Model simulations and parameter estimations were carried out with gPROMS v3.2.0 (Process Systems Enterprise, London, UK). The initial conditions (extracellular concentrations) and experimental-design parameters, such as F_{in} or V, were set to the values experimentally determined during the chemostat cultivations. The temperature profiles shown in **Figure 3.1** were given as input to the model. More details on the model can be found in the appendix (page 71).

Results

Temperature impact on growth stoichiometry: glucose limited versus glucose excess conditions

S. cerevisiae was grown in anaerobic glucose-limited chemostat cultures at a dilution rate of 0.03 h^{-1} and temperatures of 12 and 30 °C. The experimental data showed that the carbon and degree of reduction recoveries were close to 100%, allowing performing data reconciliation analysis. The results, in terms of reconciled concentrations and calculated yields of biomass and (by)products on glucose, are presented in **Table 3.1.**

For the majority of the measured compounds no significant differences in yields were observed between 12 and 30 °C chemostats. Only the yields for acetate and succinate were significantly different, whereby the acetate yield was higher at 12 °C and the succinate yield was lower. Nevertheless, these differences are small compared to the total molar amount of glucose converted, i.e. 0.5% and 0.2 % for acetate and succinate respectively.

The same trend was also observed under glucose excess conditions (anaerobic batch cultivations). The stoichiometry of growth and (by)product formation appeared independent of the cultivation temperature in the range 12 – 30 °C for the major compounds (**Figure 3.2**). The exceptions in batch conditions were acetate and glycerol yields on glucose, which appeared temperature dependent under glucose-excess conditions.

A comparison of the yields obtained for the two substrate-availability regimes shows that the biomass yield on glucose is the only stoichiometric parameter that is the same for both cultivation conditions. In glucose-limited conditions the ethanol and CO_2 yields were slightly higher compared to glucose excess conditions. This increase is stoichiometrically compensated by lower yields of glycerol and organic acids such as pyruvate and lactate (see appendix, page 74).

Table 3.1: *Reconciled extracellular concentrations and yields on substrate obtained in glucose-limited anaerobic chemostats at 12 and 30 ℃ and dilution rate of 0.03 h^{-1}. The standard errors refer to the average data of two independent chemostats.*

Metabolite	C_{out} (mM)		$Y_{i/S}$ ($mol_i.mol_{gluc}^{-1}$)	
	12 °C	**30 °C**	**12 °C**	**30 °C**
Glucose	2.33 ± 0.17	0.20 ± 0.02	---	---
Biomass [a]	2.13 ± 0.06	1.97 ± 0.14	0.58 ± 0.01	0.54 ± 0.02
CO_2 [b]	0.74 ± 0.01	0.68 ± 0.01	1.72 ± 0.05	1.74 ± 0.08
Ethanol	227 ± 4	207 ± 5	1.63 ± 0.05	1.65 ± 0.08
Glycerol	17.5 ± 0.5	17.9 ± 0.5	0.122 ± 0.004	0.122 ± 0.006
Acetate	2.4 ± 0.3	0.47 ± 0.03	0.0167 ± 0.0014	0.0033 ± 0.0004
Succinate	0.28 ± 0.01	0.59 ± 0.05	0.0019 ± 0.0001	0.0043 ± 0.0003
Pyruvate	0.21 ± 0.01	0.17 ± 0.02	0.0015 ± 0.0001	0.0013 ± 0.0001
Lactate	1.07 ± 0.11	0.78 ± 0.02	0.0075 ± 0.0006	0.0069 ± 0.0006

[a] concentrations expressed in g/kg.

[b] concentrations expressed as volume percentage of CO_2 in the off-gas.

Experimental results from dynamic temperature perturbations

The stoichiometric differences observed between glucose-limited and glucose-excess conditions raised the question if the temperature impact on

metabolism would be similar or deviate for both substrate availability regimes.

This question is particularly complex to answer for glucose-limiting chemostat conditions, because temperature perturbations will also induce changes in the residual glucose concentration (**Table 3.1**). To discriminate between the impact of temperature and residual glucose concentration on the anaerobic metabolism of *S. cerevisiae,* different experiments with dynamic temperature conditions were designed and applied to glucose-limited anaerobic chemostats (**Figure 3.1**). Because the duration of the temperature perturbations was not longer than three hours and the dilution rate was maintained at a low value (0.03 h^{-1}), it is unlikely that there were significant variations in enzyme levels during the temperature perturbations (Helbig *et al.*, 2011).

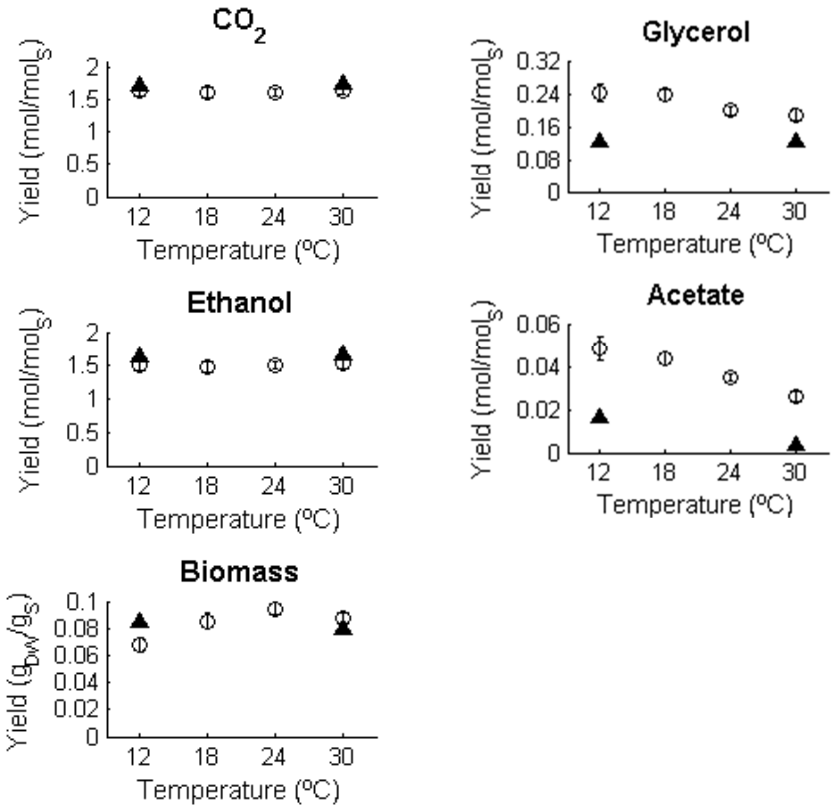

Figure 3.2: *Yields on glucose obtained in the chemostats at 12 and 30 ℃ (▲) compared to the values obtained in batch cultivations from Chapter 2 at 12, 18, 24 and 30 ℃ (○).*

The extracellular concentration profiles of glucose, ethanol, CO_2, glycerol and acetate measured during the different temperature-perturbation experiments are shown in **Figure 3.3.** As already observed during steady-state conditions at 12 and 30 °C, the residual glucose concentration displays an opposite behaviour compared to the temperature profile applied. Because during chemostat cultivations the metabolic fluxes are constrained by the dilution rate imposed, a decrease in glucose transport capacity caused by lower temperatures will be compensated by an increase of the extracellular glucose level.

Experiment C30 was designed to cover the broadest range of extracellular glucose concentrations, allowing in the end to obtain values from 0.20 to 7 mM. Experiments A30, A12 and B30 showed similar changes in residual glucose concentration (0.2 to 2 mM). Although this is a narrower range of concentrations compared to experiment C30, it represents still a considerable 10-fold difference between highest and lowest concentration.

Because the CO_2 production rate, and thus the amount of CO_2 in the off-gas, is proportional to the flux through central carbon metabolism, it can be inferred from the profiles shown in **Figure 3.3** that in experiments B30 and C30 the flux changes were larger (about eight fold) than for experiments A30 and A12 (approximately five fold). This was caused by the accumulation of glucose during the period the culture was kept at a constant temperature of 12 °C after the shift down from 30 °C, and subsequent consumption at a high rate when the temperature was rapidly increased back to 30 °C.

These results show that the experimental design was successful in achieving large fold changes in both fluxes and residual glucose concentrations. But, so far, only limited conclusions can be drawn from a qualitative analysis of the experimental data, because the effects of glucose limitation and temperature are known to be non-linear. Therefore, they cannot be separated by intuition. For instance, it is not immediately clear why in experiment C30 the residual glucose concentration accumulates to levels so much higher than in the 12 °C steady-state reference in experiment A12. Also some of the profiles obtained do not show a direct correlation between temperature of the broth and metabolite levels. The acetate levels for example, increased only during periods where the temperature increased while no significant changes were observed during periods where the temperature was maintained at 12 °C (perturbations B30 and C30). Therefore, changes in acetate levels could neither be immediately correlated

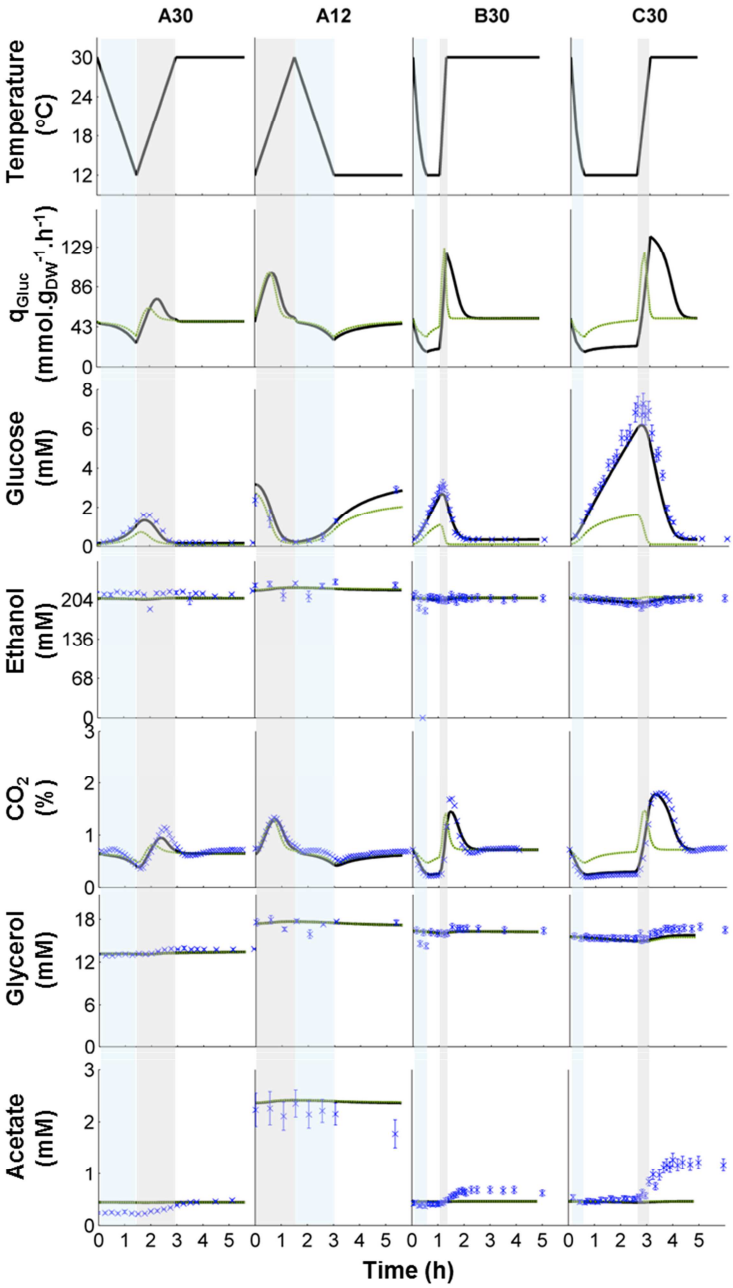

Figure 3.3: *Glucose uptake rate and extracellular concentrations of the most relevant metabolites obtained by experimental measurements (x) or by model simulations for the four temperature perturbations shown in Figure 3.1. In green are the simulated profiles using the Ratkowsky parameters from batch cultivations (Chapter 2) and the substrate-saturation constant determined by Tai et al. (2007a). The black line refers to the simulation with the optimized parameters b^* and K_S.*

to extracellular glucose concentration nor cultivation temperature. As will be shown, more insight can only be obtained from a modeling approach, which allows studying the effects of simultaneous changes in conditions (temperature, residual glucose) on the culture behavior in a more quantitative way.

Results of black-box model assuming constant yields for all products

A black-box model was developed to describe changes in extracellular metabolite levels during the different temperature perturbations applied to glucose-limited chemostat cultivations. Because the changes in yields for which a temperature-dependency was observed (acetate and succinate) represent less than 0.5% (mol/mol$_S$) of the glucose uptake rate, the first version of the black-box model was built with the assumption that the stoichiometry is constant and temperature independent for all products. The reconciled glucose-based yields used to parameterize the model and the concentrations set as initial conditions are presented in **Table 3.1**. The independent variables determined by the experimental setup used (F_{in}, V, S_{in},…) and the temperature profiles with time ($T(t)$) were set to the values described in the "Cultivation Procedures" section (see Materials and Methods for more details). The temperature impact on the maximum glucose uptake rate ($q_{S,max}$) was described by the Ratkowsky equation (3.11), using the temperature parameters as determined for glucose excess conditions in Chapter 2 (T_{min} = 0.22 °C and b^*_{gluc} = 0.0211 mmol.g$_{DW}^{-1}$.h^{-1}.°C^{-2}). Because different glucose transporters are expressed in glucose-limited chemostats at 12 and 30 °C (Tai *et al.*, 2007a), the K_S value was assumed to depend on the temperature of the steady-state chemostat preceding the temperature perturbation, whereby we used the values determined by Tai *et al.* (2007a) for the same experimental conditions as applied in this work. The K_S values were assumed not to change during the fast temperature shifts.

A good fit of the model prediction to the experimental data was obtained for the extracellular glucose profile during the linear temperature shifts applied to the 12 °C chemostat (A12) (green curve in **Figure 3.3**). It was therefore concluded that the parameters of the Ratkowsky model, which were estimated for glucose-excess (batch) experiments, were also valid to describe the effects of dynamic temperature changes under glucose-limited conditions, as applied in experiment A12. However, as can be seen from **Figure 3.3**, the glucose profiles for temperature shifts A30, B30 and C30

were not properly described (green curves). By performing a parameter estimation to obtain the best fit of the model to the measured glucose profiles for these shifts, a value for parameter b^* of 0.0121 ±0.0003 mmol.g_{DW}^{-1}.h^{-1}.°C^{-2} was obtained for biomass cultivated at 30 °C. An attempt to optimize the temperature parameter T_{min} lead to the conclusion that this parameter is the same for all the shifts performed, independently of the initial chemostat temperature or the glucose availability regime. This indicates that cells grown in batch and chemostat fermentations have similar temperature sensitivities.

The optimization of b^* for experiments A30, B30 and C30 caused an improvement of the overall fit of the model to the dynamic data, including CO_2 and ethanol (black curves in **Figure 3.3**).

The obtained profiles of the specific glucose uptake rate explains the large accumulation of residual substrate observed once the temperature was kept constant at 12 ºC for 30 minutes (experiment B30) and 2.5 hours (experiment C30) after the rapid shift down to 30 ºC. Because the glucose transport capacity is lower in the 30 °C chemostats and the biomass yield is temperature independent, the maximum growth rate achievable at 12 ºC is 0.024 h^{-1}. This value is lower than the 0.03 h^{-1} imposed as dilution rate (**Figure 3.4**), causing a partial washout of cells from the fermentor.

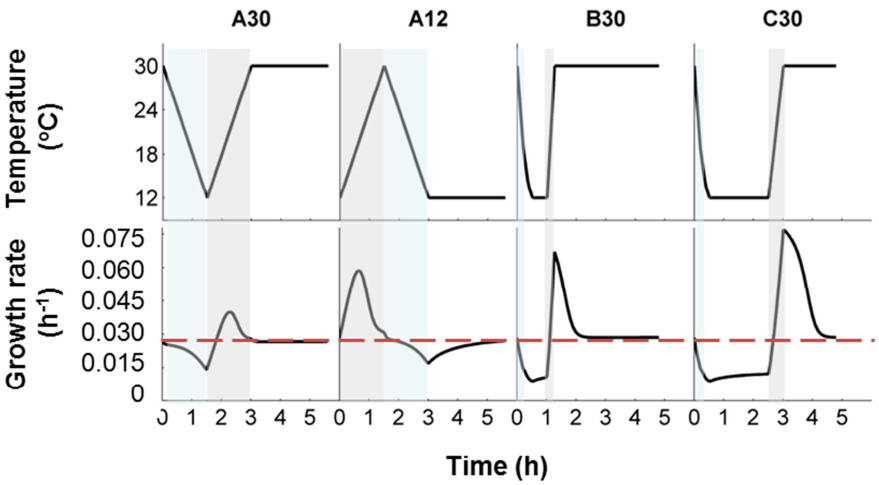

Figure 3.4: *Growth rate profiles achieved during the different temperature-perturbation experiments. The shadow areas indicate time periods where temperature was increasing from 12 to 30 ℃ (grey) or decreasing from 30 to 12 ℃ (light blue). The red line refers to the experimental dilution rate of the chemostat cultivations (0.03 h^{-1}).*

Still there were some profiles for which the model was not providing a satisfactory fit. The profiles of extracellular acetate concentrations were not being reproduced by the simulations and some inconsistencies were observed between the experimental and simulated CO_2 profiles. These last ones could neither be explained based on the temperature impact on CO_2 solubility nor the equilibrium with bicarbonate. The black-box model, as will be shown below, was used to test different hypotheses that could explain these differences.

Results of black-box model considering changes in acetate yields

Acetate production represents a small fraction of the compounds secreted by the cells grown anaerobically and, therefore, changes its conversion rates will have a small impact on the major carbon fluxes (CO_2, ethanol and biomass). However, the discrepancies between the experimental and simulated acetate profiles indicate that the yield on substrate of acetate was not constant during the shift experiments. As already shown in **Figure 3.2**, the acetate yield on substrate increases at lower temperatures, both for batch and chemostat cultivations. But because for the same temperature $Y_{Acet,S}$ is larger in glucose-excess compared to glucose-limited conditions it was not possible only from the steady-state chemostat data to evaluate to which extent glucose concentration, enzyme levels and/or temperature determine acetate production in the cell.

In order to better describe the acetate metabolism, an equation was added to the black-box model that describes $Y_{Acet,S}$ as a function of temperature and the residual substrate concentration (equation (3.12)). The choice for the kinetic format was made empirically from the data in **Table 3.1** and **Figure 3.2**, which pointed to a linear relation between temperature and the acetate yield on substrate, as well as for an activating effect of the residual glucose concentration.

$$Y_{Acet,S} = \left(Y_{Acet,S}^{\max} - \alpha.T \right) \frac{S}{K_{S,Acet} + S} \tag{3.12}$$

The kinetic parameters were estimated by solving the over-determined system of equations composed by equation (3.12) and the yields on substrate for acetate and extracellular glucose concentration of the different experimental setups (batch cultivations at different temperatures and the

steady-state chemostats at 12 and 30 ºC) presented in **Table 3.1** and **Figure 3.2**. The solution that led to the minimum squared-sum of the residues (difference between experimental and estimated values were $Y_{Acet,S}^{max}$ = 0.056 mol.mol$_S^{-1}$, α= 0.85x10^{-3} mol.mol$_S^{-1}$.ºC^{-1} and $K_{S,Acet}$= 3.26 mM. To guarantee that element balances were still satisfied when imposing changes in the stoichiometry of the model, q_{Etoh} and q_{CO2} were calculated from, respectively, the redox and carbon balances.

As it can be seen by the yellow line in **Figure 3.5**, although the trends showed some improvement compared to the model predictions where $Y_{Acet,S}$ was set to be constant (**Figure 3.3**), the results from the model simulation could still not fit satisfactory the experimental measurements once $Y_{Acet,S}$ was set to change as a function of temperature and residual glucose concentration. The underestimation of the acetate concentrations upon the temperature increase from 12 to 30 ºC indicated that the yield change is more pronounced than what predicted from the parameters of equation (3.12).

A new parameter estimation routine was applied to obtain a proper fit of the extracellular acetate concentrations. This time, the kinetic parameters $Y_{Acet,S}^{max}$, α and $K_{S,Acet}$ were obtained by fitting equation (3.12) to the acetate levels measured during the temperature-perturbation experiments A12, A30, B30 and C30 (black line in **Figure 3.5**).

The same set of parameters could be used to describe the acetate metabolism for all temperature perturbations performed ($Y_{Acet,S}^{max}$ = 0.313 mol.mol$_S^{-1}$, α = 5.90 x10^{-3} mol.mol$_S^{-1}$.ºC^{-1} and $K_{S,Acet}$ = 6.50 mM.), independently of the initial steady-state temperature. But the increase in all kinetic parameters, and especially of $Y_{Acet,S}^{max}$, caused an average three-fold increase of the acetate production rates during the dynamic temperature conditions compared to the results from the model with the parameters from steady-state conditions. If these optimized parameters would hold for batch cultivations, the acetate yields would be in average 4.6 times higher than the values determined in Chapter 2. These results, as will be further discussed, indicate the presence of overflow metabolism together with changes in the capacities of enzymes coupled to acetate metabolism between carbon-limited and carbon-excess cultivations.

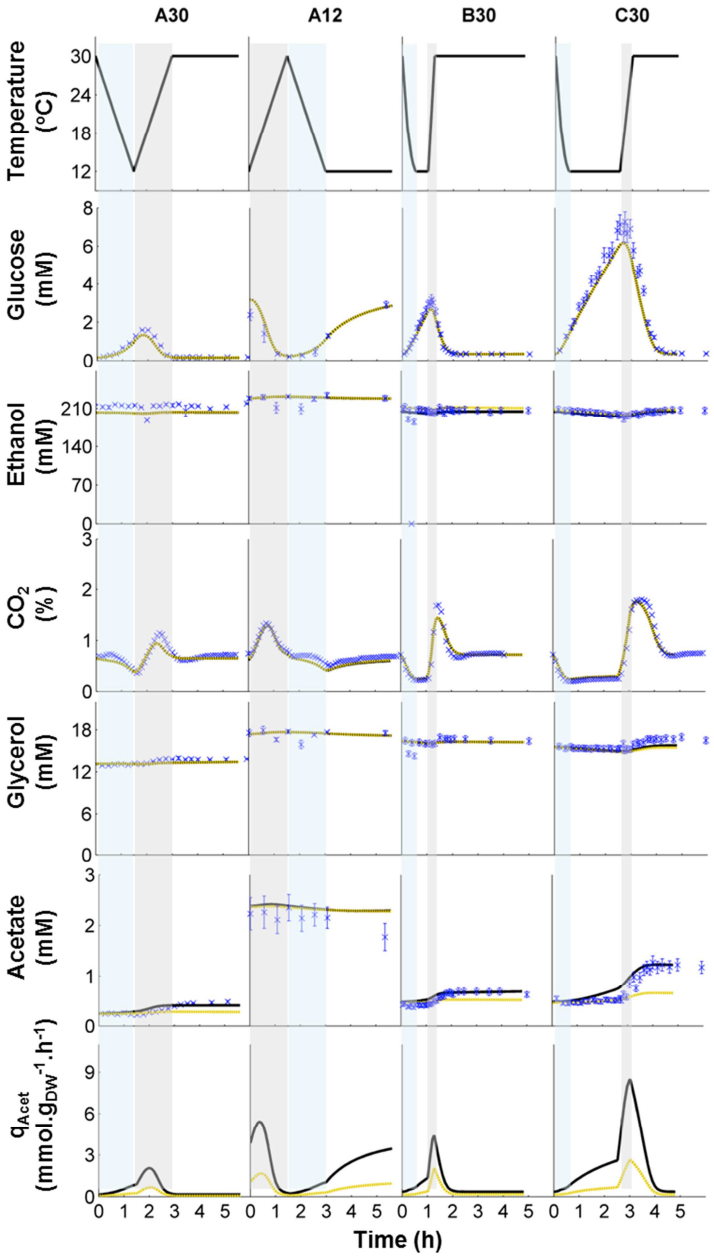

Figure 3.5: *Simulation profiles obtained when the acetate yield changes with temperature and residual substrate concentration according to equation (3.12). (x) experimental measurements; (---) simulated profiles using the parameters estimated from the acetate yields in batch cultivations at different temperatures and the steady-state chemostats at 12 and 30 ℃ (Figure 3.2); (---) simulated profiles using the parameters estimated from the acetate concentrations measured during the temperature-perturbation experiments A30, A12, B30 and C30.*

As expected, the improvements in the simulation results for acetate did not affect the simulation of other metabolite concentrations. As a result, there were still small discrepancies in the CO_2 profiles for which the available data on extracellular metabolite pools did not provide further leads. Therefore it was investigated if temperature related changes in the intracellular space did occur, such as storage-carbohydrate content (trehalose and glycogen), which are reported to play a role in the response to temperature fluctuations. The metabolism of storage carbohydrates could therefore provide an explanation for the remaining small deviations.

Impact of storage carbohydrate metabolism on the overall results of the black-box model

The incorporation of a residual-glucose dependent acetate yield in the model, which led to slight changes in $Y_{CO2,S}$ and $Y_{Etoh,S}$, improved the fitting of CO_2 profiles, namely during the period the temperature was kept at 12 ºC in shifts B30 and C30.

However, there were still misfits of CO2 predictions compared to the experimental measurements in the off-gas (black line of **Figure 3.5**). For instance, the model could not predict the increase of CO2 production during the first 30 minutes of experiment A30, nor the dynamic behavior of the CO2 composition of the off-gas after the sudden temperature increase from 12 to 30 ºC in experiments B30 and C30. An explanation could be the mobilization/accumulation of glycogen and trehalose as a consequence of changing temperature and residual glucose concentration. These two storage carbohydrates are the most relevant carbon-storage pools in S. cerevisiae grown under anaerobic conditions and it has been reported that their levels are highly dependent on temperature and growth rate (for a review see François et al., 2012). The mobilization of storage carbohydrates during temperature shifts could lead to a higher glycolytic flux and, from there, more catabolic products such as CO2.

The intracellular amounts of trehalose and glycogen measured during the different temperature perturbations can be found in **Figure 3.6**. For shifts A30 and A12, both trehalose and glycogen levels decrease with decreasing temperature. However, for shifts B30 and C30, there was no significant change in storage-carbohydrate pools during the fast temperature drop. For these two experiments (B30 and C30), storage mobilization seems to be

mostly dependent on the fast increase of glucose-uptake rate once the temperature of the broth returned to 30 °C at a high residual glucose level. Also the fold change in total storage content was independent of the time that the culture spent at 12 °C or the residual glucose level at the time of the temperature increase. The absence of a coherent behavior of the storage-carbohydrate concentrations between the four different experimental setups suggests that, besides temperature, also the glycolytic flux and/or the residual glucose concentration might be determining the metabolism of glycogen and trehalose.

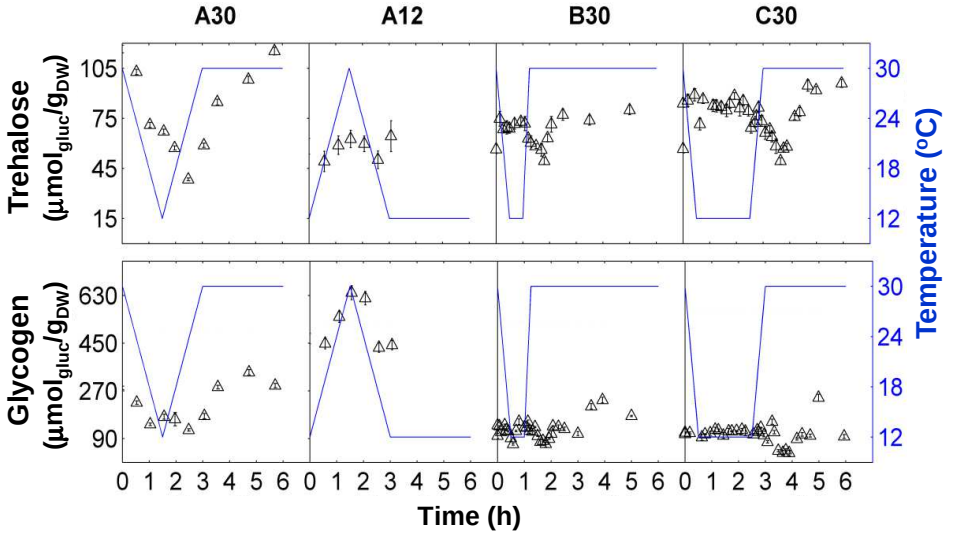

Figure 3.6: *Intracellular amounts of trehalose and glycogen during the different temperature shifts (blue line). Levels are expressed in µmol glucose equivalent per gram dry weight.*

Due to the cycling of these compounds in the cell it was not possible to determine the kinetics of storage metabolism only from concentration measurements of the storage compounds. An increase in the amount of storage compounds can be a consequence of a decrease in degradation rate or an increase in production rate. The degradation of both trehalose and glycogen leads to production of glucose, so a decrease of the levels of storage-carbohydrate metabolites indicates that there is more glucose metabolized into ethanol and CO_2. Shift C30 displays a linear decrease in total storage-carbohydrate amount of about 200 $\mu mol_S/g_{dw}$ between 3.75

and 5h (where temperature is constant at 30 ºC). This corresponds to an additional supply of glucose during this time period at a rate of 0.16 $mmol.g_{DW}^{-1}.h^{-1}$. From the CO_2 production yield it can be calculated that this additional glucose supply from storage mobilization would lead to an increase of the CO_2 production rate with 0.278 $mmol.g_{DW}^{-1}.h^{-1}$. This could explain the 0.2% (v/v) higher CO_2 in the off gas measured for this time period compared to the simulated CO_2 profiles. Therefore, storage dynamics have a significant effect in these dynamic experiments.

Discussion

The strong coupling of temperature, growth rate and residual glucose concentration in glucose-limited conditions hinders the direct interpretation of experimental data from experiments with temperature perturbations. Therefore, kinetic studies on the impact of temperature on metabolism do not frequently deliver more than an empirical analysis of the observed changes in uptake/secretion fluxes and/or extracellular metabolite concentrations. These results are not easily applicable to experimental conditions other than the ones applied. This is often caused by the narrow range of fluxes and concentrations that is obtained from standard experimental setups (e.g. batch and chemostat cultivations) and the lack of a consistent set of measurements that allows establishing proper stoichiometric relations between the substrate consumed and the production of biomass and metabolic (by)products. In previous temperature studies it has not been possible to discriminate between the impact of temperature and other simultaneously changing variables such as growth rate, residual substrate concentration and enzyme levels. This is particularly relevant in substrate-limiting conditions where the extracellular substrate concentration plays an important role in flux regulation. Relevant kinetic studies on the temperature effect on metabolism should be based on large fold changes of fluxes and concentration of the limiting substrate while maintaining the enzyme levels constant.

This study shows that applying different fast temperature perturbations under glucose-limited conditions is a useful approach to separate the impact of temperature from the effect of the extracellular concentration of the limiting substrate on the anaerobic metabolism of *S. cerevisiae*. The resulting broad range of fluxes and metabolite levels obtained in these experiments

allowed accurate estimations of most of the kinetic parameters, which cannot be easily done only from steady-state data.

For instance, in this study it could be shown that the higher acetate yield reported for chemostat cultivations at low temperatures (Pizarro *et al.*, 2008; Tai *et al.*, 2007a) is likely to be a consequence of the positive effect that higher residual glucose concentration and low temperatures have on acetate production. This is consistent with the stoichiometric differences observed between batch and steady-state chemostat cultivations at the same temperature. A similar increase of the acetate yield with increasing dilution rate (and therefore residual glucose concentration) has been reported for anaerobic chemostat cultivations performed at constant temperature (Nissen *et al.*, 1997; Verduyn *et al.*, 1990). However, it could not be determined from these published data if this was a consequence of the increasing glycolytic flux, metabolic regulation or adjustments in enzyme levels. It is generally accepted that this increase in acetate yield is a consequence of overflow metabolism by which the production of by-products from pyruvate branch-points can be increased at high glycolytic fluxes while, at the same time the activity of the enzyme that converts acetate into acetyl-CoA (acetyl-CoA synthetase) is insufficient (Postma *et al.*, 1989). It is unlikely that there were changes in enzyme expression levels during the relatively short time frames of the here reported temperature perturbation experiments (maximum three hours). Therefore, the hyperbolic stimulation of acetate production by residual glucose, leading to overflow of acetate during the temperature-perturbations, must be a consequence of metabolic regulation of one of the intermediate steps (between glucose uptake and acetate production). However, the highest acetate yield obtained during the linear temperature shifts (0.12 mol/mol_S) was 2.4 fold higher that the value measured during batch cultivations at 12 °C. This observation indicates that, in case that overflow metabolism is the only reason for the observed changes in acetate yield during temperature-perturbations in glucose-limited cultivations, the capacity of enzymes coupled to acetate metabolism should be higher under glucose-excess conditions. Further studies on acetate metabolism (namely measurements of the activity of acetyl-CoA synthetase in anaerobic conditions) should help elucidate the role of residual glucose concentration on the overflow metabolism.

No significant differences were found for the yields of ethanol, CO_2, glycerol and biomass on glucose, nor for the acetate production kinetic

parameters ($Y_{Acet,S}^{max}$, α and $K_{S,Acet}$) between the different shifts. It has also been evaluated the hypotheses of glycerol yield being dependent on temperature and/or residual glucose concentration since glycerol metabolism is often coupled to acetate production as a way to balance the redox state of the cell. However, it was not possible to obtain an empirical equation to describe the four different experiments (A30, A12, B30 and C30) with the same set of parameters. For instance, the parameters obtained by fitting an expression for the glycerol yield similar to equation (3.12) to the dataset from experiment C30, would lead to an overestimation of the glycerol profile in experiment A12 of about 1.5 fold (data not shown). Additionally, because the range of glycerol concentrations measured was not very broad, it was not possible to test different sets of kinetic parameters for each individual experiment and this way evaluate if there were changes in enzyme capacities between the different experiments. Therefore, there was not found any indication that the stoichiometry of anaerobic growth is significantly changed by mild-suboptimal temperatures, independently of the glucose availability regime (excess or limitation).

Differences in enzyme expression levels could in some cases be captured from perturbations applied to steady-state cultures grown at different temperatures. By comparing the results from shifts A30 and A12 it was concluded that only the expression of hexose transporters seems to have an impact on the kinetics of the system. The lower value of b^* for the 30 °C chemostats compared to the one obtained for batch cultivations and 12 °C chemostats matches quite well with the decrease in the glucose transport capacity observed by Tai *et al.* (2007a). Because the b^* value for 12 °C chemostats is the same as the one determined for batch experiments at different temperatures, it is possible to conclude from the black-box model results that the change in glucose transport capacity is a consequence of the residual substrate concentration in the chemostat and not temperature. Further experimental support for this conclusion is the observed change in transcripts related to hexose transporters between 12 and 30 °C chemostats and different growth rates at the same temperature. Fazio *et al.* (2008) have determined that the transcripts levels of the high affinity hexose transporters HXT2 and HXT4 are the ones that increase most significantly between a dilution rate of 0.03 and 0.2 h^{-1} whereas HXT5 and HXT16 decreased. The same observation was made by Tai *et al.* (2007a) when comparing 12 °C chemostats (high residual glucose levels) with 30 °C (low

residual glucose). This indicates that it is most likely the extracellular glucose concentration and not temperature that determines the expression of the genes related to substrate transporters.

From all these observations it was possible to construct a temperature-dependent black-box model that describes the temperature dependency of the anaerobic glucose metabolism of *S. cerevisiae* in both glucose-limiting (chemostats) and excess conditions (batch). Some minor differences between simulated and experimental measurements are still observed for CO_2, which are most likely related to complex temperature related changes in storage metabolism. Further developments with respect to kinetic modeling of trehalose and glycogen metabolism are needed to explain the observed deviations. But overall the final model reproduces quite accurately the profiles of extracellular compounds in the broth during fast temperature-shifts experiments. It can also be easily extended to other feeding regimes (e.g. fed-batch) and provides a starting point to study the temperature impact under different substrate limitations (e.g. nitrogen limitation) or different organisms.

Appendices

Description of the developed black-box model

This section resumes the equations and parameters used to construct the final version of the black-box model. Details on the meaning of the different variables and assumptions made can be found in the Materials and Methods (page 53).

Rate equations

$$F_{in} = F_{out} - F_{base} + \frac{x_{CO_2}^{out}}{\left(1 - x_{CO_2}^{out}\right)} \psi_{gas}^{in},$$

$$q_{S,\max} = b^{*}(T - T_{\min})^{2}$$

$$q_S = q_{S,\max} \frac{S}{K_S + S}$$

$$q_{Etoh} = \frac{24q_S - (4.13\mu + 14q_{Glyc} + 8q_{Acet} + 9q_{Lac} + 10q_{Pyr} + 14q_{Suc})}{12}$$

$$q_{CO_2} = 6q_S - (2q_{Etoh} + \mu + 3q_{Glyc} + 2q_{Acet} + 3q_{Lac} + 3q_{Pyr} + 4q_{Suc})$$

$$\mu = Y_{X,S}.q_S$$

$$q_{Glyc} = Y_{Glyc,S}.q_S$$

$$q_{Acet} = Y_{Acet,S}.q_S$$

$$Y_{Acet,S} = \left(Y_{Acet,S}^{\max} - \alpha.T\right)\frac{S}{K_{S,Acet} + S}$$

$$q_{Pyr} = Y_{Pyr,S}.q_S$$

$$q_{Suc} = Y_{Suc,S}.q_S$$

$$q_{Lac} = Y_{Lac,S}.q_S$$

Mass balances

$$\frac{dS}{dt} = F_{in}C_{S_{in}} - F_{out}C_S - q_S C_X V$$

$$\frac{dEtoh}{dt} = F_{in}C_{Etoh,in} - (F_{out} + k_{evap}V)C_{Etoh} + q_{Etoh}C_X V$$

$$k_{evap} = 5.74\times10^2.e^{\frac{-3510}{T(K)}}$$

$$\frac{dCO_2}{dt} = -\frac{\psi_g^{out}x_{CO_2}^{out}}{22.473\times10^{-3}} + q_{CO_2}C_X V$$

$$\frac{dX}{dt} = -F_{out}C_X + \mu C_X V$$

$$\frac{dGlyc}{dt} = -F_{out}C_{Glyc} + q_{Glyc}C_X V$$

$$\frac{dAcet}{dt} = -F_{out}C_{Acet} + q_{Acet}C_X V$$

$$\frac{dSuc}{dt} = -F_{out}C_{Suc} + q_{Suc}C_X V$$

$$\frac{dPyr}{dt} = -F_{out}C_{Pyr} + q_{Pyr}C_X V$$

$$\frac{dLac}{dt} = -F_{out}C_{Lac} + q_{Lac}C_X V$$

Temperature Profiles

The following equations have been used to define the temperature-shift profiles of experiments A30, A12, B30 and C30 (**Figure 3.1**). t is time expressed in hours.

A30

$$for\ t = [0,1.5], \quad T = 30 + \frac{(12-30)}{1.5}t$$

$$for\ t = [1.5,3], \quad T = 12 + \frac{(30-12)}{1.5}(t-1.5)$$

A12

$$for\ t = [0,1.5], \quad T = 12 + \frac{(30-12)}{1.5}t$$

$$for\ t = [1.5,3], \quad T = 30 + \frac{(12-30)}{1.5}(t-1.5)$$

B30

$$for\ t = [0,0.5], \quad T = 30 + \frac{(12-30)}{0.5}t$$

$$for\ t = [0.5,1], \quad T = 12$$

$$for\ t = [1,1.25], \quad T = 12 + \frac{(30-12)}{0.25}(t-1)$$

$$for\ t=[0,0.5],\quad T=30+\frac{(12-30)}{0.5}t$$

C30 $$for\ t=[0.5,2.5],\quad T=12$$

$$for\ t=[2.5,3],\quad T=12+\frac{(30-12)}{0.5}(t-2.5)$$

Yields on substrate obtained for lactate, succinate and pyruvate in batch and chemostat cultivations at different temperatures

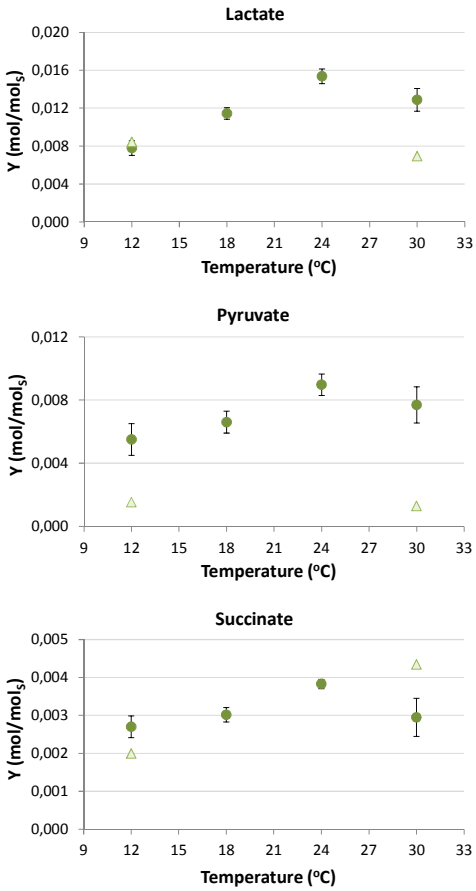

Figure 3.7: *Yields on substrate obtained for lactate, pyruvate and succinate on anaerobic chemostat cultivations at 12 and 30 ℃ (△) compared to the values obtained in anaerobic batch cultivations from Chapter 2 (●).*

4. Temperature impact on the kinetic parameters of glycolytic enzymes

Abstract

Temperature strongly affects microbial growth, and many microorganisms have to deal with temperature fluctuations in their natural environment. To understand regulation strategies that underlie microbial temperature responses and adaptation, we studied glycolytic pathway kinetics in *Saccharomyces cerevisiae* during temperature changes.

Saccharomyces cerevisiae was grown under different temperature regimes and glucose availability conditions. These included glucose-excess batch cultures at different temperatures and glucose-limited chemostat cultures, subjected to fast linear temperature shifts and circadian sinoidal temperature cycles. An observed temperature-independent relation between intracellular levels of glycolytic metabolites and residual glucose concentration for all experimental conditions revealed that it is the substrate availability rather than temperature that determines intracellular metabolite profiles. This observation corresponded with predictions generated *in silico* with a kinetic model of yeast glycolysis, when the catalytic capacities of all glycolytic enzymes were set to share the same normalized temperature dependency.

From an evolutionary perspective, such similar temperature dependencies allow cells to adapt more rapidly to temperature changes, because they result in minimal perturbations of intracellular metabolite levels, thus circumventing the need for extensive modification of enzyme levels.

Introduction

Growth and survival of microorganisms is strongly affected by environmental variables such as temperature, nutrient and oxygen availability, pH and osmolarity. Since, in natural environments, these parameters are highly dynamic, microorganisms have to cope with fluctuating, often non-optimal growth conditions. Suboptimal growth temperatures have major impacts on cell physiology including decreasing membrane fluidity and a reduced efficiency of protein synthesis and folding (Feller and Gerday, 2003; Sahara *et al.*, 2002; Thieringer *et al.*, 1998). In addition, the catalytic capacity of each enzyme in the cell decreases when the temperature is lowered. This temperature impact can, in many cases, be described by an Arrhenius equation (Russell *et al.*, 1990).

In the past decade, the response of the mesophilic yeast *Saccharomyces cerevisiae* to suboptimal temperatures has been the focus of several studies (Beltran *et al.*, 2008; Pizarro *et al.*, 2008; Tai *et al.*, 2007a). Interest in this subject is motivated by the biotechnological applications of *S. cerevisiae*. In particular, brewing and winemaking are two processes in which yeast is subjected to suboptimal temperatures (typically 12 to 15 °C) to obtain specific desired flavor compounds (Pizarro *et al.*, 2008; Redon *et al.*, 2011). Moreover, its experimental accessibility to genome-scale analysis makes *S. cerevisiae* an attractive model organism for systems biology studies on temperature responses. With a few exceptions (Sahara *et al.*, 2002; Schade *et al.*, 2004), studies on low temperature responses of *S. cerevisiae* have focussed on so-called cold shock experiments. In such experiments, instantaneous exposure to low temperatures triggers a general environmental stress response in addition to temperature-specific responses (Al-Fageeh and Smales, 2006; Homma *et al.*, 2003; Murata *et al.*, 2006; Sahara *et al.*, 2002; Schade *et al.*, 2004). To investigate long-term acclimation rather than rapid adaptation to low temperature, thereby preventing a cold shock effect, growth of *S. cerevisiae* has been studied at 30 and 12 °C in anaerobic glucose-limited chemostat cultures (Tai et al, 2007a). Since the maximum specific growth rate of *S. cerevisiae* at 12 °C is circa sevenfold lower than at 30°C (Cruz *et al.*, 2012; Tai *et al.*, 2007a), a low dilution rate of 0.03 h^{-1} was used for both temperatures in this chemostat study (Pizarro *et al.*, 2008; Postmus *et al.*, 2008; Tai *et al.*, 2007a). In anaerobic cultures, substrate-level phosphorylation in glycolysis is the sole mechanism for ATP synthesis. *Tai et al.* (2007a) observed that, despite substantially lower

specific catalytic capacities of the glycolytic enzymes at 12 °C as compared to 30 °C, chemostat cultures maintained the same glycolytic flux at these two temperatures. Because in these chemostat cultivations the growth rate was set to be the same for both conditions (0.03 h^{-1}), this indicated that the biomass yield was the same for both temperatures. Moreover, yeast did not compensate for the lower temperature by increased synthesis of glycolytic enzymes. Instead, metabolic regulation, i.e., regulation by changes in the concentrations of substrates, products and effectors (Ter Kuile and Westerhoff, 2001) was identified as the main strategy for temperature compensation. Especially for highly expressed pathways such as glycolysis, whose enzymes can account for up to 20% of the protein content of *S. cerevisiae*, repeated cycles of protein degradation and synthesis would represent a substantial burden. It was therefore hypothesized that the observed dominant role of metabolic regulation represents an evolutionary adaptation to environments with frequent (e.g. circadian) temperature fluctuations (Tai *et al.*, 2007a).

Nevertheless, physiological studies carried out at tightly controlled constant temperatures or during very fast temperature changes (e.g. cold or heat shock experiments) represent artificial conditions, considering that many microorganisms are exposed to circadian and seasonal temperature fluctuations in their natural habitats. Evolution in such habitats is likely to have resulted in regulatory strategies to optimize performance under dynamic temperature regimes. Analyzing and understanding such strategies is a typical systems biology challenge, and requires integration of biological experiments with mathematical modeling (Bruggeman and Westerhoff, 2007; Heinemann and Sauer, 2010; Westerhoff *et al.*, 2009).

The aim of this study is to identify and understand mechanisms employed by *S. cerevisiae* to control glycolytic flux and intracellular metabolite levels under dynamic temperature regimes. To this end, we investigated the impact of dynamic temperature regimes with different time constants (**Figure 4.1**) using a systems approach, integrating mathematical modeling and experimentation. Our results indicate that if the temperature dependencies of the catalytic capacities of enzymes in a pathway are highly similar, changes in metabolite levels during temperature changes are minimal.

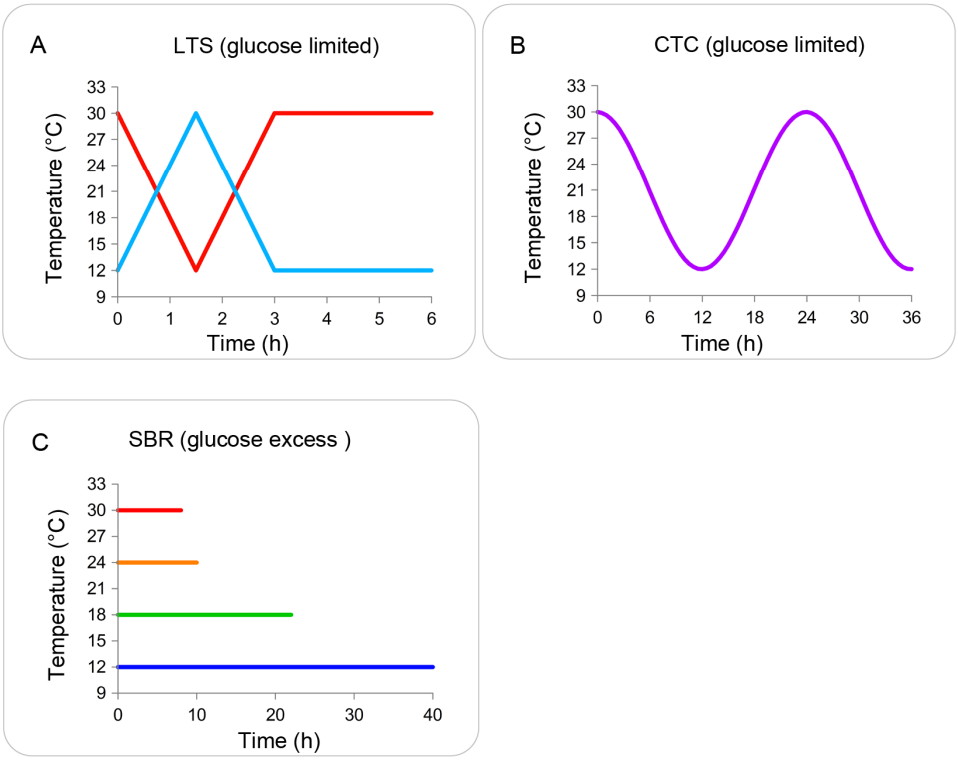

Figure 4.1: *Temperature profiles applied to the different simulations and experiments. (A) Linear temperature shifts (LTS) from 12 ℃ (blue) or 30 ℃ (red) applied to steady-state chemostats; (B) circadian temperature cycles (CTC) in glucose-limited chemostat cultures; (C) Sequential batch reactors (SBR) operated at different temperatures.*

Methods

Model description

The published kinetic model for yeast glycolysis (Teusink *et al.*, 2000) was developed to simulate a buffered cell environment where growth is absent and extracellular concentrations are constant. These constraints and the fact that this model was solely based on kinetic parameters that were estimated from *in vitro* experiments, render it unstable in simulations of dynamic conditions. To avoid stability problems when incorporating temperature changes and to better mimic the experimental setups applied in this study, several adjustments were made to the original model.

To enable simulation of scenarios in which extracellular concentrations are highly dynamic, mass balances for glucose, ethanol, glycerol and succinate were included in the model, according to equation (4.1):

$$\frac{dN_i}{dt} = q_i N_X(t) + F_{in}C_{i,in} - F_{out}C_{i,out}(t), \quad (4.1)$$

Equation (4.1) indicates how the amount of component *i* in the broth ($N_i(T)$) will change based on its biomass specific production or consumption rate (q_i) and the amount of biomass present in the broth ($N_X(T)$). The terms $F_{in}C_{i,in}$ and $F_{out}C_{i,out}$ refer to transport of the component via, respectively, the inlet and outlet streams of the fermenter. F is the flow rate ($L.h^{-1}$) whereas C_i (mM) is the concentration of component *i* in each stream. The parameters were set to be the same as in the experimental setup. The ethanol evaporation rate was taken into account in the mass balance of this compound following the same approach as in Chapter 3.

Temperature was included in the model by replacing the different catalytic activities by a temperature dependent function. In a previous study, the Ratkowsky model (Ratkowsky *et al.*, 1982; equation (4.2)) was found to better describe the temperature impact on metabolic fluxes in anaerobic, glucose-excess cultures of *S. cerevisiae* grown at temperatures between 12 to 30 °C than the Arrhenius law (Chapter 2). Therefore, the Ratkowsky model was used as the temperature-dependent function $R_i(T)$ with the parameters obtained in Chapter 2.

$$V_{\max,j}(T) = b_j(T - T_{\min})^2 \quad (4.2)$$

At temperatures between 12 and 30 °C, temperature has little impact on the yields of biomass and fermentation products in anaerobic *S. cerevisiae* cultures (Chapters 2 and 3). Therefore the stoichiometric coefficient b_j for each reaction was calculated from the ratio of its flux and the glucose uptake rate ($v_{consumption}$) in the original conditions of the Teusink model (30 °C):

$$b_j = b_{Glc}\frac{v_j^{30°C}}{v_{consumption}^{30°C}} \quad (4.3)$$

The model was implemented and run in gPROMS (Process Systems Enterprise).

Strain and growth conditions

Saccharomyces cerevisiae CEN.PK113-7D Mat**a** (Entian and Kötter, 2007; Nijkamp *et al.*, 2012) was grown anaerobically in medium containing 0.3 $g.L^{-1}$ of $(NH_4)_2SO_4$, 0.3 $g.L^{-1}$ of $K_2H_2PO_4$, 3.0 $g.L^{-1}$ $NH_4H_2PO_4$, 0.5 $g.L^{-1}$ $MgSO_4.7H_2O$, 0.4 $g.L^{-1}$ of Tween 80, 10 mg. L^{-1} ergosterol and glucose (25 $g.L^{-1}$). The medium was supplemented with 1 $ml.L^{-1}$ each of a trace element solution and a vitamin solution (Verduyn *et al.*, 1990) as well as with 0.15 $g.L^{-1}$ of antifoam (Silcolapse 5020, Bluestar Silicones, St. Fons, France).

The sequential batch experiments were performed in 1L fermenters with a working volume of 750 ml, whereas 2L fermenters were used for chemostat cultivation (Applikon, Schiedam, The Netherlands). The working volumes for linear-temperature-shifts (LTS) and circadian-temperature-cycles (CTC) experiments were 1.0 and 1.4 L, respectively. The stirring speed was set at 600 rpm for all cultures and the pH was controlled to 5.0 through automatic addition of 2.0 M KOH or 2.0M of H_2SO_4 using a Biostat Bplus controller (Sartorius BBI Systems, Melsungen, Germany). The impact of temperature on the pH measurement was taken into account by sensor calibration. In order to avoid oxygen diffusion into the cultures, Norprene tubing was used for all connections and both medium vessel and fermenter were continuously sparged with pure nitrogen gas (N_2) at a flow rate of 0.35 vvm via an Ion Science Saga digital flow meter (Cambridge, UK).

An overview of the different temperature studies made is given in **Figure 4.1**. For the experiments in glucose excess conditions (SBR), two sequential batch cycles were run at each temperature (30, 24, 18 and 12 °C) before samples were taken in the third cycle, to assure that cells were fully adapted to the new temperature (Chapter 2). Duplicate samples were taken at three different time points of the exponential phase for each temperature.

The linear-temperature-shifts (LTS) and circadian-temperature-cycles (CTC) experiments were performed in glucose-limited cultures grown at a dilution rate of 0.03 h^{-1}. After 5 residence times at constant temperature (30 or 12 °C), the temperature in LTS experiments was linearly increased or decreased at a rate of 0.2 $°C.min^{-1}$. Samples were taken when temperature reached 30, 24, 18 and 12 °C and up to 3 h after the temperature returned to the initial set-point. The temperature profiles in the SBR and LTS experiments were defined and controlled via the MFCS/ win 2.1 software (Sartorius BBI Systems, Melsungen, Germany)

For CTC-experiments, a pre-programmed sinoid temperature profile (temperature (°C) = 21+9sin(π/12·t (h) +1.57) was started after 3 residence times at a constant temperature of 30 °C. This profile was designed to mimic a circadian temperature cycle. Low-temperature thermostats (Lauda RE304, Lauda-Königshofen, Germany) ensured that the temperature was precisely controlled throughout the experiments. Samples were taken during the 5th and the 6th temperature cycle, by which time carbon dioxide profiles and metabolite concentrations during consecutive cycles were highly similar. To minimize disturbance, sampling volumes did not exceed 5 % of the reactor volume during a single temperature cycle and minimum intervals of 3 h were maintained between sampling points.

Analytical methods

Extracellular glucose was measured in 2 ml of broth samples, rapidly taken with syringes containing steel beads at -20 °C (Canelas *et al.*, 2008). The number of beads was adjusted for each initial broth temperature, such that the temperature of all samples would decrease instantaneously to 1 °C. Residual glucose concentrations were measured via high-performance liquid chromatography with a Bio-Rad Aminex HPX-87H column at 60 °C. The column was eluted with 5 mM phosphoric acid at a flow rate of 0.6 ml.min^{-1}. Glucose was detected with a Waters 2410 refractive index detector. Biomass dry weight was measured in duplicate samples as described in Mashego *et al.* (2005).

Intracellular metabolite samples were taken by withdrawing 1.2 ml of broth directly to 6 ml of 100% methanol at -40 °C via a rapid sampling setup. Samples were washed with cold methanol and extracted with boiling ethanol as described in Canelas *et al.* (2008). The concentrations of glucose-6-phosphate (G6P), fructose-6-phosphate (F6P), fructose-1,6-bisphosphate (FBP), phospho-*enol*-pyruvate (PEP), glycerol-3-phosphate (G3P), malate (MAL), fumarate (FUM), succinate (SUC), α-ketoglutarate (αKG), citrate (CIT), glucose-1-phosphate (G1P), UDP-glucose (UDPgluc), trehalose-6-phosphate (T6P), mannose-6-phosphate (M6P), 6-phosphogluconate (P6G) and sedoheptulose-7-phosphate (S7P) were measured by LC-MS according to the protocol developed by Van Dam *et al.* (2002). The nucleotide concentrations (ATP, ADP and AMP) were measured according to Seifar *et al.*

(2009). Uniformly labeled ^{13}C-cell-extract was applied in both analytical platforms as internal standard (Wu *et al.*, 2005.)

In vitro enzyme assays of the glycolytic enzymes were performed with freshly prepared cell extracts on a Hitachi model 100-60 spectrophotometer at 30 °C and 340 nm (ε_{340} of reduced pyridine-dinucleotide cofactors 6.3 mM^{-1}). All enzymes were assayed as described previously (Jansen *et al.*, 2005) with the exception of phosphofructokinase (PFK; EC 2.7.1.11), which was assayed according to De Jong-Gubbels *et al.* (1995), with minor modifications. The assay mixture contained: imidazole/HCl (pH 7.0) 50 mM, $MgCl_2$ 5 mM, NADH 0.15 mM, fructose 2,6-diphosphate 0.10 mM, aldolase (EC 4.1.2.13) (Sigma) 2.1 $U.ml^{-1}$, α-glycerophosphate dehydrogenase-triosephosphate isomerase, 1.2 U ml^{-1} and 12.4 $U.ml^{-1}$, respectively (Sigma) and cell extract. After recording background activity with 0.5 mM fructose 6-phosphate, the reaction was started with 1.0 mM ATP. All assays were performed at two concentrations of cell extract. Specific activities in duplicate experiments differed by less than 12 %. Enzyme activities are expressed as μmol substrate converted per min per mg protein ($U.mg_{protein}^{-1}$). Protein concentrations in cell extracts were determined according to Lowry *et al.* (1951), using dried bovine serum albumin (fatty-acid free; Sigma) as the standard.

Results

A minimal model to describe temperature dependency of metabolic fluxes

To understand and model the impact of temperature dynamics on metabolic fluxes, it is essential to consider the influence of temperature on the kinetic parameters of enzyme-catalyzed reactions. The *in vivo* rate of an enzyme-catalyzed reaction depends on the concentration of the enzyme (e), its specific catalytic capacity (k_{cat}), the affinities of the enzyme for substrates, products, co-factors and/or inhibitors (usually represented by the saturation constants K_P, K_S or K_E) and the thermodynamic equilibrium constant (K_{eq}) (equation (4.4)).

$$v = e.k_{cat}.f\left(K_P, K_S, K_E, S, P, E\right).\left(1-\frac{\Gamma}{K_{eq}}\right) \tag{4.4}$$

In this rate equation, the specific format of the mechanistic kinetic function $f(K_P,K_S,K_E,S,P,E)$ depends on the catalytic mechanism of the reaction. The mass-action ratio (Γ) only depends on the stoichiometry and thermodynamic properties of the reaction (Hess and Brand, 1965).

Three main questions need to be addressed when modeling the impact of temperature on metabolic networks:

1. Which kinetic parameters are temperature dependent?
2. How can temperature dependency be described for those who are?
3. Can the same mechanism be applied to all enzymes?

It is well know that each enzyme has an optimum temperature at which its catalytic capacity (k_{cat}) is maximal, while k_{cat} decreases at values below and above the optimum temperature (for a review see Feller and Gerday, 2003). Quantitative relations, describing the impact of temperature on k_{cat}, can be established by *in vitro* activity measurements at different temperatures and at saturating reactant concentrations. There are, however, only few data available on *in vitro* enzyme activity measurements at different temperatures for yeast glycolytic enzymes. A recent study focused on only two different temperatures (12 and 30 °C), thus precluding the derivation of a proper quantitative relation for the temperature dependency of k_{cat} (Tai *et al.*, 2007a).

Even when information about *in vitro* temperature-dependencies of enzymes was available, this would not necessarily provide an accurate reflection of the *in vivo* situation Teusink *et al.*, 2000. Analysis of the temperature impact on enzyme levels (e) needs to be done carefully, since these are intrinsically context dependent. For example, glycolytic enzyme levels in *S. cerevisiae* are strongly influenced by specific growth rate (Van Hoek *et al.*, 2000), nutrient limitation regimes (Van den Brink *et al.*, 2008) and number of generations (Mashego *et al.*, 2005). Tai *et al.* (2007a) minimized these influences by growing *S. cerevisiae* in anaerobic chemostat cultures at 12 and 30 °C under otherwise identical conditions. Under these conditions, the glycolytic flux was the same for both temperatures and the levels of glycolytic enzymes were found to be very similar (average absolute fold change 1.5 ± 0.1) at both temperatures. In the same experiments, k_{cat}, estimated from *in vitro* enzyme assays, was 3.9 ± 0.5 fold lower at 12 °C than at 30 °C. It was therefore inferred that changes in enzyme levels are not the primary regulation mechanism used by cells to, at equal flux, compensate for the loss of catalytic capacity at lower temperatures. Similar conclusions were

drawn by Postmus *et al.* (2008), when studying the impact of supraoptimal temperatures on the regulation of glycolytic flux in aerobically grown *S. cerevisiae*.

Changes in temperature might also affect the equilibrium constants of reactions and the binding affinities of enzymes. The temperature impact on the equilibrium constant K_{eq} is described by the Van 't Hoff equation (equation (4.5)).

$$\ln\left(\frac{K_{eq,2}}{K_{eq,1}}\right) = \frac{\Delta H_r^0}{R}\left(\frac{1}{T_1} - \frac{1}{T_2}\right) \tag{4.5}$$

When applying this equation, it can be found that the changes of the equilibrium constants for the glycolytic reactions differ by less than twofold (in average change 1.2 ± 0.2) for temperatures between 12 and 30 °C (**Table 4.1**).

Table 4.1: *Thermodynamic equilibrium constants (K_{eq}) of selected glycolytic reactions at 12 and 30 °C. K_{eq} values were calculated from Alberty, 2003 considering a reference condition of 298.15 K, I = 0.25M and pH 7.0. The fold change refers to the ratio $K_{eq}^{12\ °C}/K_{eq}^{30\ °C}$.*

Enzyme	Abrev.	K_{eq}		Fold change
		12 °C	30 °C	
Hexokinase	HXK	7.7×10^{3}	3.5×10^{3}	0.45
Phosphoglucose isomerase	PGI	0.27	0.29	-0.93
Phosphofructokinase	PFK	5.0×10^{3}	2.4×10^{3}	2.08
Fructose-1,6-biphosphate aldolase	FBA	9.3×10^{-4}	1.4×10^{-3}	-1.51
Triosphosphate isomerase	TPI	0.040	0.048	-1.20
Glyceraldehyde-3-phosphate dehydrogenase	TDH	0.66	0.69	-1.05
Phosphoglycerate kinase	PGK	20	16	1.25
Phosphoglycerate mutase	PGM	0.074	0.087	-1.18
Enolase	ENO	5.1	4.5	1.13
Pyruvate kinase	PYK	3.9×10^{4}	1.4×10^{4}	2.79

Based on a mechanistic description (Feller and Gerday, 1997), it can be assumed that temperature has a minor impact on the binding affinities of the enzymes, because they are a measure of the equilibrium between the

enzyme and the enzyme-substrate complex. Furthermore, temperature changes within the mesophilic range (10 to 40 °C) do not result in major structural alterations of the active sites of enzymes from mesophilic microorganisms (Feller, 2010; Hazel and Prosser, 1974). Therefore, changes in binding affinities caused by temperature-induced structural changes are expected to be negligible. In the mesophilic range, temperature induced changes in the glycolytic flux are therefore mainly caused by changes of k_{cat}, because this effect is by far the largest and works in the same direction for all enzymes. Consequently, the temperature sensitivity of k_{cat} for the different enzymes in a network will determine its overall response to dynamic temperature conditions.

This raises the key question whether the catalytic capacities of all enzymes of a pathway would have different or identical temperature dependencies. Consider for instance the following simple linear pathway where *A* and *B* are intracellular metabolites, while *S* and *P* are extracellular:

$$S \xrightarrow{v_1} A \xrightarrow{v_2} B \xrightarrow{v_3} P \tag{4.6}$$

Under steady-state conditions (no accumulation of metabolites) all fluxes are the same, i.e. $v_1 = v_2 = v_3$. This can be formally written by a system of equations (4.7), representing the steady-state balances of intracellular metabolites *A* and *B*, where *N* is the matrix containing the stoichiometric coefficients of the reactions.

$$\begin{bmatrix} 1 & -1 & 0 \\ 0 & 1 & -1 \end{bmatrix} \cdot \begin{bmatrix} v_1 \\ v_2 \\ v_3 \end{bmatrix} = \begin{bmatrix} 0 \\ 0 \\ 0 \end{bmatrix} \leftrightarrow N \cdot \begin{bmatrix} v_1 \\ v_2 \\ v_3 \end{bmatrix} = 0 \tag{4.7}$$

Taking into account that the fluxes v_i can be described by rate equations of the form of equation (4.4), the system of two metabolite balances becomes, for a reference temperature (T_0):

$$\mathbf{N} \cdot \begin{bmatrix} e_1 \cdot k_{cat,1}^{T_0} \cdot f(K_A, S, A, K_{eq,1}) \\ e_2 \cdot k_{cat,2}^{T_0} \cdot f(K_A, K_B, A, B, K_{eq,2}) \\ e_3 \cdot k_{cat,3}^{T_0} \cdot f(K_B, B, K_{eq,3}) \end{bmatrix} = \mathbf{0} \tag{4.8}$$

When it is furthermore assumed that the pathway is irreversible (as, for instance, anaerobic yeast glycolysis), the concentration of *P* plays no role. This set of algebraic relations can then be solved to obtain the intracellular

metabolite levels at the reference temperature, for given values of the extracellular concentration of *S*, thus yielding relations for the intracellular levels of *A* and *B* as a function of the extracellular concentration of substrate *S* for the reference temperature. It should be noted here that this conclusion is also valid for pathways containing reversible reactions, as long as the steady-state assumption is fulfilled.

Assuming that the catalytic capacity of each enzyme as a function of temperature can be described by the function $R_i(T)$ and the rate at the reference temperature, such that $k_{cat,i} = k^{To}_{cat,i} R_i(T)$ and that the stoichiometry does not change significantly with temperature (Chapters 2 and 3), the description of the system at a temperature *T* different from T_0 becomes:

$$\mathbf{N} \cdot \begin{bmatrix} e_1 \cdot R_1(T) \cdot k_{cat,1}^{T_0} \cdot f(K_A, S, A, K_{eq,1}) \\ e_2 \cdot R_2(T) \cdot k_{cat,2}^{T_0} \cdot f(K_A, K_B, A, B, K_{eq,2}) \\ e_3 \cdot R_3(T) \cdot k_{cat,3}^{T_0} \cdot f(K_B, B, K_{eq,3}) \end{bmatrix} = \mathbf{0} \tag{4.9}$$

If each enzyme has its own temperature dependent function $R_i(T)$, the ratio between *A*, *B* and *S* will be different for each temperature and dependent on the parameters of the corresponding temperature function. If, on the other hand, the temperature function of the single enzymes follows the same mechanism with the same parameters, e.g. $R_1(T)=R_2(T)=R_3(T)$, then eq. (4.9) will become equal to eq. (4.8). This would then imply that the relations describing the intracellular concentrations of *A* and *B* as a function of the extracellular substrate concentration are temperature independent. The differences between these two scenarios can be tested *in vivo* to provide insight into the temperature dependency of enzymes.

Considering the simple network described above, we now assume a dynamic temperature situation in which the concentration of *S* is high and non-limiting and thus fluxes v_1 to v_2 are at their maximum values. If the catalytic capacities of the enzymes in a pathway or network share the same temperature dependency, changes in temperature will cause all enzyme activities to change with the same factor. In such a scenario, no changes in intracellular metabolite levels will occur and thus the cells maintain complete homeostasis during temperature changes, without the need to adjust enzyme levels. If, however, for a substrate-limited system (i.e. the flux through the pathway is limited by the supply of *S*) it is experimentally imposed that the fluxes remain the same even at lower temperature (e.g. in a

chemostat cultures at constant dilution rate), S as well as the metabolite concentrations A and B will change to compensate for the lower enzymatic capacities.

In silico evaluation of different k_{cat}-temperature relationships in yeast glycolysis

To evaluate the impact of different or identical temperature dependencies of the k_{cat} of the enzymes in yeast glycolysis, simulations were carried out with a detailed kinetic model of this pathway developed by Teusink *et al*. (2000). Several modifications were made to the published version of the model to, amongst others, account for biomass growth and to include temperature dependency of enzyme capacities (see Materials and Methods). Using this model different substrate feeding regimes and temperature profiles were simulated to distinguish between the effects of temperature and of extracellular glucose concentration on glycolytic flux. This distinction is especially important for glucose-limited conditions, where the glycolytic flux is highly correlated with the extracellular glucose concentration because, as shown by Diderich *et al.* (1999) and Schaaff *et al.* (1989), glucose transport is a key growth-rate-controlling process. Therefore, in glucose-limited chemostat cultures, temperature dynamics will affect the extracellular glucose concentration via changes in glycolytic capacity. These changes in the extracellular glucose concentration will then propagate through all intracellular metabolite levels, yielding temperature-independent relations between intracellular metabolite and extracellular glucose levels. If, on the other hand, a different relationship between intracellular metabolite levels and extracellular glucose concentrations is observed for different temperature profiles, this would indicate that the temperature impact on k_{cat} differs for the different enzymes in yeast glycolysis (see simple example in the preceding paragraph).

Two distinct rounds of simulations with different substrate feeding regimes were performed to evaluate the impact of the parameters of the temperature-dependent function $R_i(T)$ on the intracellular metabolite profiles. In the first round, the temperature sensitivity of one of the glycolytic enzymes was set to be different from all others. In the second round, temperature sensitivities were set to be identical for all enzymes, implying that a decrease in temperature resulted in the same relative decrease of k_{cat} for all enzymes. In both rounds, simulations were performed for circadian

temperature cycles, linear temperature shifts starting from 30 °C steady-state conditions and batch cultures grown at 12, 18, 24 and 30 °C (temperature profiles are illustrated in **Figure 4.1**).

All simulations resulted in trends between intracellular metabolite levels and the extracellular glucose concentration. As expected, different temperature profiles or substrate-feeding regimes caused different trends when at least one of the enzymes was set to have a different temperature sensitivity compared to the others. For instance, when the temperature sensitivity of the k_{cat} of glyceraldehyde 3-phosphate dehydrogenase (TDH) was set to be two fold lower than that of the other glycolytic enzymes, the simulated values of the intracellular G6P, F6P and FBP levels under glucose-excess conditions clearly decreased with decreasing temperature (**Figure 4.2A**).

Differences were less pronounced for the model simulations of glucose-limited conditions, where metabolites upstream of TDH (G6P, F6P) showed no differences and only FBP was mildly affected by the change in temperature sensitivity. Furthermore FBP levels correlated poorly with the extracellular glucose concentration, especially for the fastest temperature shifts applied (circles in **Figure 4.2A**). Similar results were obtained when changing the sensitivity of the other glycolytic enzymes (see Appendix 0), indicating that this observation is not related to the flux towards the reaction, nor to its kinetic mechanism or reversibility. It was noticed that only metabolites upstream of the reaction with the different temperature sensitivity displayed such deviating trends. These observations are consistent with experimental and modeling results of Fendt *et al.* (2010) on the impact of changes in the abundance of single enzymes in metabolic pathways and with the 'passive network mechanism' proposed by these authors.

When temperature sensitivities were assumed to be identical for all glycolytic enzymes, the intracellular concentrations of glycolytic intermediates under glucose-excess conditions were predicted to be temperature independent (**Figure 4.2B**). Conversely, simulations of glucose-limited conditions revealed strong changes of intracellular metabolite concentrations during the temperature shifts. The range of intracellular levels was broader than in the previous simulation (**Figure 4.2A**).

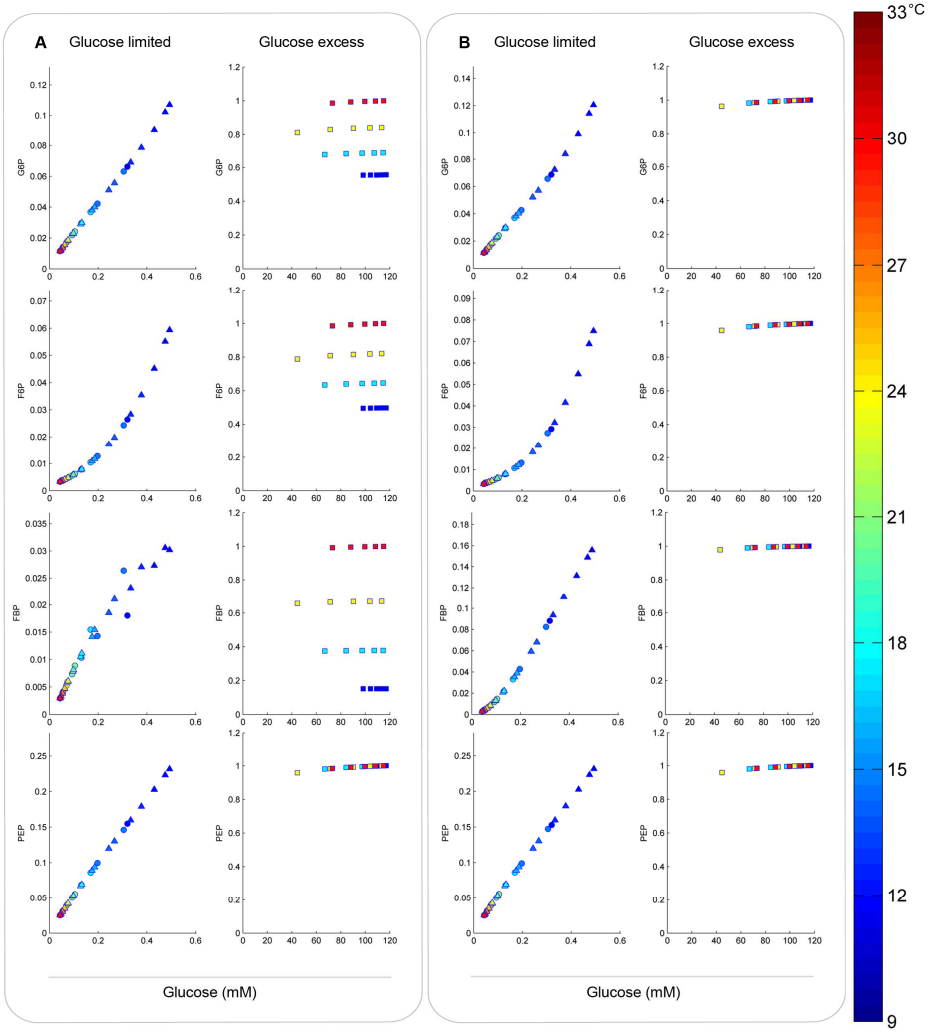

Figure 4.2: *Simulation results of intracellular metabolite levels, normalized to the levels under glucose-excess conditions at 30 ℃. (A) k_{cat} of glyceraldehyde 3-phosphate dehydrogenase (TDH) was set to be 2 times less sensitive to temperature than the other glycolytic enzymes; (B) all were set to have the same temperature dependency. The symbols refer to simulations of: sinoidal temperature cycles (Δ), linear temperature shifts applied to 30 ℃ steady-state chemostats (○) and batch fermentations at different temperatures (□). The colors indicate the culture temperature at the time of sampling. Simulation results considering different temperature sensitivities for phosphofructokinase and pyruvate kinase can be found in the appendix (page 101).*

Nevertheless, because the temperature sensitivity was set to be identical for all enzymes, intracellular metabolite concentrations showed highly similar correlations with the extracellular glucose concentration, irrespective of the simulated temperature profile. The results of these simulations agree with the results obtained with the simple example network (equation 4.6), thus showing that model predictions are independent of the assumed kinetic mechanisms of the enzymes involved, as long as the assumption of temperature independent K_i holds true. Therefore, experimental analysis of the relations between the extracellular glucose concentration and intracellular metabolite levels for different cultivation conditions and temperature regimes should resolve the question whether or not all enzymes in a pathway share the same k_{cat}-temperature relationship. Although based on model simulations the major differences between the two hypotheses are expected in glucose-excess conditions, *in vivo* there might be more than one enzyme with significantly different temperature dependency. Therefore, the deviating trends of intracellular metabolite levels simulated in glucose-limited conditions compared to glucose-excess conditions might be augmented. Experimental analysis under both conditions is important to decipher and quantify the temperature dependency of the glycolytic enzymes.

Experimental evaluation of model predictions

To experimentally investigate k_{cat}-temperature relationships in yeast glycolysis, anaerobic cultures were grown under different substrate feeding regimes and dynamic temperature conditions. The experimental setups used included batch cultures at 12, 18, 24 and 30 °C, to evaluate the temperature impact on intracellular metabolite levels under glucose excess conditions (sequential batch experiments (SBR)) and different sets of dynamic temperature shifts between 12 and 30 °C performed in glucose-limited chemostat cultures. These dynamic experiments comprised short term (3 h) linear temperature shifts (12→30→12 °C) and (30→12→30 °C) applied to steady-state cultures at 12 and 30 °C (LTS12 and LTS30) and sinoidal circadian temperature cycles (CTC) with 24 h frequency (**Figure 4.1**).

Experiments LTS12 and LTS30 aimed at understanding if different pre-cultivation temperatures would affect the metabolic response to temperature shifts. The different timescale of the temperature perturbations between LTS and CTC allowed to better discriminate between impact of

temperature and substrate concentration (see previous paragraphs). The CO_2 production rate was monitored on-line during all experiments since, in anaerobic cultures, it provides an accurate measure for (changes in) glycolytic flux.

In vitro enzyme activity assays were performed during CTC cultivation, since this setup had the slowest temperature dynamics and, consequently, the highest chance of hierarchical regulation of the glycolytic flux (*i.e.*, changes in enzyme levels). Nevertheless, levels of glycolytic enzymes did not significantly change during the temperature cycles (**Figure 4.3** and Appendix 0). This observation, together with previous results (Tai *et al*., 2007a), confirms that temperature changes have negligible impact on glycolytic enzyme levels in *S. cerevisiae*. On the other hand, intracellular metabolite levels and extracellular glucose concentrations showed a dynamic behavior in the CTC and LTS experiments (**Figure 4.4**).

In the SBR experiments, glucose was present in excess, and therefore the glycolytic flux depended exclusively on the cultivation temperature, through its impact on k_{cat}. Even though the glycolytic flux in batch cultures was observed to be six-fold lower at 12 °C than at 30 °C, intracellular metabolite levels were independent of the growth temperature (**Figure 4.4D**)

When temperature dynamics were applied to anaerobic glucose-limited chemostat cultures (LTS and CTC experiments), the residual glucose concentration was observed to increase with decreasing temperature as response to a decrease of the glucose transport capacity. As a result, the metabolite profiles show the inverse dynamics when compared to the temperature profiles applied to the chemostat cultivations (**Figure 4.4A-C**). When the intracellular metabolite levels, measured during the LTS and CTC experiments, were plotted in one graph as a function of the residual glucose concentration, a single relation between metabolite level and residual glucose was obtained (**Figure 4.5** and appendix on page 104). It can be inferred from these results that the metabolic response was independent of the initial steady-state temperature (12 or 30 °C) or the dynamics of the temperature perturbation applied, indicating that hierarchical regulation of yeast glycolytic flux does not play a significant role during temperature dynamics. Furthermore, based on the *in silico* evaluation of different scenarios, these results support the notion that all glycolytic enzymes in *S. cerevisiae* share a similar temperature- k_{cat} relationship.

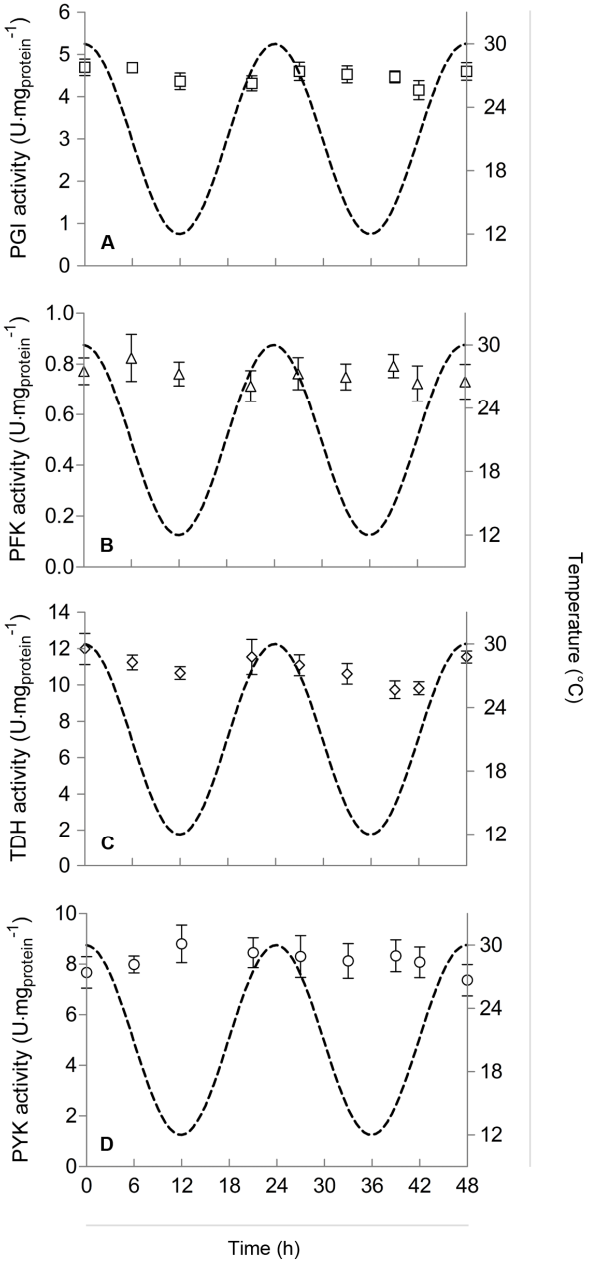

Figure 4.3: *Measured biomass specific capacities (V_{max}) of four glycolytic enzymes, during circadian temperature cycles in glucose limited chemostats. V_{max} values were obtained from in vitro enzyme activity assays performed at 30 °C in cell free extracts. A. Phosphoglucose isomerase (PGI); B. Phosphofructokinase (PFK); C. Glyceraldehyde-3-phosphate dehydrogenase (TDH); D. Pyruvate kinase (PYK). Results for the other glycolytic enzymes can be found in appendix (page 101).*

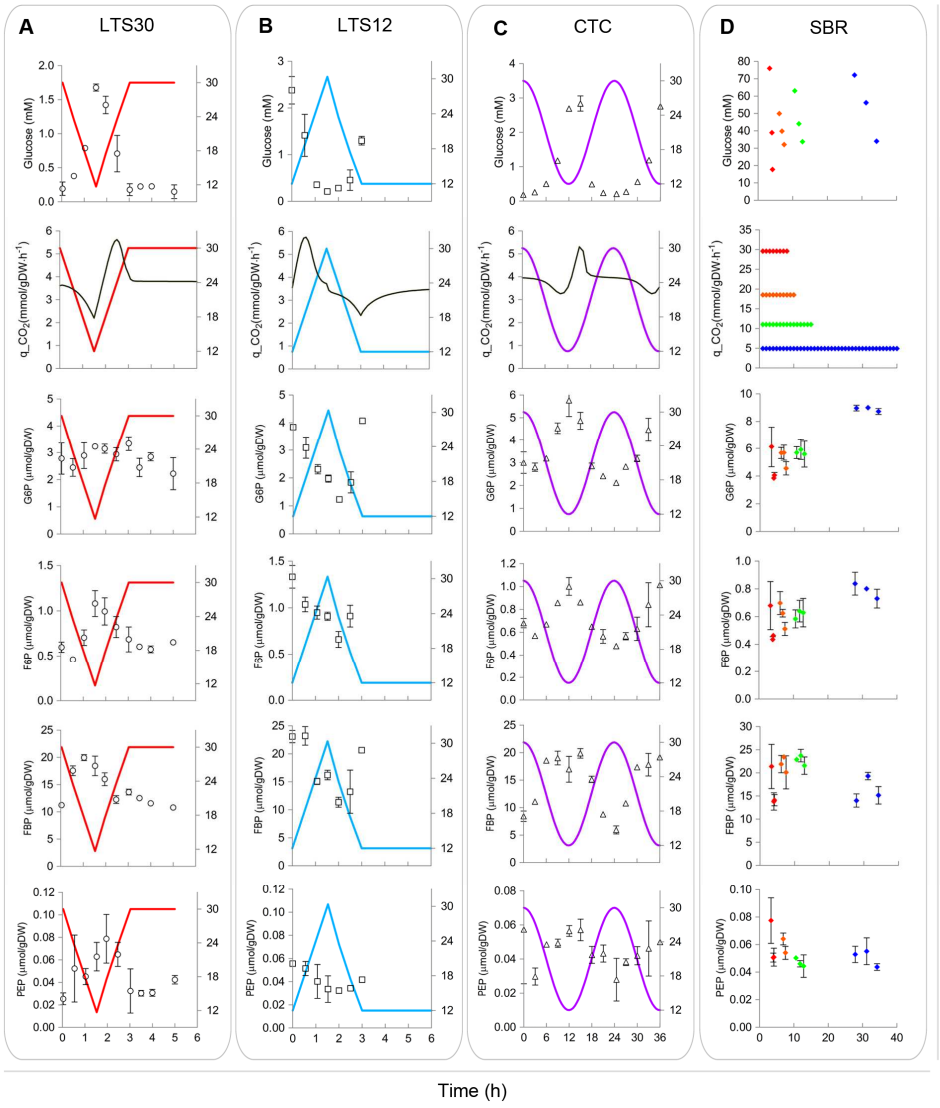

Figure 4.4: *Experimental results of residual glucose concentration, CO_2 production and intracellular glycolytic metabolite levels versus time for fast linear temperature shifts (A and B), circadian temperature cycles (C) and batch cultivations (D) at different temperatures. The coloured solid lines in panels A, B and C represent the applied temperature profiles. Error bars indicate the standard error of the average from at least two duplicate samples and two independent cultures.*

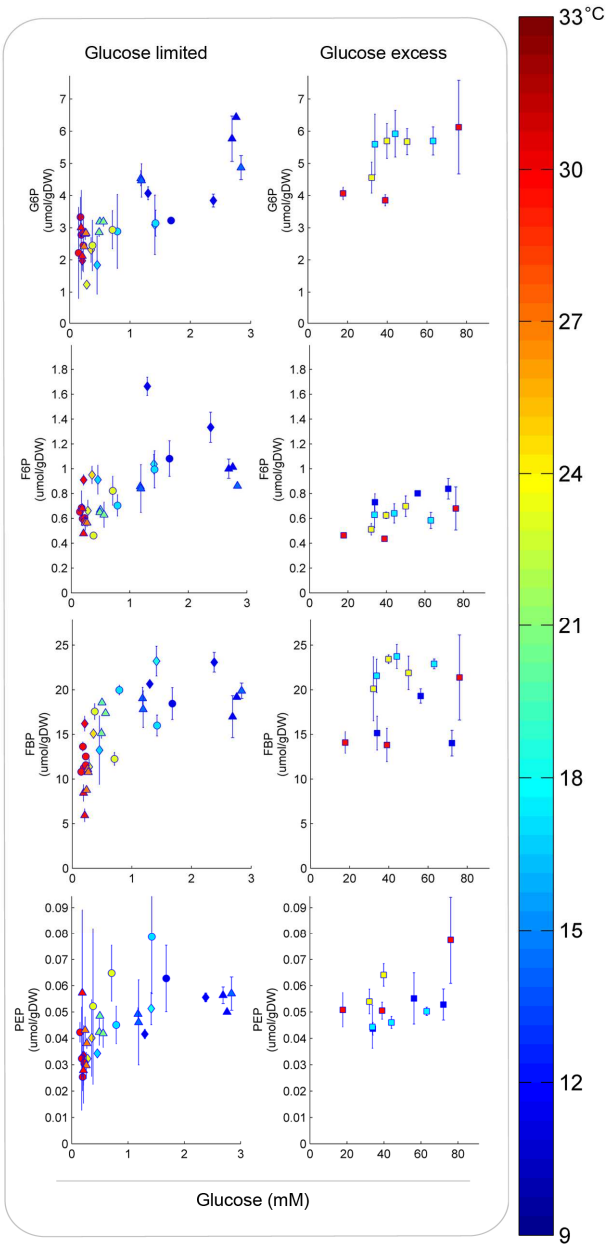

Figure 4.5: *Experimentally obtained relations between intracellular levels of glycolytic intermediates and extracellular glucose concentration. The different symbols represent data from different experiments, i.e. sinoidal temperature cycles (Δ), linear temperature shifts starting at 30 °C (○) or 12 °C (◇) and batch cultivations at different temperatures (□). Error bars refer to the standard error of the average of at least two duplicate samples and two independent runs of experiments. Colors indicate the temperature of the culture at the time of sampling.*

Discussion

Considering that chemical reactions in aqueous solutions have activation energies between 42 and 125 kJ.mol^{-1}, it can be estimated that reaction rates change by two fold for every 10 °C temperature change (Connors, 1990). However, temperature effects on individual enzyme-catalysed reactions can deviate substantially from this 'rule of thumb', for example due to the impact of temperature on protein structure. As illustrated with a simple linear metabolic pathway (equation (4.6)), different temperature dependencies of enzyme reactions inevitably result in (large) changes in concentrations of pathway metabolites. Similar changes in metabolite levels are observed when expression levels of individual enzymes in a pathway are modified (Fendt *et al.*, 2010). Hierarchical regulation, i.e. regulation at the level of enzyme synthesis (Ter Kuile and Westerhoff, 2001), would then be needed to restore and maintain homeostasis.

Previous *in vitro* assays in cell extracts, performed at 12 and 30 °C, suggested large differences in temperature dependency for the ten glycolytic enzymes in *S. cerevisiae* (Tai *et al*., 2007a). However, *in vitro* studies with optimized assays, in which parameters such as pH and concentrations of salts, cofactors and effectors differ for each enzyme, are not representative for the intracellular environment (Van Eunen *et al.*, 2010). The differences in, among others, protein content, osmotic pressure, substrate diffusion between the *in vitro* and *in vivo* conditions might lead to different flux versus temperature relationships.

To avoid the inherent problems of *in vitro* studies on enzyme kinetics, we developed a novel systems biology approach for analyzing kinetic regulation strategies under temperature dynamics. By combining *in silico* simulation of different strategies with experimental analysis of metabolite and substrate concentrations under various controlled temperature and substrate-feeding regimes, regulation strategies could, for the first time, be analyzed without relying on kinetic parameters derived from *in vitro* experiments. The *in silico* simulations predicted that similar temperature dependencies of the k_{cat} of all glycolytic enzymes should result in a single relation between metabolite level and residual substrate concentration for each metabolite, independent of temperature. Consequently, in batch cultures growing at saturating substrate concentrations, intracellular concentrations of glycolytic

intermediates should be independent of the growth temperature. In glucose-limited chemostat cultures, each metabolite level is then predicted to solely depend on the residual glucose concentration and not on the temperature as such (**Figure 4.6**).

Experimental results obtained under conditions of glucose excess, were consistent with this scenario and could not be reconciled with the alternative scenario in which temperature dependencies of the k_{cat} values of individual glycolytic enzymes were different. Although the experimental results of metabolite levels versus residual glucose for the glucose limited chemostat experiments (LTS and CTC) showed similar trends as the model simulations, the experimental errors of the metabolite data did not allow discriminating between the two simulated scenarios (i.e. the same temperature dependency for all enzymes versus a single enzyme different). However, if several glycolytic enzymes have different temperature sensitivities, the differences should be larger. Unfortunately, simulations in which several glycolytic enzymes have different temperature sensitivities did not result in a stable model.

All simulations were carried out using the model parameters published by Teusink *et al*. (2000). It should be realized, however, that different initial conditions, in our case anaerobic glucose-limited chemostat cultures at 12 and 30 °C, could have resulted in different expression levels of glycolytic isoenzymes, which could have led to differences in enzyme kinetic properties in both conditions. A genome wide transcriptome analysis of cells cultivated under both conditions (Tai *et al*., 2007a) did not provide indications for significant differences in the expression of glycolytic isoenzymes. Nevertheless, changes were observed in the expression levels of the different hexose transporters between the 12 and 30 °C chemostat cultivations. Determination of the glucose transport kinetics for both conditions indeed showed that the glucose transport capacity of cells grown in 12 °C chemostats was higher than that of cells grown at 30 °C (Tai *et al*., 2007a). Changes in the kinetics of glucose transport could have had a repercussion on the metabolite profiles as a function of the residual glucose concentration between shifts LTS12 and LTS30. Nevertheless, it was measured that the increase in the k_{cat} of glucose transport at 12 °C was coupled to an increase in the glucose saturation constant (K_S), in such a way that the ratio K_S/k_{cat} is not significantly different for the two conditions. Moreover, the increase in glucose transport capacity observed for the 12 °C chemostat (1.59) is

significantly lower than the decrease in glucose transport capacity caused by the temperature decrease (6.4 fold change). Considering the similar K_S/k_{cat} ratio and the limited difference in k_{cat} at 30 °C for both conditions, the effect must have been small in our experiments.

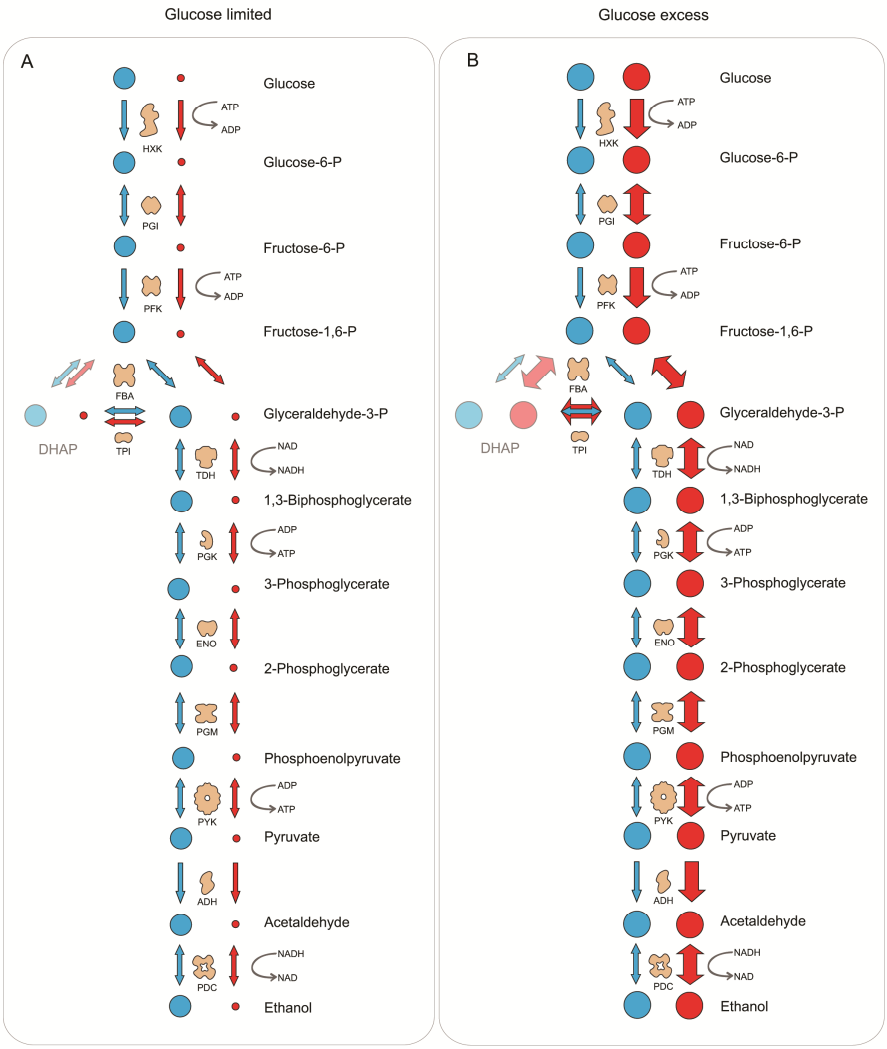

Figure 4.6: *Overview of the impact of temperature on glycolytic flux in anaerobic cultures of S. cerevisiae. The two panels represent growth under glucose-limited (A) and glucose-excess (B) conditions. The thickness of the arrows and diameter of the circles reflect the relative flux through the glycolytic enzymes and the intracellular concentrations of glycolytic intermediates, respectively. Blue and red symbols indicate growth at 12 ℃ and 30 ℃, respectively.*

Although this study was focused on yeast glycolysis, pentose phosphate pathway (PPP) metabolites were also found to correlate primarily with extracellular glucose concentration rather than with the temperature. Conversely, tricarboxylic acid pathway (TCA) and storage carbohydrate-related metabolites showed a different behavior, as their levels seemed to be primarily dependent on the initial steady-state temperature (**Figure 4.7**). It should be noted that under anaerobic conditions, the TCA, PPP and storage metabolism fluxes are generally much lower than the glycolytic flux (Nissen *et al.*, 1997). Therefore, changes in metabolites from these pathways will be slower under dynamic conditions. In the SBR experiments no significant difference was observed in the TCA pathway metabolite levels at different temperatures. This was likely due to the higher turnover times (time needed to refill or empty a metabolic pool), rather than different temperature sensitivities. Levels of precursors of storage carbohydrates (e.g. T6P) were too low in glucose-excess conditions to allow a good analysis of the temperature impact in this pathway. However, T6P levels under glucose limited conditions indicate a different regulation mechanism of trehalose-6-phosphate synthase or trehalose-6-phosphate phosphatase compared to glycolytic enzymes. Further model developments and experimental investigations should help to determine if the differences observed for the TCA and storage carbohydrate metabolism are a consequence of transcriptional regulation (reflected, for instance, in different enzyme levels), higher turnover times or significantly different temperature sensitivities. Analyzing the correlation between residual substrate levels and intracellular metabolite concentrations in different temperature conditions might enable to pinpoint which metabolic pathways are the most sensible to temperature perturbations and likely to be relevant in the overall response of *S. cerevisiae* to temperature perturbations.

Evolutionary 'synchronization' of the temperature dependencies of the catalytic capacities of enzymes in a metabolic pathway, may confer selective advantages to microorganisms that are subjected to frequent temperature changes. Firstly, changes of metabolite levels in response to temperature changes are minimized, thereby avoiding the need for energetically costly cycles of *de novo* synthesis and degradation of enzymes. This preservation of homeostasis may be particularly important for central metabolism, of which intermediates serve as precursors for several biosynthetic pathways. Secondly, based on metabolic control analysis, it can be inferred that this minimization of changes in metabolite concentrations causes pathway fluxes

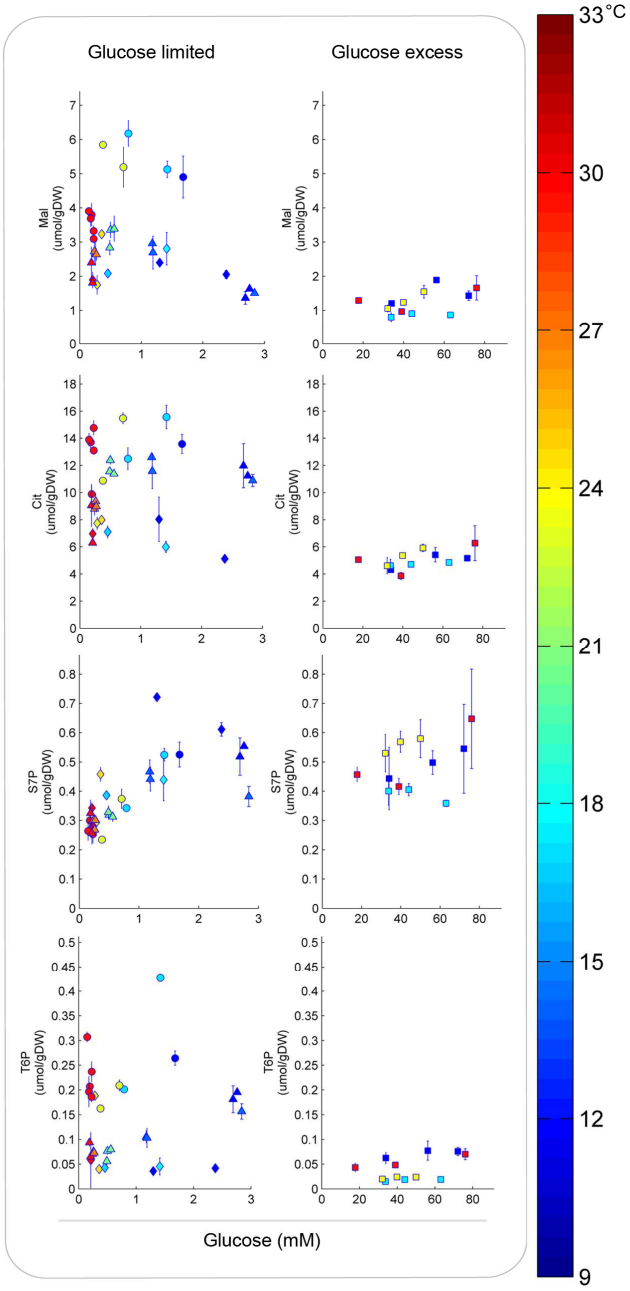

Figure 4.7: *Intracellular concentrations of metabolites from the tricarboxylic acid pathway, pentose-phosphate pathway and storage carbohydrate metabolism. Malate (Mal) and citrate (Cit) from the TCA pathway; sedoheptulose-7-phosphate (S7P) from the PPP; trehalose-6-phosphate (T6P) as a precursor of storage carbohydrates. Samples were taken during sinoidal temperature cycles (Δ), linear temperature shifts from 30 °C (○) or 12 °C (◇) and from batches at different temperatures (□).*

Figure 4.7 (cont.): *Error bars refer to the standard error of the averages of at least two duplicate samples and two independent experiments. The different colors indicate the temperature of the culture at the time of sampling.*

to be minimally sensitive to temperature variations (see Appendix, page 105).

Recent studies on temperature as an evolutionary pressure indicate that temperature optima for growth are a key factor for survival of sympatric strains (Gonçalves *et al.*, 2011; Libkind *et al.*, 2011; Salvado *et al.*, 2011). Our results indicate that, in addition to temperature optima, microbial strategies for kinetic adaptation to temperature dynamics (e.g. circadian temperature cycles) may play a key role in determining microbial fitness in natural environments. Further research should reveal whether microorganisms evolved in environments with a steady temperature (e.g. obligate commensals of homoeothermic vertebrates) show a different kinetic regulatory strategy than found for glycolysis in *S. cerevisiae*.

Appendices

In vitro enzymatic capacities of glycolytic enzymes during circadian temperature cycles

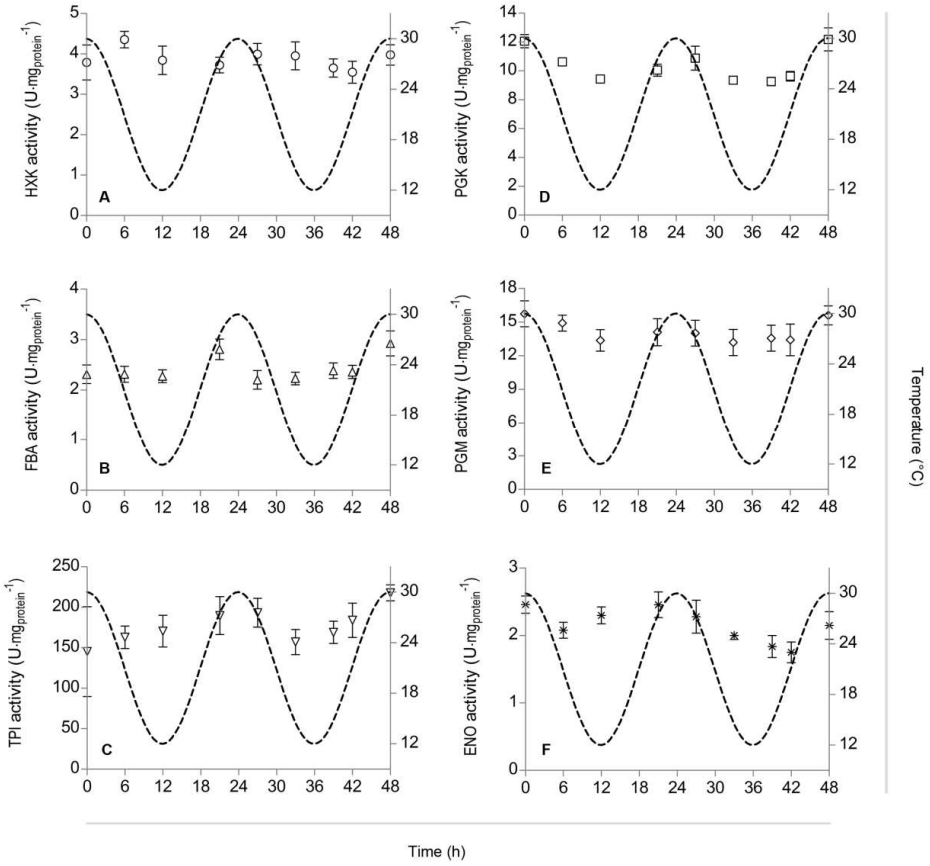

Figure 4.8: *Enzymatic capacities (V_{max}) of the glycolytic enzymes that are not shown in* ***Figure 4.3*** *(page 92), estimated from in vitro enzyme activity assays measured at 30 °C in cell free extracts of S. cerevisiae cultivated in glucose-limited anaerobic chemostats subjected to circadian temperature cycles (CTC). A. Hexokinase (HXK); B. Fructose bi-phosphate aldolase (FBA); C. Triose phosphate isomerase (TPI); D. Phosphoglycerate kinase (PGK); E. Phosphoglycerate mutase (PGM); F. Enolase (ENO).*

Simulation results considering different temperature-sensitivities

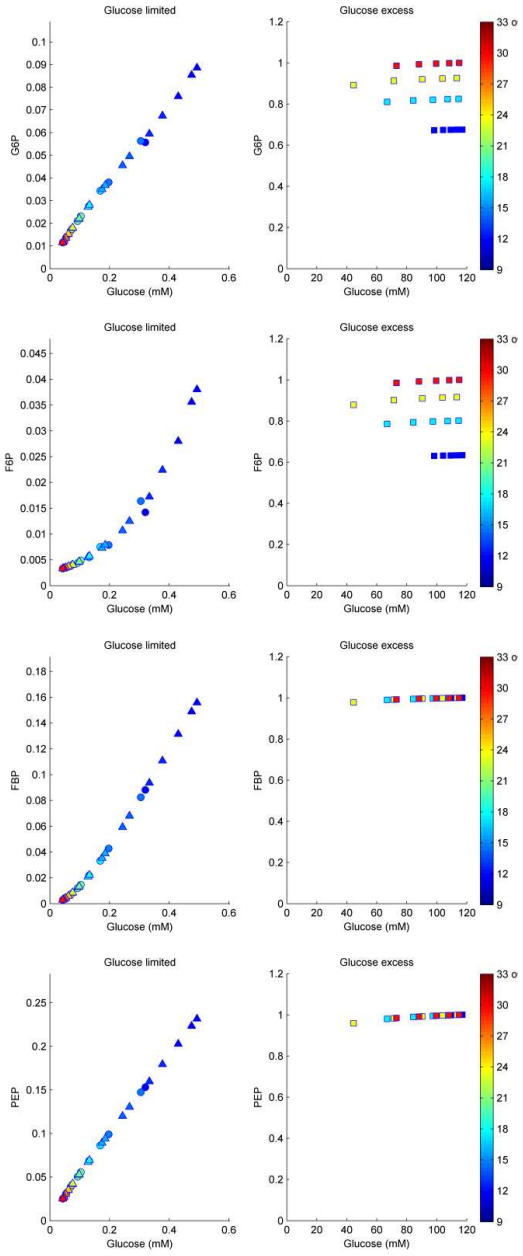

Figure 4.9: *Intracellular concentrations derived from model simulations considering that k_{cat} of phosphofructokinase (PFK) is 2 times less sensitive to temperature than the other glycolytic enzymes. The symbols refer to simulations of: sinoidal temperature cycles (Δ) and linear temperature shifts from 30 ℃ steady-state chemostats (○); batch fermentations at different temperatures (□). The colors indicate the culture temperature at the time of sampling. All concentrations are normalized to the levels under glucose excess conditions at 30 ℃.*

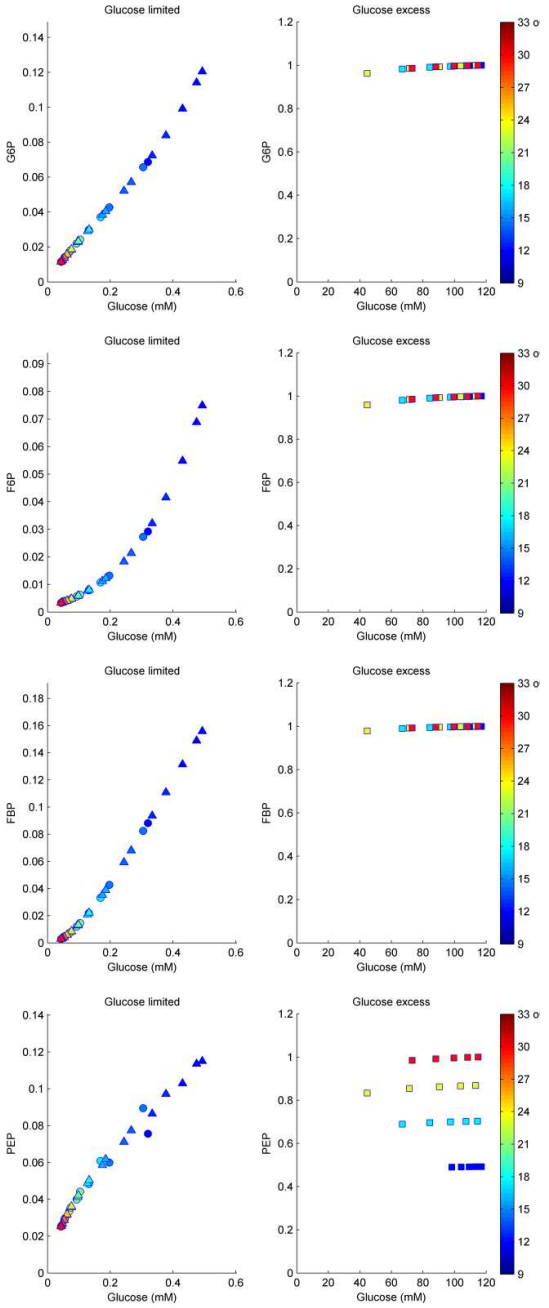

Figure 4.10: *Intracellular concentrations derived from model simulations considering that k_{cat} of pyruvate kinase (PYK) is 2 times less sensitive to temperature than the other glycolytic enzymes. The symbols refer to simulations of: sinoidal temperature cycles (Δ) and linear temperature shifts from 30 ℃ steady-state chemostats (○); batch fermentations at different temperatures (□). The colors indicate the culture temperature at the time of sampling. All concentrations are normalized to the levels under glucose excess conditions at 30 ℃.*

Nucleotide levels profiles measured during different temperature perturbation experiments

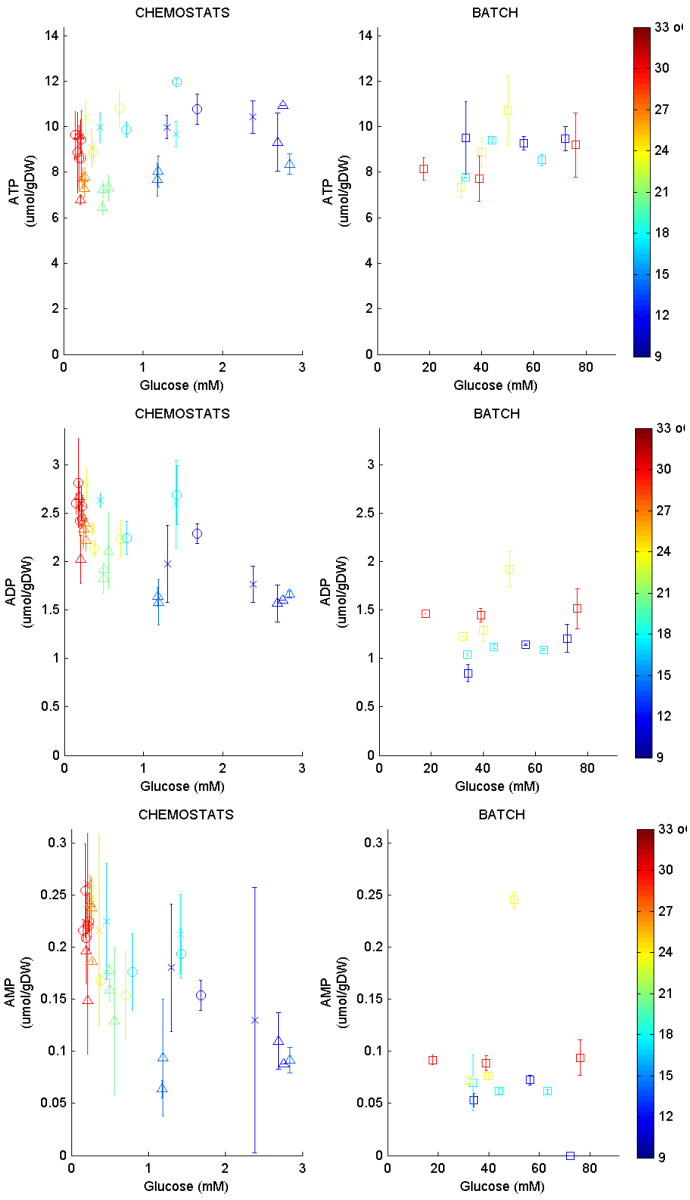

Figure 4.11: *Nucleotide levels profiles as a function of the extracellular glucose from experiments with sinoidal temperature cycles (Δ), linear temperature shifts from 30 ℃ (○) or 12 ℃ (X) and from batches at different temperatures (□). The error bars refer to the standard error of two duplicate samples from at least two independent runs of experiments. The different colors indicate the temperature of the sample.*

Demonstration that similar temperature-dependencies of k_{cat} lead to minimal flux change upon temperature perturbations

To demonstrate how the temperature dependency of k_{cat} influences the flux change, we will consider once more the simple network (4.6) (page 82). According to metabolic control analysis (Van Gulik *et al.*, 2003), the change in flux through the pathway (J) compared to the flux at a reference condition (with flux J^0 and biomass specific capacity V_i^0) can be quantified based on the change in enzymatic capacity of the three different enzymes (V_i/V_i^0) and the flux control coefficients $C^{J_i^0}$, in such way that $\sum_{i=1}^{3} C^{J_i^0} = 1$.

$$\frac{J}{J^0} = \frac{1}{C^{J_1^0}\frac{V_1^0}{V_1} + C^{J_2^0}\frac{V_2^0}{V_2} + C^{J_3^0}\frac{V_3^0}{V_3}} \qquad (4.10)$$

As we have discussed in the main section, the enzyme levels are not affected by temperature, meaning that the change in V_i^0/V_i will be uniquely a consequence of the temperature impact on the catalytic activity (k_{cat}) according once more to function $R_i(T)$.

$$\frac{V_i^0}{V_i} = \frac{k_{cat\,i}^{\;0}}{k_{cat\,i}} = \frac{1}{R_i(T)} \qquad (4.11)$$

From equation (7.11) and knowing that for temperatures below the optimal growth temperature (this study) k_{cat} decreases with decreasing temperature, it can be seen that:

$$\begin{cases} T < T^0 \rightarrow 0 < R_i(T) < 1 \\ T = T^0 \rightarrow R_i(T) = 1 \\ T > T^0 \rightarrow R_i(T) > 1 \end{cases} \qquad (4.12)$$

By replacing equation (4.11) in (4.10) we obtain the relation between the change in flux with temperature:

$$\frac{J}{J^0} = \frac{1}{\frac{C^{J_1^0}}{R_1(T)} + \frac{C^{J_2^0}}{R_2(T)} + \frac{C^{J_3^0}}{R_3(T)}} \tag{4.13}$$

We will now consider that, for temperatures lower than the reference temperature (T^0), the catalytic activity of enzyme 1 decreases less severely than for enzymes 2 and 3. This means that $R_1(T)$ will be higher than $R_2(T)$ or $R_3(T)$. Multiplying equation (4.13) by $R_1(T)$ we obtain equation (4.14) where the ratios $R_1(T)/ R_2(T)$ and $R_1(T)/ R_3(T)$ will always be higher than 1.

$$\frac{J}{J^0} = \frac{R_1(T)}{C^{J_1^0} + C^{J_2^0}\frac{R_1(T)}{R_2(T)} + C^{J_3^0}\frac{R_1(T)}{R_3(T)}} \tag{4.14}$$

If, on the other hand, we speculate that evolution led to a situation where all k_{cat} have the same low-temperature-sensitivity, all enzymes would have the same temperature function as the one of enzyme 1 ($R_1(T) = R_2(T) = R_3(T)$). This means that, when multiplying equation (4.13) by $R_1(T)$ equation (4.15) can be derived.

$$\frac{J}{J^0} = \frac{R_1(T)}{C^{J_1^0} + C^{J_2^0} + C^{J_3^0}} = R_1(T) \tag{4.15}$$

Because the denominator in equation (4.15) will always be higher than 1, the flux decrease as a consequence of temperature drop is minimal only if k_{cat} values of the different enzymes have the same temperature dependency.

Even in cases where J/J^0 is different than $R_1(T)$ (for instance if the overall change in flux is the average of the functions $R_1(T)$, $R_2(T)$ and $R_3(T)$), only in the extreme cases where the enzyme with the highest temperature sensitivity has no impact on the flux through the pathway ($C^{J_i^0}$ close to 0), will the flux change be less than in the situation where all enzymes have similar temperature sensitivities (**Figure 4.12**).

This points out that, besides minimizing changes in intracellular metabolite levels, identical temperature sensitivities of the enzymes in a pathway can also minimize the changes in flux in response to temperature fluctuations. This can be beneficial in competitive environments since the growth rate of the microorganisms would not be drastically reduced when temperature decreases.

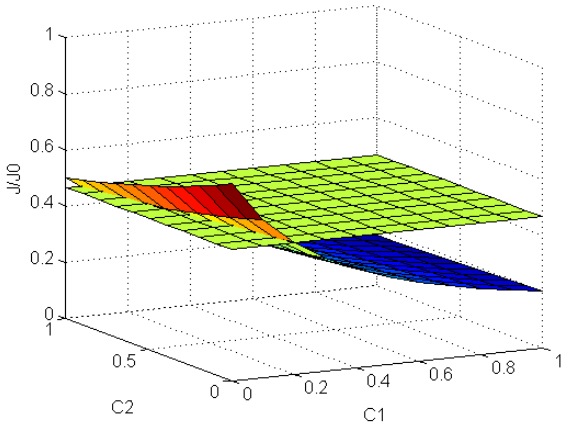

Figure 4.12: *Impact of the control coefficients $C^{J_i^0}$ in the overall change in flux with temperature. For the simulation considering different temperature sensitivities of the different enzymes it was assumed that the function $R_i(T)$ was 0.7, 0.5 and 0.2 for, respectively, enzymes 1, 2 and 3. The green surface represents the situation where all the enzymes have the same temperature dependencies, considering that the overall change in flux J/J^0 would be the average of the $R_i(T)$ values used in the previous simulation.*

5. Temperature and glucose-dependent *in vivo* kinetic model of anaerobic yeast glycolysis

Abstract

The results from the previous chapters have indicated that mild suboptimal temperatures have no major impact on the stoichiometry of growth, nor they require adjustment in the levels of the glycolytic enzymes to compensate for the loss of specific catalytic activity at temperatures lower that the optimal one. It was on the other hand clearly demonstrated that the residual glucose concentration has a major impact on the uptake and secretion rates during temperature perturbations done to glucose-limited chemostat cultivations. Nevertheless, it is not possible at this moment to predict the impact of residual glucose concentration on intracellular metabolite concentrations and glycolytic fluxes, as there are no models that can describe the metabolite levels measured from anaerobic chemostat cultivations as function of residual glucose concentration and temperature.

This work aimed at developing an *in vivo* kinetic model of anaerobic yeast glycolysis that can provide insight to the impact of residual glucose concentration, growth rate and temperature on the central-carbon metabolism of *Saccharomyces cerevisiae*. Such models will allow a better understanding of the kinetic mechanisms used by the cell to cope with several environmental perturbations at the same time (e.g. changes in substrate concentrations and temperature).

To construct the kinetic model it was first needed to gather a dataset capable to cover a sufficiently broad range of metabolite concentrations and fluxes. Such a large range is needed to estimate the *in vivo* kinetic parameters of each glycolytic enzyme. Steady-state glucose-limited anaerobic chemostats were run at different dilution rates (from 0.025 to 0.26 h^{-1}) and

constant temperature (30 °C). Samples were taken to measure extra-and intracellular metabolite concentrations, elemental biomass composition and enzyme activities. By applying data reconciliation and metabolic flux analysis it was possible to estimate the intracellular fluxes together with the uptake and secretion rates. Enzyme levels could be predicted because it appeared that the production rates of most glycolytic enzymes are only dependent on the residual glucose concentration, following a Hill-type saturation function.

With all the collected data (fluxes, metabolite levels and enzyme activities) it was possible to parameterize the kinetic function of each glycolytic enzyme that describes the flux through a reaction as a function of the concentrations of the effectors (substrates, products and co-factors). The choice of which kinetic format to use was made based on thermodynamic analysis. Mechanistic equations were used to describe the kinetics of reactions operating far-from-equilibrium while the Q-linear-kinetic format was used for reactions operating at near-equilibrium. Reactions operating in pseudo-equilibrium did not require the use of kinetic equations as they were assumed to be in equilibrium. The K_{eq} estimated from the *in vivo* data could be used to describe such reactions.

The developed model could successfully describe the profiles of glycolytic metabolites measured during the experiments and the changes in enzyme activities measured from the *in vitro* assays. To further test the robustness of the model, temperature was included as a variable. The resulting model was validated using the experimental data obtained from linear temperature perturbations applied to glucose-limited chemostat cultivations.

Introduction

The results presented in the previous chapters regarding the black-box behavior at different temperatures and glucose regimes (excess and limitation) have allowed understanding how *Saccharomyces cerevisiae* has evolved to cope with dynamic temperature conditions. It has been concluded that, in the mild-suboptimal range, temperature has no major impact on the stoichiometry of growth. Also no significant influence on the equilibrium constant (K_{eq}), saturation constants (K_S, K_P, K_i,…) and enzyme levels could be found. The only kinetic parameter that is sensitive to temperature conditions is the catalytic activity of the enzymes (k_{cat}), where temperature changes lead to the same alterations in the k_{cat} of all the glycolytic enzymes.

As shown in Chapter 4, when comparing the measured intracellular concentrations with the ones estimated *in silico*, the currently available kinetic models of yeast glycolysis are still unable to describe *in vivo* intracellular metabolite data or to be stable for the range of fluxes and residual glucose concentrations covered by dynamic temperature conditions. A predictive kinetic model of yeast central metabolism, describing the intracellular metabolite concentrations, enzyme levels and fluxes as a function of residual glucose and cultivation temperature, is a valuable tool. It can be used to predict the metabolism under other dynamic temperature conditions, but also for a comprehensive analysis of the impact of those variables under other complex experimental settings where fluxes and residual substrate concentrations change concomitantly (e.g. fed-batch setups).

To build such a model it is important to have a dataset that gives information on the behavior of all the kinetic effectors of the individual enzymes in glycolysis. These include metabolite concentrations, enzyme activities and fluxes.

In spite of the high industrial relevance of *Saccharomyces cerevisiae*, there is very few data concerning the influence of growth rate or residual substrate concentration on the anaerobic metabolism of this yeast. Some of the available literature (e.g. Nissen *et al.*, 1997; Verduyn *et al.*, 1990) presents a black-box description, but no insight concerning the impact of the growth rate or residual glucose on the intracellular metabolites and enzyme levels. Another study from Fazio *et al.*, 2008 gives very relevant information on changes in transcript levels at different growth rates but no extrapolation could be made to changes in the kinetics of anaerobic growth. So, before modeling the anaerobic glycolytic metabolism at different growth rates or temperatures, it is important to gather a dataset that allows a global analysis of the central-carbon metabolism and to accurately parameterize the kinetics of each enzymatic reaction.

Another crucial point to consider when building a kinetic model is the mathematical format used to describe the relation between rates and the metabolite concentrations. Mechanistic rate equations, such as the ones derived from *in vitro* studies of the enzyme reaction rates, often have many parameters. This hinders their proper *in vivo* quantification and complicates the analysis of which effectors play the most relevant role in regulating the reaction rate (e.g. substrates, products, co-factors,…). Some strategies have

been developed to minimize the number of parameters of kinetic models, such as the application of approximate kinetic formats (e.g. lin-log kinetics, log-linear kinetics, power-law,…) and model reduction (for a review see Nikerel, 2009). But one of the problems is that these formats may fail to provide accurate simulations when applied to a broad range of fluxes and/or metabolite concentrations. Canelas *et al.*, 2011 have recently tried to overcome these problems by developing a reaction classification method. By carrying out a thermodynamic analysis of each reaction, using the measured metabolite concentrations for a wide range of reaction rates, it is possible to group enzymatic reactions as operating in pseudo-, near- or far-from equilibrium. It has been reported by Canelas *et al.* (2011), that only 25% of the reactions from aerobic central-carbon metabolism have to be classified as irreversible and need to be described by mechanistic equations. A linear equation with only two parameters can be used to describe the rates of near-equilibrium reactions (Q-linear kinetics), while no parameters besides the equilibrium constant need to be used for pseudo-equilibrium reactions since they operate very close to thermodynamic equilibrium. Another benefit of this method is that the parameters obtained for the near-equilibrium reactions are obtained from *in vivo* data, guaranteeing that, when used in the glycolytic model, they will describe the measured intracellular concentrations at least for the range of fluxes used to parameterize the equation.

This chapter presents the development of a temperature-dependent *in vivo* kinetic model of anaerobic yeast glycolysis. To build the model it was first necessary to carry out experiments to characterize the metabolic state of *Saccharomyces cerevisiae* in anaerobic, glucose-limiting conditions for a wide range of growth rates (0.026 to 0.27 h^{-1}). By using well-defined and tightly controlled steady-state chemostat cultivations it was possible to accurately quantify the intracellular fluxes, the concentrations of intra- and extracellular metabolites and the changes in enzyme levels. This comprehensive dataset, together with measurements of enzyme activities and biomass composition, allowed setting up an *in vivo* kinetic model according to the reaction classification method developed by Canelas *et al.* (2011). The model was validated with an independent dataset from the temperature shift experiments.

Materials and Methods

Fermentation setup

Strain and Media

All cultivations were done with *Saccharomyces cerevisiae* strain CEN.PK113-7D (MATa) (Entian and Kötter, 2007; Nijkamp *et al.*, 2012).

Pre-cultures were grown in 100 ml of synthetic medium containing 5.0 g.L^{-1} $(NH_4)_2SO_4$, 3.0 g.L^{-1} KH_2PO_4, 0.5 g.L^{-1} $MgSO_4.7H_2O$, 18 g.L^{-1} glucose and 1.0 ml.L^{-1} of a trace element solution and vitamin solution with the composition described by Verduyn *et al.* (1990). This medium was filter sterilized directly into sterile 500 ml shake-flasks, using 0.2 µm PVDF membranes (Millipore, Massachusetts, USA).

The glucose-limited chemostat cultivations were fed with medium composed by 0.3 g.L^{-1} $(NH_4)_2SO_4$ and $K_2H_2PO_4$, 3.0 g.L^{-1} $NH_4H_2PO_4$, 0.5 g.L^{-1} $MgSO_4.7H_2O$, 0.4 g.L^{-1} of Tween 80, 10 mg.L^{-1} ergosterol, 25 g/L glucose, 0.15 g.L^{-1} antifoam C (Sigma-Aldrich, Missouri, USA) and 1 ml.L^{-1} of the same trace element and vitamin solutions used to prepare the pre-culture medium. A solution composed by the salts, glucose, vitamin and trace-element solutions were filter sterilized with a Sartopore 150 filter (Sartorius, Goettingen, Germany) into a previously heat sterilized vessel (20 min at 121 °C) containing the antifoam. The Tween 80 and ergosterol were mixed together in 30 ml pure ethanol to assure its total dissolution and sterility and later added to the medium vessel.

Steady-state chemostat cultures at different dilution rates

Five chemostat cultivations were run in parallel under anaerobic glucose-limited conditions. For each chemostat, the dilution rate was changed stepwise (up or down) according to the diagram presented in **Figure 5.1**. All chemostats were sampled at the 4th and 5th residence time after each change in dilution rate, which corresponds respectively to 6.2 and 7.2 generations. After the second sample, the set point of the feed pump was manually changed to match the new dilution rate. This experimental approach was used to reduce the number of fermentations needed to study a broad number of growth rates while assuring that steady state conditions are achieved. The total number of generations per fermentation was kept below

22, to avoid long-term adaptation (Mashego *et al.*, 2005). Nevertheless, to check that there was indeed no long-term adaptation, the last dilution rate of each chemostat was set to be the same as the first one and the measurements of extracellular metabolite concentrations were compared. Instead of running duplicate fermentations, dilution rates were split in an intercalated way between fermentations runs such that the results obtained could indicate the reproducibility of this experimental approach.

All cultivations were carried out at 30 °C in 2 L fermenters (Applikon, Schiedam, The Netherlands) containing a working volume of 1.4 L of medium and were continuously stirred at 800 rpm. A 2.0 M solution of KOH was automatically added to maintain the pH of the broth at 5.0. Nitrogen gas (N_2) was sparged at a rate of 0.5 $L.min^{-1}$ to both fermentation broth and medium vessel to maintain fully anaerobic conditions throughout the experiments. The stirrer speed, temperature, pH and gas-inflow set points were controlled by a Biostat Bplus controller (Sartorius BBI Systems, Melsungen, Germany).

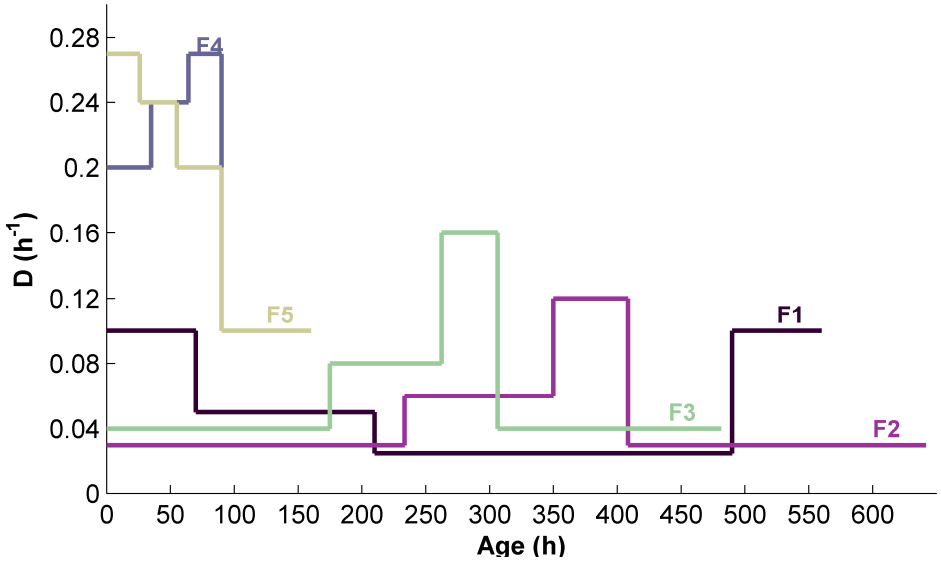

Figure 5.1: *Dilution rate profiles applied to the five different chemostats (F1 – F5). Sampling took place when steady state was reached, and twice for every dilution rate, one volume change apart. After the second sample, the dilution rate was changed up or down, according to the setup.*

Analytical methods

Off-gas analysis

The flow rate of the N_2 stream was determined with an Ion Science Saga digital flow meter (Cambridge, UK). The amount of CO_2 present in the off-gas was measured online with a Rosemount NGA 2000 gas analyzer (Minnesota, USA). Before measurement of the CO_2 mol fraction, the part of the gas stream entering the off-gas analyzer was dried with a Permapure dryer (Inacom Instruments, Overberg, The Netherlands) to avoid the interference of other compounds (e.g. water and ethanol).

Sampling and analysis of extracellular metabolite concentrations

2.0 ml of broth were sampled directly into syringes containing 64.5 g of cold steel beads (-20 °C). This resulted in immediate cooling of the sample to a temperature slightly above 0 °C for quenching of metabolic activity. Immediately thereafter the sample was filtered through 0.2 µm membrane filters as described by Canelas *et al.* (2008) to remove the cells.

The concentrations of glucose, ethanol, glycerol, acetate and lactate were measured by high-performance liquid chromatography, using an Aminex HPX-87H column (Bio-Rad Laboratories, California, USA) at 60 °C and eluted with 5 mM phosphoric acid at a flow rate of 0.6 $ml.min^{-1}$. Glucose, ethanol and glycerol were detected by Waters 2410 refractive index detector whereas acetate and lactate with a Waters 2487 dual-wavelength absorbance detector (Waters Corporation, Massachusetts, USA) at 214 nm. Acetaldehyde concentrations were determined by GC, using a HP Innowax 19095N-121 column (Agilent, California, USA) coupled to a FID detector. The column temperature was 70 °C while the injector and detector were, respectively, at 180 °C and 200 °C. The injection volume was set to 0.2 µl.

Pyruvate and succinate concentrations in the fermentation broth were quantified with GC-MS using U-^{13}C-labeled cell extract as internal standard, as described by Wu *et al.* (2005).

Sampling and analysis of intracellular metabolite concentrations

1.2 ml of broth were withdrawn within 0.9 seconds into 6 ml of 100% (v/v) cold methanol (-40 °C) using the rapid sampling setup described by Lange *et*

al. (2001). Biomass was collected and washed using the filtration setup developed by Douma *et al.* (2010). Uniformly labeled ^{13}C-cell-extract was added to the biomass cake as internal standard in the same ratio as previously reported by Wu *et al.* (2005) (100 µl extract per 1 g sample). The intracellular metabolites were extracted with boiling ethanol (75% v/v) following the protocol described by Canelas *et al.* (2008). The concentrations of G6P, F6P, F16P, GAP, DHAP, 2PG, 3PG and T6P were measured by GC-MS using the protocol described by Cipollina *et al.* (2009). Pyruvate concentrations were also measured by GC-MS, but using the protocol described by De Jonge *et al.* (2011). The concentrations of nucleotides (ATP, ADP and AMP) were quantified by ion-pair reverse-phase LC-MS/MS (Seifar *et al.*, 2009).

The volume of the cytosol was assumed to be 1.7 $ml.g_{DW}^{-1}$ when converting the measured concentrations to $mmol.L^{-1}$ (Canelas *et al.*, 2011).

Biomass concentration and composition (elemental and macromolecular)

15 ml of broth was sampled at 4th and 5th residence times and filtered through 0.45 µm pore-diameter filters (Supor-450, Pall Corp., Michigan, USA). Biomass dry weight was determined after drying the filters for 48h at 75 °C as described by Wu *et al.* (2005).

Samples for elemental composition determination were processed as follows: 10 ml of broth was withdrawn from chemostat fermentations at a dilution rate of 0.026, 0.03, 0.05, 0.1, 0.206, 0.232 and 0.263 h^{-1} and centrifuged. After discarding the supernadant, the pellets were washed twice with 40 ml demi water, and after freeze-dried for 48h. Samples were then sent to the Energieonderzoek Centrum Nederland (ECN, Petten, Netherlands) where the carbon (C), hydrogen (H), nitrogen (N) and oxygen (O) content was determined with an element analyzer (Interscience, Breda, The Netherlands).

The molecular weight of dry biomass (MW_X in $g_{DW}/Cmol_X$) was calculated from the carbon percentage in the dry biomass (g_C) according to equation (5.1).

$$MW_X = \frac{g_{DW}}{g_C} MW_C = \frac{100}{g_C} \times 12.01 \qquad (0.1)$$

To derive the macromolecular composition it was assumed that the proteins, lipids, carbohydrates and nucleic acids had the elemental compositions determined by Lange and Heijnen (2001) who used the same strain growing under aerobic conditions. Based on the measured elemental composition of biomass and the one of the macromolecules, a data reconciliation routine was set to calculate the macromolecular biomass composition. Details on the assumptions made and overall procedure can be found in the supplementary information (page 154).

Enzyme activity measurements

Enzyme activities from 0.03, 0.05, 0.16, 0.20, 0.22 and 0.27 h^{-1} cultivations were measured with *in vitro* assays at 30 °C and 340 nm, using the protocol described by Jansen *et al.* (2005). Measurements were done to two different concentrations of freshly prepared cell extracts and the protein concentrations were determined with the Lowry assay (Lowry *et al.*, 1951) using dried bovine serum albumin as standard.

Statistical and modeling procedures

Stoichiometric model and data reconciliation

The intracellular fluxes were calculated by combining a data reconciliation approach with flux balance analysis. More precisely, the measured concentrations of the extracellular compounds, the in- and outflows, the evaporation rate of ethanol and acetaldehyde, their errors, and the biomass composition were used as input to solve the over determined system comprised by the steady-state molar balances of the extracellular components on the broth and gas phase and the stoichiometric model previously described by Daran-Lapujade *et al.* (2004). The extracellular components considered were glucose, CO_2, ethanol, biomass, glycerol, acetate, lactate, succinate, pyruvate and acetaldehyde. Standard data reconciliation techniques, as explained by Verheijen (2009), were used to obtain the flux distributions and respective errors.

Having the stoichiometric model it was also possible to estimate the amount of glycolytic intermediates needed for biomass formation and the fluxes from the model boundaries as a function of growth rate. Functions were fitted to these profiles and added as input to the kinetic model.

Reaction classification according to thermodynamic analysis

The approach followed to select the kinetic format to be used in the final model was the one used by Canelas *et al.* (2011). Resuming, the flux through a reaction (v) can be expressed as a function of its mass-action ratio (Γ) according to the general equation:

$$v = V_{\max}\beta(x,p)\left(1-\frac{\Gamma}{K_{eq}}\right) \tag{5.2}$$

K_{eq} is the equilibrium constant, V_{max} the catalytic capacity of the enzyme and $\beta(x,p)$ is the mathematical expression that describes the binding of reactants and effectors (x) to the enzyme according to the affinity parameters (p) and the mechanism of the enzyme-catalyzed reaction. The term $1-\Gamma/K_{eq}$ represents the dimensionless thermodynamic driving force, which can be directly related to the Gibbs-free-energy of the reaction (Canelas *et al.*, 2011).

By plotting the flux as a function of the mass-action ratio (Γ), it is possible to determine the thermodynamic state of the reaction (i.e. its displacement from equilibrium) by comparing the magnitude of Γ with K_{eq} and the overall profile of v versus Γ for the entire range of fluxes. If the order of magnitude of Γ is significantly lower than K_{eq} for the entire range of conditions evaluated, the reaction is likely to be far-from-equilibrium and mechanistic rate equations are needed to describe the kinetics of the enzyme reaction. If the order of magnitude of Γ is similar to K_{eq} and no significant displacement from equilibrium is measurable for the range of conditions evaluated (i.e. $\Gamma/K_{eq} \approx 1$), the reaction operates at pseudo-equilibrium. No rate equation is needed to describe the kinetics of pseudo-equilibrium reactions and the mass balance of one of its effectors (product P_i or substrate S_i) can be replaced in the model by the algebraic equilibrium equation:

$$K_{eq} = \frac{\prod P_i^{p_i}}{\prod S_i^{s_i}} \tag{5.3}$$

Finally, if the order of magnitude of Γ is similar to K_{eq} but there is a statistically significant displacement from equilibrium that increases with increasing flux (Γ/K_{eq} becomes increasingly lower than 1), the reaction

operates at near-equilibrium. For such cases, Canelas *et al.* (2011) have hypothesized that the rate equation (5.2) containing generally a highly parameterized and non-linear $\beta(x,p)$ function can be simplified to a linear relation containing only two parameters.

The statistical methodology applied to classify the different reactions from the *in vivo* metabolite concentrations and fluxes was the same as the one used by Canelas *et al.* (2011). The threshold p-value of the weighted linear regression of Γ versus v was set at 0.005.

Kinetic model for different growth rates at constant temperature (30 °C)

The reactions described by the developed kinetic model of anaerobic yeast glycolysis are presented in **Figure 5.2**. Because no data was available on the concentrations of 1,3-phosphoglycerate, the reactions catalyzed by glyceraldehyde phosphate dehydrogenase (TDH) and phosphoglycerate kinase (PGK) were lumped. The first version of the model was built to describe steady-state fluxes and intracellular metabolite concentrations at different growth rates/residual substrate concentrations but constant cultivation (30 °C). The choice of the kinetic format to use for each enzymatic reaction and consequent parameterization was made according to the reaction classification method developed by Canelas *et al.* (2011). For the reactions classified as being far-from-equilibrium, a literature survey was made to gather mechanistic equations used to describe the kinetics of that reaction. The one that provided the best fit for the range of *in vivo* concentration measured was the one selected for the kinetic model. The growth rate was given as input to the model and the glucose uptake rate was calculated using the Herbert-Pirt relation obtained from the experimental data. Detailed information on the structure and parameters of the kinetic model, including the functions used to describe the boundary fluxes and coefficients of the biomass formation reaction, are given in Appendix 5.2 (page 156).

Validation of the model

Data from cultivations subjected to dynamic-temperature conditions were used for an independent validation of the kinetic model. Temperature was added as a variable by including the Ratkowsky equation to describe the temperature impact on the catalytic activity of each glycolytic enzyme

(Ratkowsky *et al.*, 1982). Following the results from the previous chapter, the decrease in catalytic activity as a consequence of a temperature drop was set to be the same for all enzymes and all other kinetic parameters (equilibrium and saturation constants) were fixed to be temperature independent. Because no information was found regarding the impact of mild suboptimal temperatures on the enzyme production and degradation rates, it was initially set that the temperature impact on these reactions is the same as for the glycolytic enzymes. For this version of the model, the black-box model developed in Chapter 3 was coupled to the kinetic model of yeast glycolysis, including the hyperbolic function to describe the glucose uptake rate.

To validate the temperature-dependent kinetic model, temperature perturbations were simulated from 30 and 12 °C steady-state conditions. Temperature was linearly changed between 30 and 12 °C for 1.5h and after set back to return to the initial steady-state vale in the same amount of time. These temperature profiles are the same as shifts A30 and A12 reported in Chapters 3 and 4 (see, for instance, page 51), allowing comparing the simulated metabolite levels with the experimental measurements obtained in the previous chapters. Because the simulated temperature perturbations did not take longer than 3h, it was assumed that there were no significant changes in biomass composition. As a consequence, the coefficients of biomass formation were set to be constant (temperature and growth rate independent) at the values determined for the initial steady-state growth rate (0.03 h^{-1}).

Results

Primary data obtained from anaerobic glucose-limited chemostats run at different dilution rates and 30 °C

Five glucose-limited anaerobic fermentations were carried out with stepwise increases/decreases of the dilution rate (**Figure 5.1**). In this way it was possible to cover a broad range of dilution rates (0.026 to 0.27 h^{-1}) with a limited number of experiments, without compromising steady-state results. By sampling at different growth rates it was possible to gather a rich dataset containing information on intra- and extracellular metabolite levels, biomass composition, *in vitro* enzyme activities and reaction fluxes. This section

presents an overview of the main results obtained from the performed chemostat experiments.

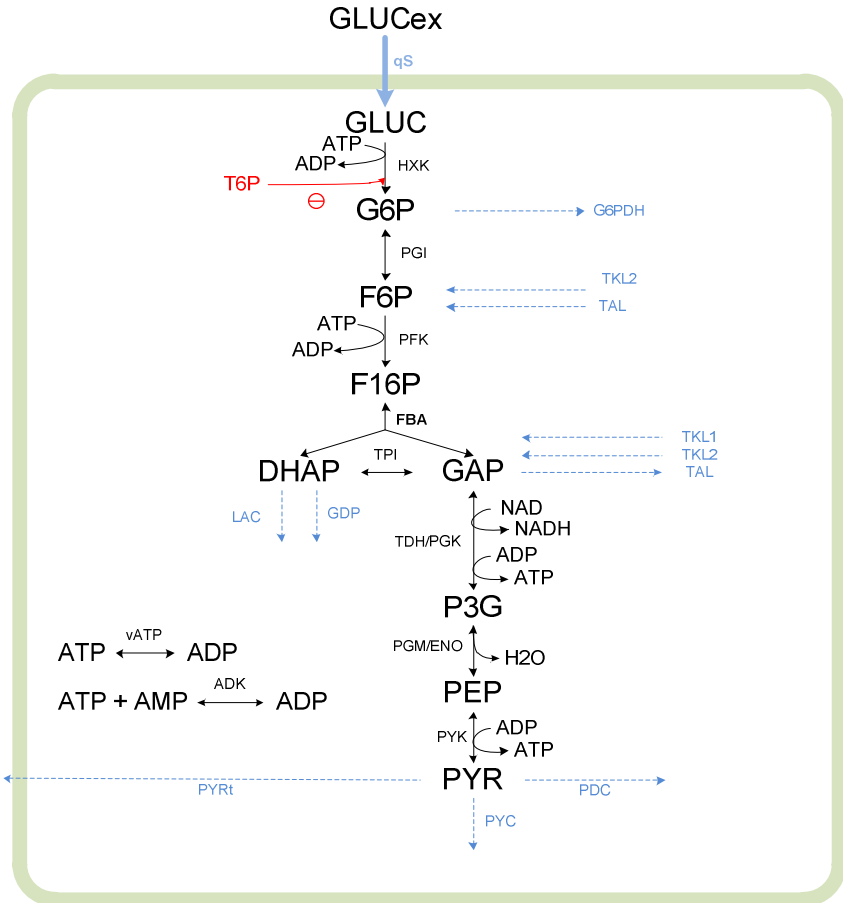

Figure 5.2: *Network described by the model (glycolysis and boundary conditions). The boundary reactions, for which the flux values were set as a function of glucose uptake rate, are represented in blue. The biomass reaction has been included in the mass balances of all metabolites except GLUC, F6P, F16P and AMP. Because no measurements are available for 13PG, the reactions catalyzed by glyceraldehyde phosphate dehydrogenase (TDH) and phosphoglycerate kinase (PGK) were lumped together into one reaction (TDH/PGK) as well as phosphoglycerate mutase (PGM) and enolase (ENO). T6P was included as an inhibitor of hexokinase (HXK).*

Extracellular metabolome and net production/consumption rates

The measured concentrations of residual glucose, biomass and main by-products can be seen in **Figure 5.3**. No significant differences could be found

between the results obtained towards the end of the fermentations and the ones obtained for the same dilution rate during the first five volume changes. This pointed out that neither long-term adaptation nor evolution occurred during these experiments.

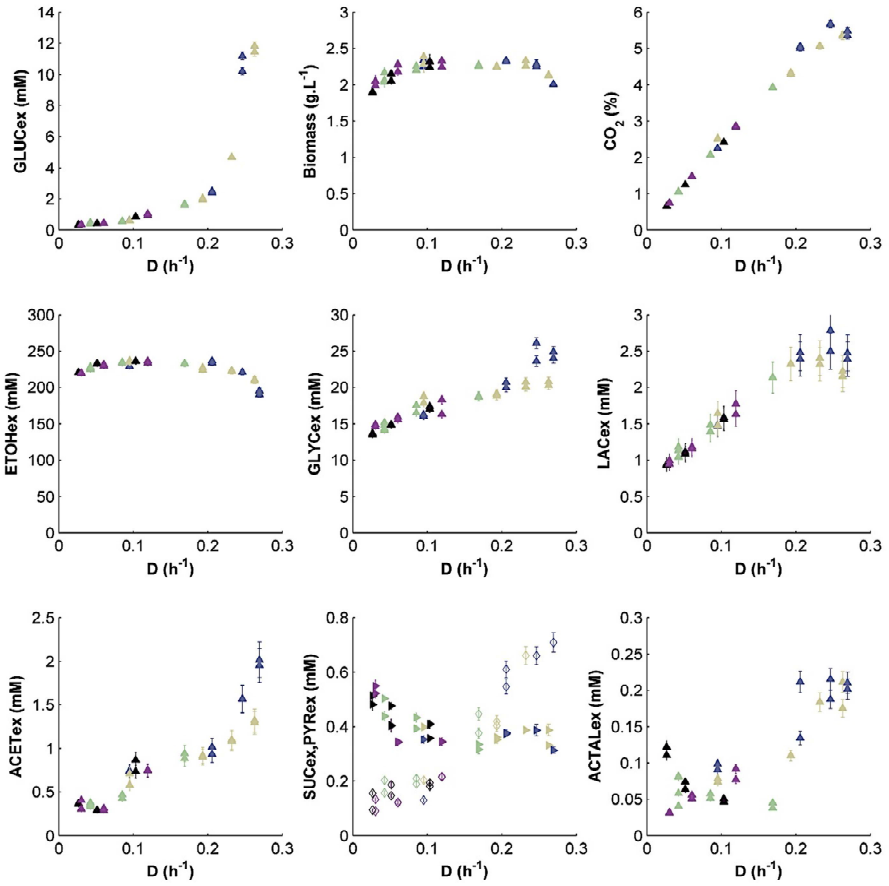

Figure 5.3: *Steady-state concentrations of extracellular metabolites measured during anaerobic glucose-limited chemostat cultivations. The different colors indicate the fermentation run from where the samples were obtained, as depicted in Figure 5.1. Succinate concentrations are the closed symbols while pyruvate levels are depicted in the open symbols.*

For the range of dilution rates applied, the most significant changes in concentrations occurred for the extracellular glucose, where levels increased with growth rate from 0.3 to 12 mM. This increase was steeper at higher dilution rates, likely as a consequence of both the glucose transport capacity

being closer to its maximum value and near-washout conditions being reached, as can be seen from the decrease of biomass concentration for dilution rates (D) higher than 0.25 h^{-1}. As expected, lower biomass concentrations are also observed at low dilution rates (< 0.1 h^{-1}) as a consequence of the energy necessary for maintenance reactions. Changes in trends of extracellular metabolite concentrations versus growth rate were also observed for the other by-products. To better evaluate these variations one should analyze the changes in the biomass-specific production rates and stoichiometry with growth rate.

Uptake and secretion fluxes

A data reconciliation routine was applied to obtain best estimates of the biomass-specific-net-conversion rates (q_{rates}) and to evaluate if there were gross measurement errors that could cause the observed changes in monotony of the trends (Verheijen, 2009). The measurements of the extracellular concentrations, the values of experimental settings (flow rates, broth volume, gas inflow rate,…) and their respective errors were used to estimate the uptake and production rates that satisfied the elemental carbon and redox balances, as described in the Materials and Methods section. The estimated q_{rates} can be found in **Figure 5.4**.

For most of the experimental data obtained the reconciliation appeared statistically acceptable, i.e. there was no indication for gross measurement errors. The only exception was the data from fermentation 4 at the dilution rates of 0.24 and 0.27 h^{-1}, indicating that it was not possible to achieve steady state within five generation-times. This was not the case for fermentation 5 at the same growth rates. The only difference between the two cultivations was the sequence of dilution rates (see **Figure 5.1**). This points out to the need of more time to reach steady-state conditions in setups operating at high dilution rate. The results from fermentation 4 were not taken into account for the steady-state analysis of anaerobic metabolism.

No large deviations were found in the trends of biomass specific conversion rates (q-rates) versus dilution rate for the five fermentations, indicating that the results from the different runs were consistent. Therefore, the data obtained from fermentations 1 to 5 could be combined to one dataset.

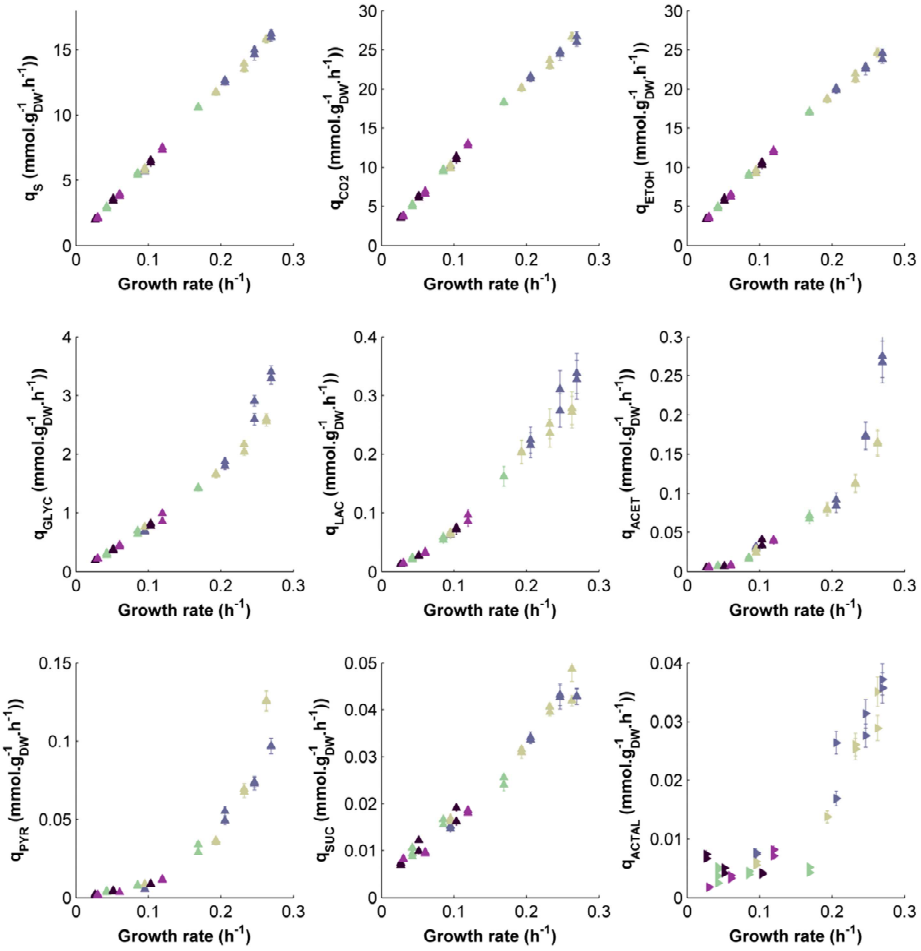

Figure 5.4: *Steady-state conversion rates of extracellular metabolites estimated from the data reconciliation routine. The different colors indicate the fermentor from where the samples were obtained, as depicted in Figure 5.1.*

Plotting the glucose uptake rate (q_S) as function of growth rate (μ) resulted in a linear relation, and could thus be described by the Herbert-Pirt equation (5.4). Using this relation it was possible to estimate the maximum theoretical yield of biomass production ($Y_{XS,max}$= 17.35 ±0.09 $g_{DW}.mol_S^{-1}$) and the flux of glucose metabolized for maintenance of the cell (m_S = 0.41 ±0.05 mmol. $g_{DW}^{-1}.h^{-1}$).

$$q_S = \frac{1}{Y_{XS,\max}}.\mu + m_S \qquad (0.4)$$

The fold increases in production rates between 0.026 and 0.27 h^{-1} was different for the different metabolites. For instance, ethanol and CO_2 show a total fold increase similar to the glucose uptake (approximately 7.5 fold change) whereas glycerol and lactate increased respectively 15 and 24 fold. This observation, together with the non-linearity of q_{Acet} and q_{Pyr} profiles, points to changes in the stoichiometry of growth.

To evaluate this, the yields of the different (by)products on glucose were calculated. Because previous observations (described in Chapter 3) had suggested that the extracellular substrate concentration is a regulator of the production of some metabolites, the yields on substrate from all the experimental setups investigated in this thesis (glucose-limited chemostats at 30 °C and different dilution rates, chemostats cultivated at 12 °C (D=0.03 h^{-1}), and the batches at 12, 18, 24 and 30 °C) were plotted together as a function of growth rate and the residual glucose level (**Figure 5.5**).

Acetate, lactate and pyruvate were the metabolites for which the yield on glucose changed the most. For the majority of the compounds there seems to be a change in monotony at a dilution of 0.1 h^{-1}. For example, the biomass yield increased with growth rate until a dilution rate of 0.1 h^{-1}, remaining constant afterwards. The opposite behavior was observed for pyruvate production. The yields on substrate of glycerol, acetate and lactate increased faster when growth rate was higher than 0.1 h^{-1}.

By comparing the plots of the different yields on substrate as function of growth rate (**Figure 5.5A**) or residual glucose (**Figure 5.5B**) it was possible to conclude that growth rate determines the yield of lactate and biomass production (i.e. the data from all different experimental setups fall within the same curve when plotting $Y_{Lac,S}$ and $Y_{X,S}$ as a function of growth rate).

On the other hand the residual glucose concentration is likely to control the production of CO_2, ethanol, pyruvate and lactate. It is still not clear the mechanism underneath regulation of acetate and glycerol production. For acetate, the trends of $Y_{Acet,S}$ obtained from batch cultivations are similar to the ones obtained in glucose-limited conditions when plotted as a function of glucose concentration. Nevertheless, the order of magnitude is significantly higher in substrate-excess fermentations. At this stage it cannot be excluded a potential effect of both residual glucose and temperature that determines the changes in acetate metabolism. For glycerol, on the other hand, is not possible to establish a correlation with any of the variables (temperature, residual glucose concentration or growth rate).

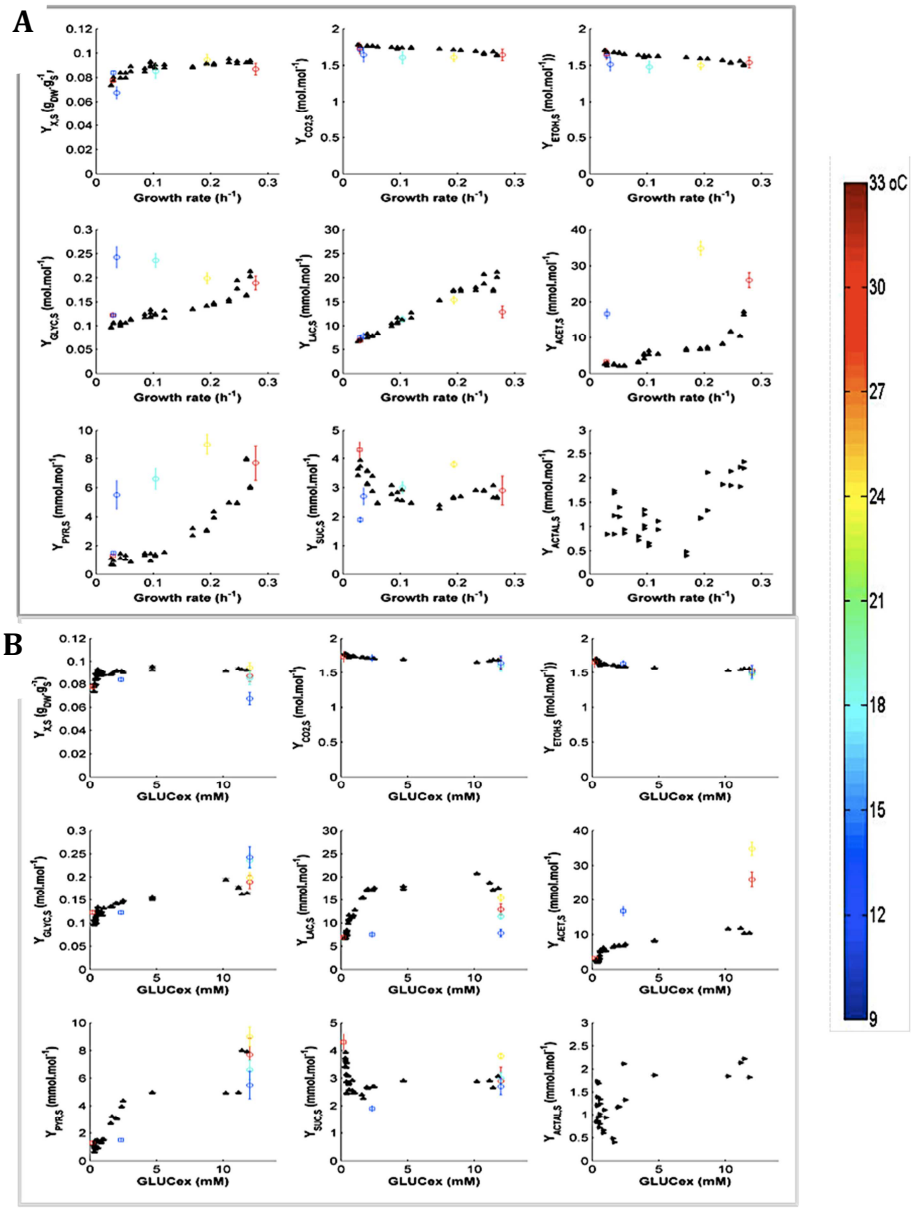

Figure 5.5: *Yields on substrate of biomass and anaerobic by-products as a function of growth rate (upper panel) and residual glucose concentration (lower panel) calculated from reconciled q_{rates}. (▲) yields from glucose-limited chemostat cultivations carried out at 30 °C and different growth rates (this chapter); (□) yields obtained from glucose-limited chemostat cultivations carried out at 30 and 12 °C (Chapter 3); (○) yields from the sequential batch cultivations carried out in Chapter 2. The different colors indicate the temperature of the broth.*

Intracellular metabolome

In order to build and validate a kinetic model it is essential to measure the intracellular metabolite levels from the pathway of interest. Therefore, the concentrations of the glycolytic metabolites and adenylate nucleotides were measured for all the dilution rates (**Figure 5.6**).

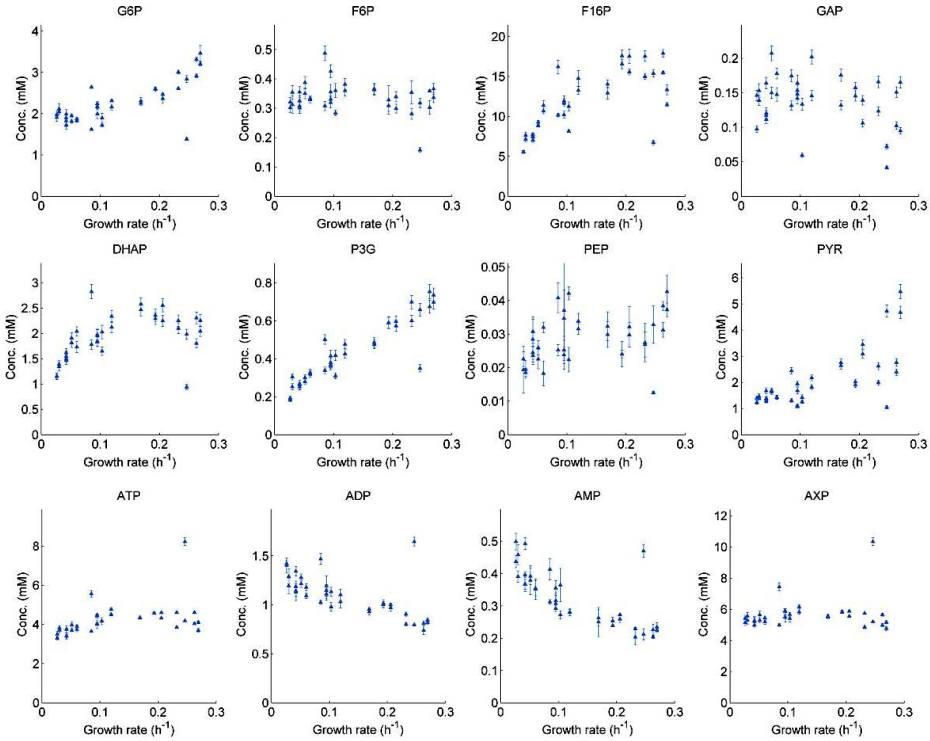

Figure 5.6: *Glycolytic metabolites and adenosine nucleotides measured for the different dilution rates. AXP refers to the sum of ATP, ADP and AMP.*

It could be observed that, although the residual glucose concentration changed approximately 65 fold, the intracellular metabolite levels do not change more than two to three fold for the 10 fold change of growth rates applied in this study (0.026 to 0.27 h^{-1}). Except for F6P and GAP, the levels of the glycolytic metabolites increased with growth rate, although there seems to be a change in the slope when the dilution rate is higher than 0.1 h^{-1}. The ATP concentrations increased with increasing growth rate, while the opposite trend was observed for ADP and AMP. The total level of adenylate

nucleotides (ATP+ADP+AMP) did not change significantly with growth rate. The average value for the entire range of growth rates applied was calculated to be 5.63 ±0.15 mM.

An overview of the range of concentrations measured compared to intracellular metabolite levels obtained from temperature shift experiments can be seen in **Figure 5.7**. All the measured glycolytic metabolites present a correlation with the extracellular glucose concentration that is similar to the one previously reported for dynamic temperature conditions, despite the changes in the catalytic activity of the enzymes upon temperature perturbations. This observation supports the conclusions from Chapter 4, whereby it is more likely that it is the residual glucose concentration and not temperature that determines the intracellular metabolite concentrations in glucose-limited cultivations at different temperatures.

Biomass composition as a function of growth rate

Information on the macromolecular biomass composition is important to calculate the amount of key metabolites needed for biomass synthesis. Also it could provide an explanation for the observed changes in the stoichiometry of (by)product formation under anaerobic conditions, as well as the metabolic shift at $\mu = 0.1\ h^{-1}$, characterized by the change in monotony of the fluxes and concentration profiles of as a function of growth rate.

The elemental biomass composition was determined for samples taken from the steady states carried out at D = 0.026, 0.03, 0.05, 0.1, 0.2, 0.23 and 0.27 h^{-1}. The results are presented in **Table 5.1**. It was observed that, per Cmol, the H content did not change significantly with growth rate (average value 1.882±0.008 mol_H/Cmol) whereas the N and O contents respectively increased and decreased with increasing dilution rate. With the values of elemental composition as a function of growth rate it was possible to apply a reconciliation procedure similar to the one used by Lange *et al.* (2000) to determine the macromolecular biomass composition, i.e. the levels of carbohydrates, protein, lipids and nucleic acids, for the different growth rates. Details on the procedure and assumptions made to deduce the macromolecular content from the elemental composition can be found in Appendix 5.1 (page 154).

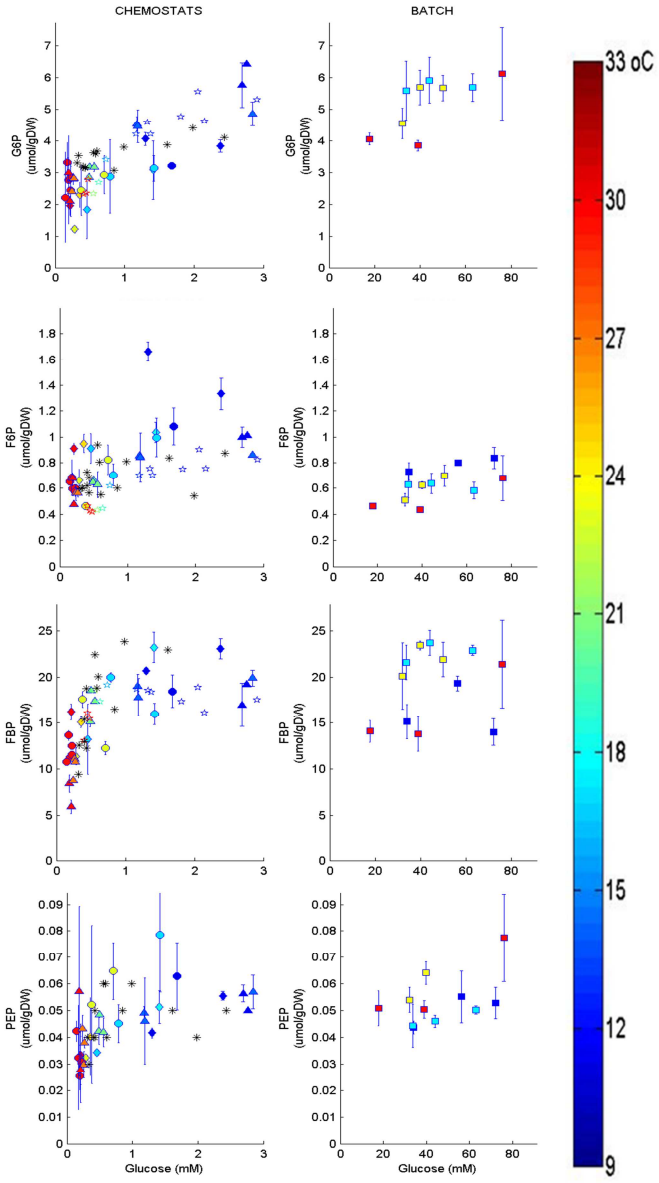

Figure 5.7: *Intracellular metabolite profiles as a function of the residual glucose concentration for the different growth rates at 30 ℃ (*) and the different dynamic temperature conditions shown in Figure 4.1. Samples were taken during sinoidal temperature cycles (Δ), linear temperature shifts from 30 ℃ (○) or 12 ℃ (◇) and from batches at different temperatures (□). Error bars refer to the standard error of the averages of at least two duplicate samples and two independent experiments. The different colors indicate the temperature of the culture at the time of sampling.*

Table 5.1: *Elemental composition of biomass (mol/Cmol) obtained for different dilution rates. The error was obtained by propagation of the analytical errors of at least two measurements of the same sample.*

D (h^{-1})	C	H	N	O
0.026	1.00 ±0.00	1.89 ±0.00	0.14 ±0.00	0.67 ±0.00
0.030	1.00 ±0.01	1.86 ±0.06	0.14 ±0.00	0.66 ±0.00
0.052	1.00 ±0.00	1.88 ±0.01	0.15 ±0.00	0.63 ±0.00
0.100	1.00 ±0.01	1.87 ±0.03	0.17 ±0.00	0.62 ±0.00
0.206	1.00 ±0.00	1.90 ±0.03	0.18 ±0.00	0.59 ±0.00
0.232	1.00 ±0.00	1.86 ±0.06	0.19 ±0.00	0.58 ±0.00
0.263	1.00 ±0.00	1.91 ±0.01	0.19 ±0.00	0.57 ±0.00

Overall there seems to be a 35% increase of the total protein amount in the biomass with increased growth rate, which is compensated by a similar decrease in the total carbohydrate amount (**Figure 5.8**). The RNA content in the cell doubles between the lowest and highest growth rate, while the total lipid content is constant (0.1083 $Cmol_{lipid}/Cmol_X$).

From the reconciled elemental composition it was possible to calculate the biomass molecular weight. Apparently the symmetrical behavior of the most abundant components (carbohydrates and protein) allows the cell to maintain a constant molecular weight. The average value obtained for the different growth rates was 25.98 ±0.11 $g_{DW}/Cmol_X$.

In vitro enzyme activities

To be able to simulate fluxes and metabolite concentrations, it is important to determine if there are changes in the enzyme levels for the entire range of growth rates studied. If that is the case, functions need to be added to describe variations in enzyme activities with growth rate. *In vitro* enzyme activity assays were carried out with cell extracts from the anaerobic chemostat cultivations. A survey was made to gather *in vitro* enzyme activity measurements done to different steady-state cultures of *S. cerevisiae* CEN.PK113-7D grown in glucose-limited chemostats.

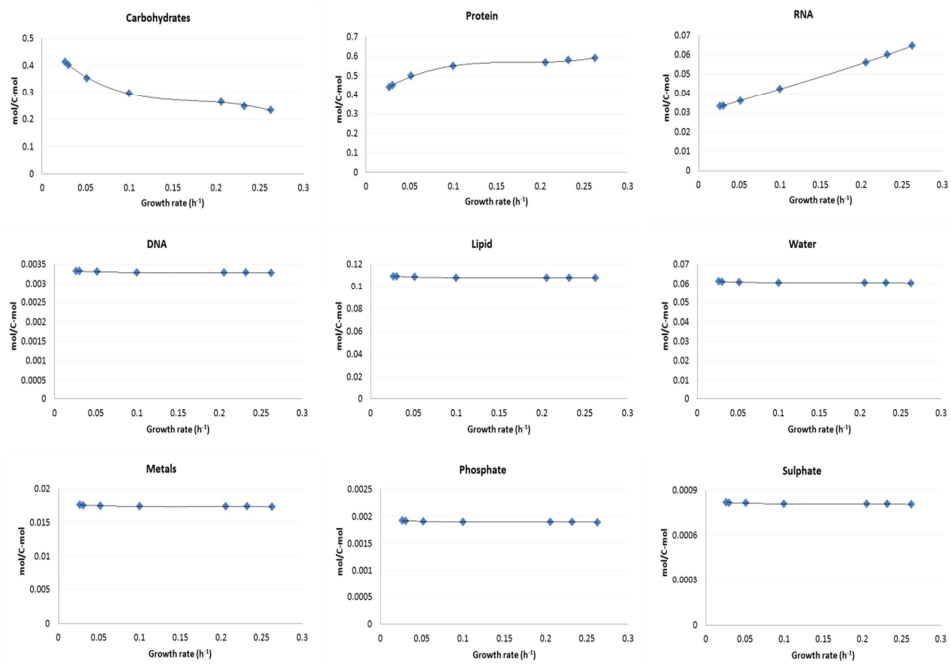

Figure 5.8: *Macromolecular composition of biomass as a function of the growth rate.*

The aim was to determine if there could be a conserved relation between enzyme activities and growth rate between aerobic and anaerobic conditions that could be used to extrapolate the enzyme activities for which no experimental measurement was available under anaerobic conditions. Only literature data with measurements obtained using similar *in vitro* protocols was taken into account. This minimized the impact of experimental differences on the search for correlations between aerobic and anaerobic conditions. The data sources used are described in **Table 5.2** and the results gathered are presented in **Figure 5.9**.

Different relations between *in vitro* activity and growth rate were obtained for the six glycolytic enzymes measured. It was observed that hexokinase was the enzyme for which activities change the most with growth rate (approximately a six fold decrease at increasing growth rate between 0.03 and 0.27 h^{-1}). Enolase (ENO) and phosphoglycerate mutase (PGM) present a two-fold difference in activity while the other enzymes

analyzed did not change more than 1.5 fold. Although overall the changes in enzyme activity are not as significant as the changes in flux, they are of the same order of magnitude as the measured changes in intracellular metabolite concentrations. Therefore it must be expected that changes in enzyme capacity with growth rate can have an impact on the parameterization of the model.

Table 5.2: *Resume of data sources for enzyme activity measurements of S. cerevisiae CEN.PK 113-7D grown at 30 °C and using glucose as carbon source. (Aer.) and (Anaer.) refer, respectively, to aerobic and anaerobic conditions.*

	Reference	Aer.	Anaer.	D (h^{-1})
■	This study		x	From 0.03 to 0.27 h^{-1}
□	Mashego *et al.* (2005)	x		0.1 h^{-1}
▲	Tai *et al.* (2008)		x	0.03 h^{-1}
◇	Canelas *et al.* (2010)	x		0.4 (batch) and 0.1 h^{-1}
△	Van Hoek *et al.* (2000)	x		From 0.05 to 0.375 h^{-1}
x	Van den Brink *et al.* (2008)	x		0.1 h^{-1}
○	Abbot *et al.* (2009)	x		0.1 h^{-1}

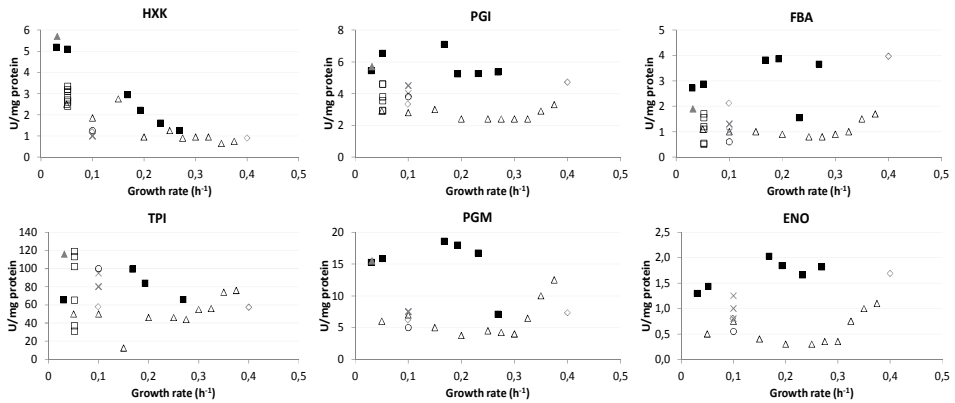

Figure 5.9: *Enzyme activities as a function of the growth rate in aerobic (open symbols) and anaerobic conditions (closed symbols). For a more detailed reference of the data sources used, please consult the symbols in Table 5.2.*

The activities under anaerobic conditions where more than two fold higher that the ones measured for aerobic cultures ate the same growth rate. But no unique relationship was found between the measured enzyme activities and growth rate, neither for anaerobic nor aerobic data. Also no

correlation was found when plotting the enzyme activities as a function of the residual glucose concentration or the substrate(s) of the enzymatic reactions (data not shown).

Stoichiometric model, lumped biomass reaction and flux distribution

Description of the full stoichiometric model

Besides the concentrations of the kinetic effectors (substrate, products, enzyme levels,…), also the fluxes through the reactions are needed to parameterize a kinetic model. When samples are taken in steady-state conditions (i.e. when there is no accumulation of intracellular metabolites), the intracellular fluxes can be estimated by metabolic flux analysis, such as exemplified by Van Gulik and Heijnen (1995). The same approach has been followed to determine the fluxes through the central carbon metabolism in the anaerobic chemostat cultivations carried out in this study.

An anaerobic stoichiometric model of *S. cerevisiae* was developed from a previously published compartmented stoichiometric model (Daran-Lapujade *et al.*, 2004). Literature data were used to make a thorough revision of this scaffold model and to adapt it to anaerobic conditions. Transcript data from Fazio *et al.* (2008) was used to support decisions on cofactor specificity of reactions (NADH or NADPH coupling reactions) caused by the expression of different isoenzymes under anaerobic conditions. For instance, it was set that under anaerobic conditions, acetaldehyde dehydrogenase uses $NADP^+$ as cofactor. Another example is lactate production that, under anaerobic conditions, can occur in the methylglyoxal bypass via methylglyoxal reductase (resulting in NADPH consumption and NADH production) or via methylglyoxal glyoxylase using glutathione. It was observed from the RNA expression data under different conditions and different growth rates of Fazio *et al.* (2008) that the Gre2 expression of the gene related to methylglyoxal redutase (Gre2) is negligible under anaerobic conditions compared to Glo1. It can therefore be concluded that lactate is produced via methylglyoxal glyoxylase and not redutase.

No changes of the anaerobic model were made regarding the stoichiometry of anabolic reactions, except for the desaturation of fatty acids. Because palmitoleate and stearate cannot be desaturated in the absence of oxygen (Bloomfield and Bloch, 1960), these reactions have been replaced by

transport of oleic and palmitoleic acid from the extracellular medium in anaerobic conditions. Furthermore, a reaction was introduced to account for the maintenance energy requirements and, in this way, satisfy the ATP and ADP balances.

However, from the set of reactions used in the full-anaerobic-stoichiometric model it was not possible to satisfy the balances for the NAD^+ and NADH species. For dilution rates lower than 0.1 h^{-1} there is a 35% surplus gap in the NADH balance. This gap decreases linearly to 5% when increasing the growth rate from 0.1 to 0.26 h^{-1}, and could not be closed, even considering different co-factor specificity of some reactions (e.g. proline dehydrogenase:pyrroline-5-carboxylate reductase (Matsuzawa and Ishiguro, 1980), methylenetertrahydrofolate reductase (Raymond *et al.*, 1999) and isocitrate dehydrogenase (Haselbeck and McAlister-Henn, 1993)). Because the redox balance is satisfied when considering the extracellular components alone (black-box model) it must be concluded that there are reactions missing in the intracellular stoichiometric model that act as NADH sink. Because it was not possible from genome databases (www.yeastgenome.org) neither from available literature on redox metabolism to find a candidate for the missing reaction, the NAD^+/NADH balance was not used as constraint in the stoichiometric model.

Lumped model and final biomass reaction

Full stoichiometric models of organisms can be used to perform metabolic flux analysis and determine the rates of production/consumption of most intracellular metabolites in the cell. However, because this study targets specifically the kinetic behavior of anaerobic yeast glycolysis under different growth rates, it seemed appropriate to lump the anabolic reactions of the full stoichiometric model towards biomass in order to focus on central carbon metabolism. By lumping the full stoichiometric model it is also possible to estimate the amounts of glycolytic metabolites consumed for biomass formation and include these in the kinetic model of anaerobic yeast glycolysis.

A stoichiometric matrix with all anabolic reactions was put in row echelon form and used to calculate the quantity of the precursors from central metabolism needed to form one Cmol biomass with the macromolecular composition determined in page 131 for each growth rate. As expected from

the changes in the biomass composition versus growth rate, the demand for precursors normally associated with carbohydrate synthesis (e.g. G6P) decreased with increasing growth rate, opposed to the higher requirements of metabolites from lower glycolysis (e.g. 3PG and PEP), which are precursors of aminoacid biosynthesis. Although statistically significant, the changes in the coefficients of the lumped biomass formation reaction were relatively mild (average fold change was 1.38±0.13) compared to the 10-fold range of growth rates applied.

By performing a metabolic flux analysis using the lumped-stoichiometric model described above it was possible to estimate the intracellular flux distribution of the network depicted in **Figure 5.2**. The measured concentrations of extracellular glucose and (by)products with their standard errors were used as input for the model and the network fluxes were obtained in a similar way as described for the data reconciliation procedure. The only difference was that also the molar balances for the intracellular compound were used as constraints.

No significant differences were found between the predictions of the full and lumped stoichiometric model, indicating that the latter one can be used to describe the central carbon metabolism of anaerobic yeast glycolysis (data not shown). The intracellular fluxes obtained from the lumped stoichiometric model were used to parameterize the kinetic model as will be described below.

Thermodynamic reaction classification

From the measured intracellular levels of the glycolytic metabolites and the flux estimates it is possible to classify the different enzymatic reactions in the network according to their displacement from thermodynamic equilibrium (see Materials and Methods, page 118). In a previous study, Canelas *et al.* (2011) carried out a thermodynamic reaction classification using aerobic *S. cerevisiae* data. In this study the enzyme levels were assumed constant. However, as already shown in this chapter, the changes in enzyme activities under anaerobic conditions were of the same order of magnitude as the changes in metabolite levels, and neglecting these could compromise the analysis of thermodynamic displacement. Therefore the changes of enzyme levels with growth rate were taken into account in the reaction classification procedure for anaerobic conditions. Assuming that adjustments in enzyme

capacity (V_{max}) are a consequence of changes in enzyme levels (e) and that $V_{max} = e.k_{cat}$, equation (5.2) can be rewritten as:

$$\frac{v}{e} = k_{cat}\beta(x,p)\left(1-\frac{\Gamma}{K_{eq}}\right) \quad (5.5)$$

The specific catalytic activity of each enzyme (k_{cat}) is in this way considered to be constant for the range of conditions evaluated. Because the data gathered from the *in vitro* enzyme activity assays in this study did not cover all the glycolytic enzymes for all dilution rates studied, an attempt was made to determine kinetic functions that could describe the changes in enzyme levels (e) with growth rate based on literature data.

Kinetics of enzyme production

Most kinetic models available in literature do not include changes in enzyme levels. However, as presented in **Figure 5.9**, this assumption is not realistic for the current conditions. The kinetics of enzyme production should then be included in the kinetic model so the changes in enzyme levels for each growth rate are properly described in the final model from the balance to the enzyme amounts.

In general, the production rate of an enzyme ($v_{e,i}$ in $U.g_{DW}^{-1}.h^{-1}$) can be calculated from a mass-balance including the enzyme activities (e_i in $U.mg_{prot}^{-1}$) and the whole cell protein amount ($Prot$ in $mg_{prot}.g_{DW}^{-1}$), which reads:

$$\frac{de_i}{dt} = v_{e,i} - \left(k_{\deg,i} + \mu\right).e_i.Prot \quad (5.6)$$

For steady-state conditions the accumulation term vanishes, and thus the production rate will be the same as the sum of the degradation rate ($k_{deg,i}.e_i.Prot$) and the dilution term ($\mu.e_i.Prot$).

$$v_{e,i} = \left(k_{\deg,i} + \mu\right).e_i.Prot \quad (5.7)$$

A study from Van Eunen (2010) regarding protein degradation rates in aerobic glucose-limited chemostat cultivations at 0.1 h^{-1}, has shown that at 30 °C $k_{deg,i}$ is lower than 10% the value of μ. Therefore, in the absence of other data regarding the degradation rates for all glycolytic enzymes, it was assumed that $k_{deg,i}$ is negligible compared to the growth rate when calculating

the enzyme production rate. This means that the protein production rate can be calculated from the experimental measurements of enzyme activities and the whole cell protein amount obtained from the biomass composition.

$$v_{e,i} = \mu.e_i.Prot \tag{5.8}$$

Having the estimates for the enzyme production rates it was possible to test different hypothesis for regulation mechanisms. It has been tried to plot $v_{e,i}$ of each enzyme as a function of its substrate and/or product concentration but no correlation was found (data not shown). The opposite was seen when plotting the enzyme production rates as a function of the extracellular glucose concentration for the different data sources (**Figure 5.10**). This indicates that glucose can be acting as a signaling molecule for expression of genes related to glycolytic enzyme production under glucose-limited conditions. Except for hexokinase, all enzymes showed a hyperbolic curve when plotting their production rate as a function of the extracellular glucose. More interestingly is that, except for TPI, both aerobic and anaerobic data appear to fall on the same curve.

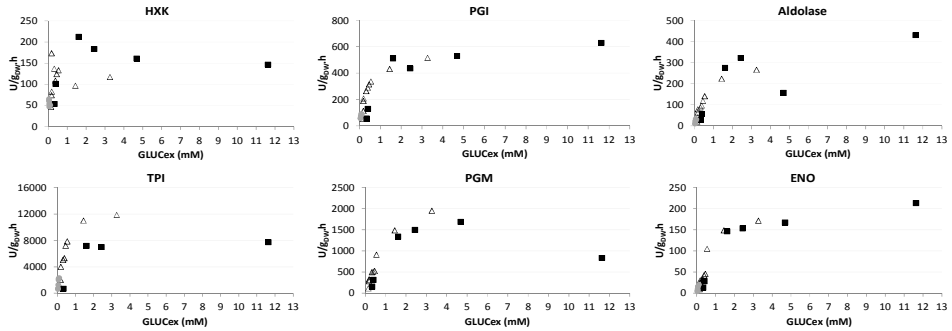

Figure 5.10: *Enzyme production rates as a function of the extracellular glucose concentration in aerobic (open symbols) and anaerobic conditions (closed symbols). For a more detailed reference of the data sources used, please consult the symbols in Table 5.2.*

A Hill type function was used to describe the enzyme production rate ($v_{e,i}$), using the residual glucose concentration as the activator:

$$v_{e,i} = V_{\max,e_i} \frac{1}{1+\left(\frac{K_e^{\,m}}{GLUC_{ex}^{\,m}}\right)} \tag{5.9}$$

wherein K_e is the dissociation constant, m is the Hill coefficient and $V_{max,e}$ is the maximum enzyme production rate. Initial estimates of the parameters of the Hill function were obtained by regression of the experimentally determined enzyme production rates (equation (5.7)) and equation (5.8). The values obtained for each individual enzyme are presented in **Table 5.3**.

Table 5.3: *Parameters of the Hill function used to calculate the enzyme-production rate as a function of the residual glucose concentration, and the average enzyme activity from the in vitro assays (* $\overline{e_i.Prot}$ *).*

Enzyme	$V_{max,e}$ ($U.g_{DW}^{-1}.h^{-1}$)	K_e (mM)	m (--)	$\overline{e_i.Prot}$ ($U.g_{DW}^{-1}$)
PGI	700	1.20	1	2540
PFK	60	0.29	3	291
FBA	400	1.42	1	1345
TPI	9795	0.35	3	34372
TDH	1202	0.97	1	3666
PGM	2183	0.83	2	6660
ENO	184	0.81	2	733
PYK	1082	0.61	2	2375

By substituting the parameters of **Table 5.3** in equation (5.8) it was possible to calculate the enzyme production rates for all the anaerobic cultivations carried out in this study. Having $v_{e,i}$ it was possible to establish the mass balances of the different enzymes and estimate the enzymatic activity for the different growth rates or residual glucose concentrations.

Results from the reaction classification

Having the estimates of enzyme activities for all the growth rates it was possible to normalize the fluxes through the different enzymatic reactions with the changes in enzyme levels. It is important to note here that e_i, as

calculated from the parameters in **Table 5.3**, would express the *in vitro* enzyme activity ($U.mg_{prot}^{-1}$). However, it is known that the activities measured from such assays are not likely to represent the *in vivo* enzyme capacity (Van Eunen *et al.*, 2010). The values of $e_i.Prot$ estimated from the enzyme balance (5.6) were normalized with the average *in vitro* enzyme capacity measured for the range of dilution rates considered in this study ($\overline{e_i.Prot}$ values in **Table 5.3**). By doing so it was possible to avoid any impact of using *in vitro* measurements when estimating the kinetic parameters of the reactions operating near- and far-from-equilibrium.

The mass-action ratios were calculated for each individual reaction and plotted as a function of the flux corrected with the changes in enzyme activities (**Figure 5.11**). Because it was not possible to measure the intracellular glucose concentrations, the glucose uptake was lumped together with the glucose phosphorylation step catalyzed by hexokinase (HXK). Also the reactions catalyzed by TDH and PGK were lumped into one and classified as such due to the unavailability of measurements of 1,3-phosphoglycerate (13BPG). The resulting reaction (TDH/PGK) was assumed to operate in pseudo-equilibrium so it would allow estimating the NAD^+/NADH ratio according to equation (5.10).

$$K_{eq}^{TDH} = \frac{P3G.ATP.NADH}{GAP.ADP.NAD.Pi} \tag{5.10}$$

The equilibrium constant assumed was the one reported by Visser *et al.* (2000) (139.2 ±7.5 M). The phosphate level (P_i) was assumed to be constant at 50 mM for all growth rates, as used in the study of Canelas *et al.* (2011).

The profiles of the mass-action ratios as a function of the fluxes are displayed in **Figure 5.11**. Similar to what reported by Canelas *et al.* (2011) for aerobic glucose-limited cultivations, it was concluded that most reactions operate near-equilibrium (more precisely PGI, FBA, TPI, ENO and ADK). The reactions HXT/HXK, phosphofructokinase (PFK) and pyruvate kinase (PYK) were classified as far-from-equilibrium and, therefore, require the use of mechanistic equations to describe the relation between flux and metabolite levels. No other reaction besides TDH/PGK was classified as being in pseudo-equilibrium. Triosephosphate isomerase (TPI) appears to operate in near-equilibrium whereas it had been classified as being in pseudo-equilibrium under aerobic conditions (Canelas *et al.*, 2011). Aerobically, a p-value of 0.0056 was obtained when classifying TPI. This is quite close to the

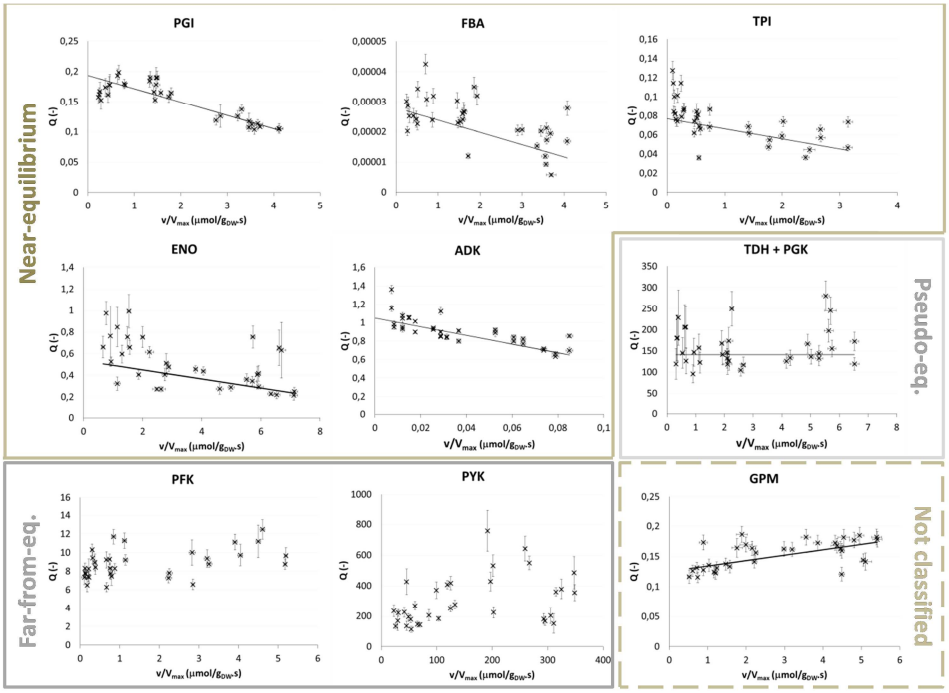

Figure 5.11: *Mass-action ratios (Γ) as a function of the flux (v) divided by the normalized enzyme level* $((e_i.Prot).(\overline{e_i.Prot})^{-1})$.

threshold value of 0.0050 used as a statistical boundary to distinguish reactions operating near- from pseudo-equilibrium.

Phosphoglycerate mutase (PGM) displayed a profile that, according to equation (5.5), goes against thermodynamic impositions. The mass-action ratio is increasing with increasing flux, to values that are higher than the estimated equilibrium constant. No error or problems could be detected in the measurements of the metabolites 2PG and 3PG or the *in vitro* activity measurements of PGM. So analytical error was excluded as being the cause for this observation. An explanation could be a positive correlation between flux and the phosphorylation state of PGM as shown by Oliveira *et al.* (2012). But because there is very few data to support this theory and quantify the changes in enzyme activity as a consequence of post-transcriptional regulation, PGM was lumped with enolase (ENO) for the current kinetic model of yeast glycolysis.

Assuming constant enzyme activities of the entire range of fluxes, as done by Canelas *et al.* (2011), did not change the classification for none of the enzymatic reactions.

Construction of the kinetic model of anaerobic yeast glycolysis for different growth rates

TDH/PGK, as discussed on the previous section, was the only reaction in the kinetic model considered to be in pseudo-equilibrium. Therefore, no mass balance was included for 3-phosphoglycerate (3PG) and its concentrations were calculated from equation (5.10).

Because the redox-balance was not included in the stoichiometric model, it was not possible to include the mass balances of the redox co-factors (NAD^+ and NADH) in the kinetic model. As an alternative, the NAD^+/NADH ratio for the different growth rates was calculated from equation (5.10). This resulted in a linear relation between the NAD^+/NADH ratio and growth rate (**Figure 5.12**), which was used in the kinetic model to obtain the changes in the redox status of the cell (equation (5.11) with μ in mmol.Cmol^{-1}.h^{-1}).

$$\frac{NAD^+}{NADH} = 0.0132\mu + 0.1665 \qquad (5.11)$$

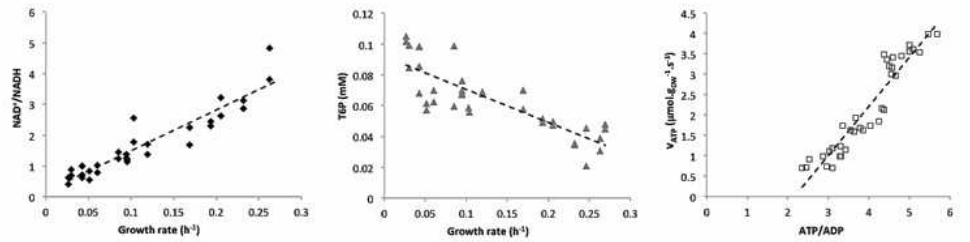

Figure 5.12: *Empirical relation used to describe the redox ratio as a function of growth rate (left graph), the concentrations of trehalose-6-phosphate (T6P) (central graph) and the flux of ATP hydrolysis (v_{ATP}) as a function of the ATP/ADP ratio (right graph).*

The reactions classified as being in near-equilibrium were parameterized according to the Q-linear kinetics (equation (5.5)). The parameters were estimated by applying a weighted linear regression to the profiles of PGI,

FBA, TPI, ENO/PGM and ADK presented in **Figure 5.11**. The values obtained can be found in

Table 5.4.

Table 5.4: *Kinetic parameters used for PGI, FBA, TPI, TDH/PGK, PGM/ENO and ADK. The $\beta.k_{cat}$ values are expressed in $\mu mol.g_{DW}^{-1}.s^{-1}$. K_{eq} has no units except for FBA and TDH/PGK where it is expressed in mM.*

		PGI	***FBA***	***TPI***	***PGM/ENO***	***ADK***
Anaerobic	K_{eq}	0.193 ± 0.004	0.028 ± 0.002	0.077 ± 0.005	0.084 ± 0.006	1.05 ± 0.02
	$\beta.k_{cat}$	8.78 ± 0.65	6.56 ± 1.50	7.29 ± 2.14	14.31 ± 3.01	0.22 ± 0.019
Aerobic *(a)*	K_{eq}	0.259 ± 0.003	0.010 ± 0.000	0.039 ± 0.002	0.464 ± 0.011	0.96 ± 0.02
	$\beta.k_{cat}$	4.07 ± 0.17	3.68 ± 0.64	--------	n.d. *(b)*	--------

(a) Parameters obtained by Canelas *et al.* (2011).
(b) Not determined for the lumped reaction.

The mechanistic expressions used in the models of Teusink *et al.* (2000) and Rizzi *et al.* (1997) were tested to describe the observed change in fluxes as a consequence of the measured intracellular metabolite concentrations of the reactions far-from-equilibrium (phosphofructokinase (PFK) and pyruvate kinase (PYK)). Due to the high number of parameters, the parameter estimation was started by estimating the V_{max} values (taking into account the changes of enzyme levels with growth rate) while maintaining the affinity parameters constant. Thereafter the best estimates of the affinity parameters were obtained, while maintaining the V_{max} values constant.

The kinetic expression from the model of Van Eunen *et al.* (2012) was used to describe HXK. It is an extension of the equation used by Teusink *et al.* (2000), with competitive inhibition by trehalose-6-phosphate (T6P):

$$v_{HXK} = \frac{V_{\max,HXK}\left(\frac{GLUC_{ex}}{K_{m,GLUC}}\frac{ATP}{K_{m,ATP}} - \frac{G6P \cdot ADP}{K_{m,GLUC} \cdot K_{m,ADP} \cdot K_{eq,HXK}}\right)}{\left(1+\frac{GLUC_{ex}}{K_{m,GLUC}}+\frac{G6P}{K_{m,G6P}}+\frac{T6P}{K_{i,T6P}}\right)\cdot\left(1+\frac{ATP}{K_{m,ATP}}+\frac{ADP}{K_{i,ADP}}\right)} \quad (5.12)$$

The T6P concentrations were set as a linear function of growth rate, as observed in **Figure 5.12**.

For estimation of the kinetic parameters it was set that the $V_{max,HXK}$ should change with growth rate according to the enzyme activity measurements (**Figure 5.9**).

Table 5.5: *Kinetic parameters estimated for the lumped reaction for glucose transport and hexokinase (HXT/HXK).*

	Van Eunen et al. (2012)	***This study***
K_{eq}	3800	3800
$K_{m,GLUC}$ (mM)	0.08	0.572
$K_{m,ATP}$ (mM)	0.15	0.144
$K_{m,G6P}$ (mM)	30	39.61
$K_{m,ADP}$ (mM)	0.23	0.0181
$K_{i,T6P}$ (mM)	0.2	0.0129
$_{ax}$ [(a)](mmol.Cmol^{-1}.h^{-1})	559.6	3769.3
$\Delta V_{max}/\Delta mu$	-------	-10.092

[(a)] In the case V_{max} is not constant, the value presented refers to the intercept (growth rate = 0 h^{-1}).

For PFK and PYK, the best solution was found using the equations from Rizzi *et al.* (1997). Specially the activation of PYK by fructose-1,6-biphosphate, which was not included in the Teusink model, has shown to be essential for a good description of the *in vivo* data (data not shown). For both enzymes no major readjustments had to be made to the affinity constants as long as the enzyme capacity (V_{max}) was allowed to change with growth rate. However, V_{max} has been predicted to change more than what was initially estimated from the kinetics of enzyme production discussed in the previous section (page 136).

$$v_{PFK} = V_{\max,PFK} \frac{ATP}{ATP + K_{ATP4}} \frac{F6P}{F6P + K_{F6P4}} \frac{1}{1 + L_4}; \qquad (5.13)$$

$$K_{ATP4} = K_{ATPS,4}\left(1+\frac{ADP}{K_{ADPC,4}}\right); \qquad L_4 = \frac{L_{0,4}}{\left(1+\frac{F6P}{K_{F6P4}}\right)^8};$$

$$K_{F6P4} = K_{F6PS,4}\frac{\left(1+\frac{ATP}{K_{ATP1,4}}+\frac{ADP}{K_{ADP2,4}}+\frac{AMP}{K_{AMP2,4}}\right)}{\left(1+\frac{ADP}{K_{ADP1,4}}+\frac{AMP}{K_{AMP1,4}}\right)}$$

Table 5.6*: Kinetic parameters used to describe the kinetics of phosphofructokinase (PFK).*

	Rizzi et al. (1997)	***This study***
$K_{AMP\,2,4}$ (mM)	0.01	0.010
$K_{AMP\,1,4}$ (mM)	8.74	9.019
$K_{ADP\,C,4}$ (mM)	0.36	0.36
$K_{ADP\,2,4}$ (mM)	0.25	0.251
$K_{ADP\,1,4}$ (mM)	239	171.287
$K_{ATP\,S,4}$ (mM)	0.004	0.004
$K_{ATP\,1,4}$ (mM)	0.25	0.250
$K_{F6P\,S,4}$ (mM)	0.008	0.0080
$L_{0,4}$	4357	4320.2
V_{max} **(a)** (mmol.Cmol^{-1}.h^{-1})	367.2845	6283.138
$\Delta V_{max}/\Delta mu$	-------	31.407

(a) In the case V_{max} is not constant, the value presented refers to the intercept (growth rate = 0 h^{-1}).

$$v_{PYK} = V_{max}\frac{\frac{PEP}{K_{PEP}}\left(\frac{PEP}{K_{PEP}}+1\right)^{n-1}}{L\left(\frac{\frac{ATP}{K_{ATP}}+1}{\frac{F16P}{K_{F16P}}+1}\right)^n+\left(\frac{PEP}{K_{PEP}}+1\right)^n}\frac{ADP}{ADP+K_{ADP}} \qquad (5.14)$$

Table 5.7: *Kinetic parameters used for PYK.*

	Rizzi et al. (1997)	***This study***
K_{ADP} (mM)	0.6	0.5515
K_{PEP} (mM)	0.6	0.4474
K_{ATP} (mM)	2	2.3028
K_{F16P} (mM)	3.9	1.7152
L	100	92.3759
n	4	4
V_{max} [(a)] (mmol.Cmol^{-1}.h^{-1})	5780	13196
$\Delta V_{max}/\Delta mu$	------	33.408

[(a)] In the case V_{max} is not constant, the value presented refers to the intercept (growth rate = 0 h^{-1}).

The flux of ATP being hydrolyzed to maintenance of the cell (v_{ATP}) was set to be a linear function of the ATP/ADP ratio (equation (5.15)) as observed in **Figure 5.12**. No other correlation was found between v_{ATP} and nucleotides concentrations or ratios (data not shown).

$$v_{ATP} = 0.378\frac{\text{ATP}}{\text{ADP}} - 0.025 \qquad (5.15)$$

Simulation results

A model of anaerobic yeast glycolysis was built by combining the equations obtained by the reaction classification method to describe the kinetics of the enzymatic reactions with the molar balances of the different metabolic intermediates and the kinetic equations that describe the enzyme production rates. Simulations were run by setting a stepwise increase in growth rate (0.02 to 0.28 h^{-1}) after a steady state was reached (every seven generation times). The obtained intracellular fluxes as a function of growth rate can be seen in **Figure 5.13**. The deviations from linearity of the fluxes from lower glycolysis and, more significantly, from lactate, glycerol and pyruvate branches reflect the changes in the stoichiometry of the network caused by the change of the biomass composition and the product yields on glucose of organic acids (acetate, lactate, pyruvate and succinate) with the growth rate.

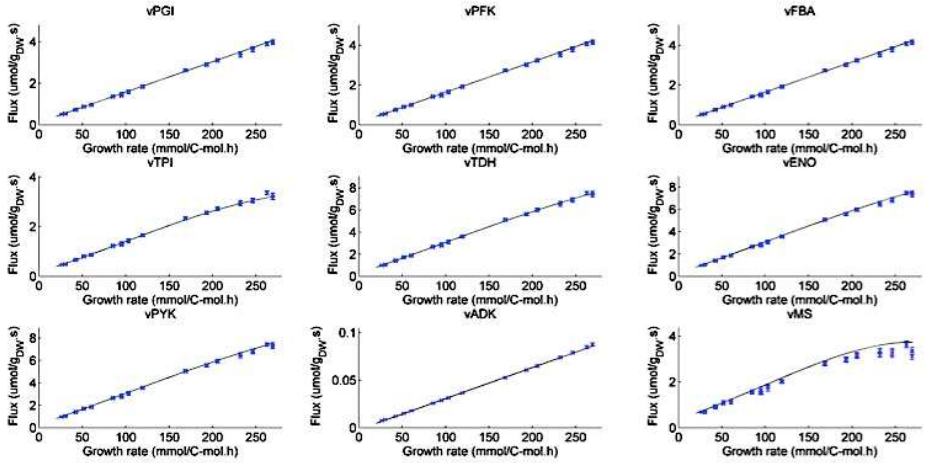

Figure 5.13: *Fluxes simulated from the kinetic model (black line) compared to the steady-state values estimated by flux balance analysis of anaerobic chemostat cultivations at 30 ℃ (x).*

With increasing growth rate, more carbon is channeled towards the pentose phosphate pathway, biomass formation and, consequently, glycerol formation. The carbon being redirected to lower glycolysis and ethanol production decreases.

The simulated enzyme production rates were very close to the values estimated from experimental data (**Figure 5.14**).

The model could also provide quite a good description of the changes in metabolite concentrations with growth rate under anaerobic conditions (**Figure 5.15**). This observation, together with the similar correlation between extracellular glucose and intracellular metabolite concentrations obtained with this setting compared to previous temperature-shift experiments done to anaerobic glucose-limited chemostats (**Figure 5.7**) motivated to extend this model to dynamic temperature conditions.

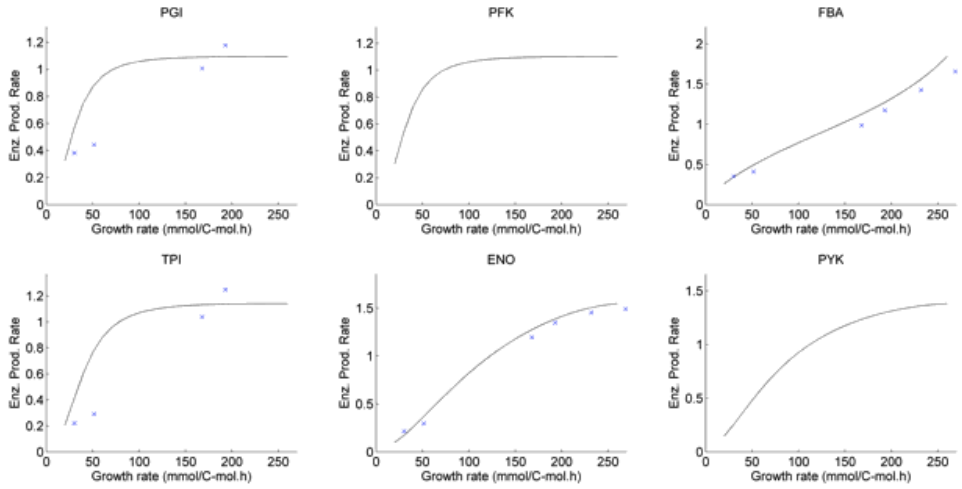

Figure 5.14: *Normalized enzyme production rates simulated by the kinetic model (black line) compared to the values estimated by the in vitro enzyme activity measurements and equation (5.7) (x). Because no data was available regarding changes in activity of PFK and PYK under anaerobic conditions, the kinetic parameters were taken from aerobic data.*

Model validation using data from experiments with dynamic temperature conditions

Previous studies on the impact of temperature on the kinetic parameters of enzymes from central carbon metabolism have allowed quantifying the drop in the catalytic activities of the glycolytic enzymes with decreasing temperature in the mild suboptimal range. By incorporating this relation into the model it was possible to include temperature as a variable and simulate dynamic temperature conditions. The temperature impact on the maximal enzyme production rate ($V_{max,ei}$) in equation (5.9) was not included in the model.

The metabolite profiles obtained when simulating the linear temperature-shifts A30 and A12 from Chapter 3 are shown in **Figure 5.16**.

The temperature-dependent model could reproduce the major trends of the metabolite concentrations, even when simulating temperature perturbations applied to 12 °C chemostats. The simulated profiles that deviated the most when compared to experimental measurements were the nucleotide concentrations (**Figure 5.17**). Somehow the model could not

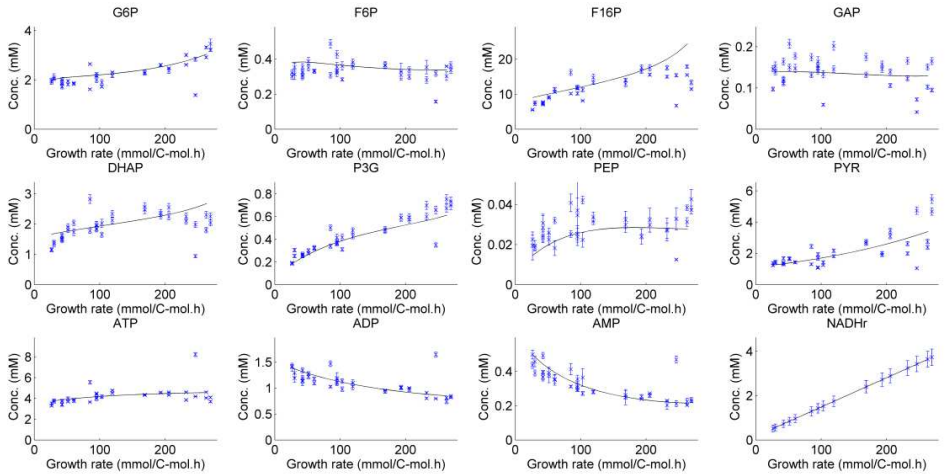

Figure 5.15: *Simulated concentrations of glycolytic metabolites (black line) compared to the steady-state values measured in anaerobic chemostats cultivations at 30 °C (x).*

capture the increase in ATP levels measured during time periods where temperature decreased. Because the flux estimates from the kinetic model were consistent with the profiles obtained from the black-box model, it is not likely that the demand of ATP for maintenance reactions changes with temperature. Despite these differences between experimental and simulated nucleotides concentrations, the overall model fit seemed to indicate that the model could be used to make *in silico* predictions on the temperature impact on parameters not easily assessed by experimental approaches.

Because no information was available on changes in the redox state of the cell (NAD^+/NADH ratio) during temperature changes, some simulations were run to test if the linear relation obtained with growth rate from the anaerobic chemostats at different growth rates but constant temperature was valid also for dynamic conditions. By simulating a scenario where the NAD^+/NADH ratio would be constant during the temperature perturbations it was observed that most of the metabolite levels would change considerably less compared to the conditions where the redox ratio is changing. This strongly indicated that changes in NAD^+/NADH are a consequence of metabolic regulation and not adjustment of the levels of redox-related enzymes.

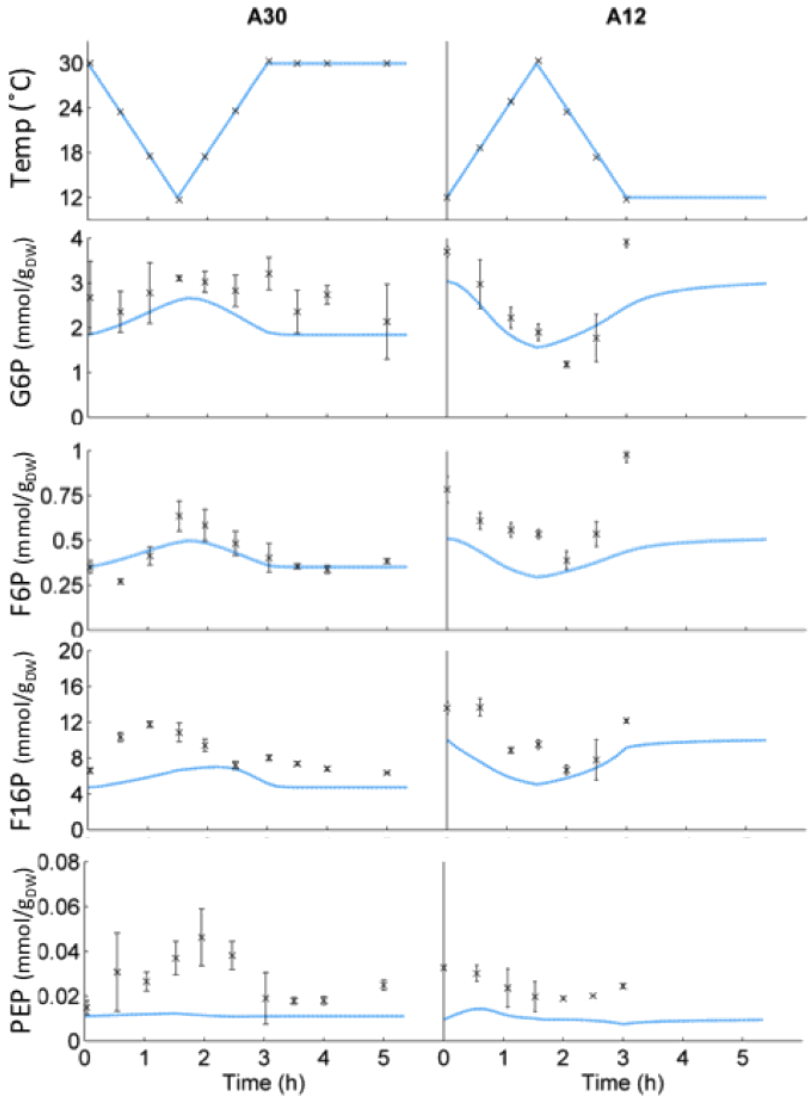

Figure 5.16: *Experimental and simulated concentrations of glycolytic metabolites during dynamic temperature conditions.*

Another interesting point of analysis is the temperature impact on the enzyme production rate. A first simulation had been carried out where it was imposed that the temperature impact on the maximum enzyme production rate was the same as for the glycolytic enzymes. However, by doing so, the higher residual glucose concentration obtained under steady-state conditions in 12 °C chemostats compared to 30 °C was not enough to

compensate for the loss of capacity of enzyme production at the lower temperature. As a consequence, the enzyme levels in 12 °C chemostats were significantly lower than at 30 °C, leading to significant deviations in the simulated metabolite trends compared to the experimental measurements. This *in silico* analysis has allowed concluding that the temperature impact on protein production rate is likely to be milder compared to the one quantified for catabolic reactions.

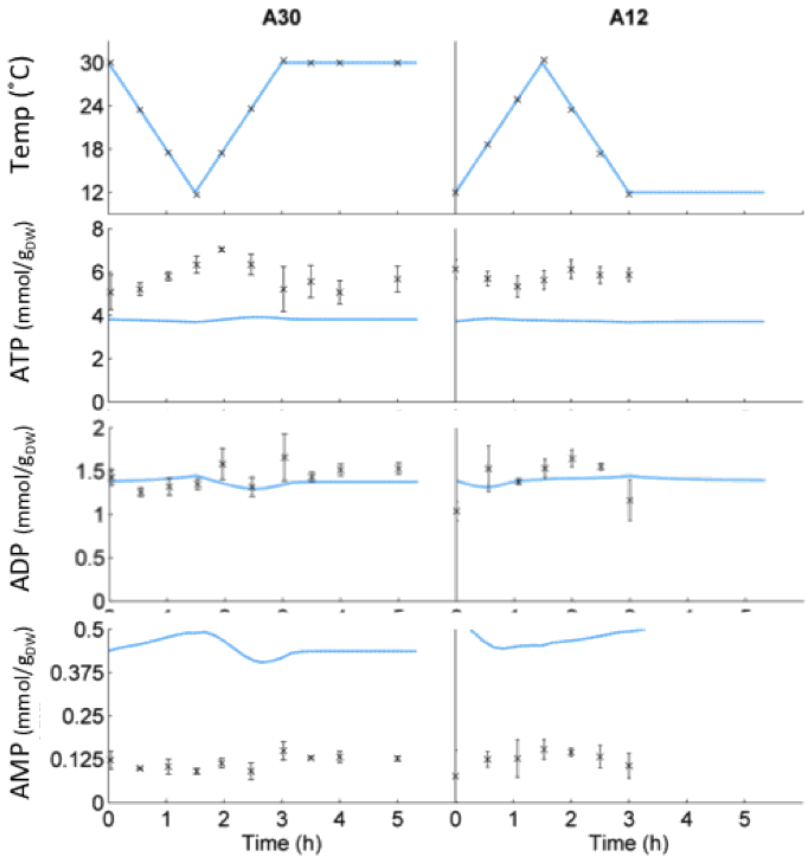

Figure 5.17: *Simulated and measured concentrations of the adenosine nucleotides during linear temperature perturbations.*

Discussion

Robust kinetic models capable of describing the *in vivo* central carbon metabolism of *S. cerevisiae* can be extremely useful not only to develop

industrial fermentation processes, but also to better study and understand the regulation mechanisms used by yeast to change its growth rate upon environmental changes (temperature, substrate availability…). This chapter aimed at delivering an *in vivo* model that can be easily scalable to other experimental conditions (e.g. aerobic conditions) and further optimized to test the impact of different factors on the regulation of central carbon metabolism in yeast.

The first step done was to gather a relevant dataset containing information on the behavior of the different effectors of enzyme-catalyzed reactions. By performing parallel chemostat fermentations with different stepwise changes in dilution rate it was possible to collect steady-state data from twelve growth rates between 0.026 and 0.27 h^{-1} with a limited number of chemostat experiments. The measured metabolite concentrations and the estimated rates of production of the most relevant (by)products have shown that the results between the different cultivations were reproducible and that long-term adaptation was avoided by limiting the maximum number of generations per fermentation to 22. The reproducibility of this approach was also supported by the agreements of the estimated yields on substrate compared to previously published data. For instance, the parameters of the Herbert-Pirt equation match the values reported by Boender *et al.* (2009).

The gathered data on extra- and intracellular metabolite levels, glycolytic fluxes and changes in enzyme activities with growth rate have allowed to apply the reaction classification method developed by Canelas *et al.* (2011) and parameterize the reactions operating near- and in pseudo-equilibrium. Although the thermodynamic classification obtained for anaerobic conditions is quite similar to the one reported for aerobic conditions, the kinetic parameters were not the same for the two conditions. This was particularly unexpected regarding the values of the equilibrium constants (K_{eq}), because these should reflect the thermodynamic equilibrium of the chemical reaction, which is independent of the nature or quantity of the catalyst (e.g. enzyme amounts or expression of isoenzymes). Because the analytical methods and strains used were similar in both studies, the difference in kinetic parameters between aerobic and anaerobic datasets provides an indication that the Q-linear approach might be simply the result of an empirical observation and caution should be used when trying to give a thermodynamic meaning to the estimated parameters.

Another difference compared to previous work from Canelas *et al.* (2011) is that, for anaerobic conditions, changes in enzyme activity might need to be taken into account when describing the kinetics of glycolytic reactions. The absolute change in enzyme activities measured from *in vitro* assays indicated that, although small when compared to the change in growth rate, it is in the same order of value as the changes in metabolite levels and mass-action ratio. This means that it cannot be excluded that, contrary to what assumed for aerobic conditions where the metabolite concentrations changed a factor 3 to 4 more, enzyme activities play a significant role in regulating the glycolytic flux at different growth rates in anaerobic conditions. Nevertheless, the similarity in the reaction classification between anaerobic and aerobic conditions and, most of all, the comparable kinetic functions obtained for the enzyme production rates as a function of the extracellular glucose concentration indicate that a modification of the theory underneath the Q-linear kinetics approach or a different (approximate) kinetic format might help to construct a kinetic model valid for both aerobic and anaerobic conditions.

However some problems still remain to be tackled. The high dependency of intracellular metabolite levels and enzyme production rates on the extracellular glucose concentration stresses the need for accurate models of the kinetics of glucose uptake. This would allow modeling separately the glucose uptake and phosphorylation steps and understand the apparent decrease in capacity of hexokinase with increasing growth rate. Further analytical developments to measure intracellular glucose content and studies on the link between storage-carbohydrate metabolism and glycolysis are expected to shed some light on this topic.

Also the *in silico* results did not allow explaining the observed shift in metabolite profiles and yields on glucose for growth rates higher than 0.1 h^{-1}. For instance, no enzymes were operating near their maximum capacity and the same set of kinetic parameters could be used to describe the whole range of fluxes and metabolite concentrations. Therefore, it is unlikely that the metabolic shift comes from changes in the kinetics of enzyme conversion due to the expression of other isoenzymes. An explanation could be the observed changes in biomass composition with growth rate, namely the increase in protein and decrease in carbohydrate contents at higher growth rates. A specific growth rate of 0.1 h^{-1} could mark the transition to a metabolic state where energy supply is saturated considering the higher biosynthetic

demands. To expand the current model to other pathways, namely carboxylic acid and glycerol production, could provide more clues to explain this observation.

Another observation from the simulation results is the mild impact temperature has on the enzyme production rates. This is likely the consequence of both the increased transcription of genes related to ribosome biogenesis (Tai *et al.*, 2007b) and higher RNA stability at lower temperatures. This means that the conclusions of Chapter 4, where it was seen that the activity of the glycolytic enzymes decreased with the same fold-change with decreasing temperature, cannot be extended to complex polymeric reactions, such as protein production.

Nevertheless, applying a simplified kinetic approach using only two kinetic parameters for reactions operating at near-equilibrium, it was possible to developed a model that reproduces quite well the glycolytic metabolite levels and fluxes for the range of anaerobic growth rates evaluated. More interestingly, it could be shown that a kinetic model built exclusively from steady-state data can be used to describe mild dynamic conditions such as temperature-shifts. This opens possibilities to study *in silico* the impact of other regulation mechanisms, such as enzyme phosphorylation, on the metabolism under more drastic conditions (e.g. glucose pulses).

Appendices

5.1 Methods used to derive the macromolecular biomass composition

To derive the macromolecular composition it was set that the proteins, lipids, carbohydrates and nucleic acids had the elemental compositions determined by de Lange *et al.* (2001) for the same strain growing in aerobic conditions (**Table 5.8**).

Table 5.8: *Elemental composition of the macromolecular components as determined by de Lange et al. (2001). MW refers to the molecular weight (g/Cmol).*

	C	H	O	N	P	S	metal	charge	MW
water	0.00	2.00	1.00	0.00	0.00	0.00	0.00	0.00	18.02
phosphate	0.00	1.00	4.00	0.00	1.00	0.00	0.00	-2.00	95.98
sulphate	0.00	0.00	4.00	0.00	0.00	1.00	0.00	-2.00	96.06
DNA	1.00	1.26	0.61	0.38	0.10	0.00	0.00	0.00	31.52
protein	1.00	1.58	0.32	0.27	0.00	0.00	0.00	-0.01	22.63
carbohyd.	1.00	1.67	0.83	0.00	0.00	0.00	0.00	0.00	27.03
RNA	1.00	1.23	0.74	0.39	0.11	0.00	0.00	0.00	33.76
lipid	1.00	1.87	0.15	0.01	0.01	0.00	0.00	0.00	16.72
metal	0.00	0.00	0.00	0.00	0.00	0.00	1.00	0.00	37.24

Based on the elemental composition of biomass estimated from ECN measurements and the one of the macromolecules. a data reconciliation routine was set to calculate the macromolecular biomass composition.

Because no measurements were available regarding the total lipid, DNA, water and sulphate content in the cell, it was set that its values were independent of the growth rate and to have the same average value calculated by de Lange *et al.* (2001). This meant that the variables to be determined were the protein, RNA and total carbohydrate.

The RNA content can be set as being a function of the protein production rate (q_{prot}) which is obtained by multiplying the amount of protein in the cell by the growth rate. This observation can be seen for both the data of de Lange *et al.* (2001) as for the anaerobic data from Nissen *et al.*, 1997, as presented in **Figure 0.18**. To be sure that the regression applied to obtain the correlation between RNA amount and q_{prot} would be valid for the entire

range of dilution rates in this study, it was decided to also take into consideration the data from Nissen *et al.* (1996), even though it refers to measurements done in other strain. The equation obtained was (R^2=0.88):

$$RNA(g/g_{DW}) = (0.33 \pm 0.04) \times q_{prot}(g_{prot}/g_{DW}.h) + (0.039 \pm 0.004) \quad (5.16)$$

From the work of de Lange *et al.* (2001) it was also possible to observe that the phosphate content in the cell has an inverse correlation with the protein content and production rates (**Figure 0.18**).

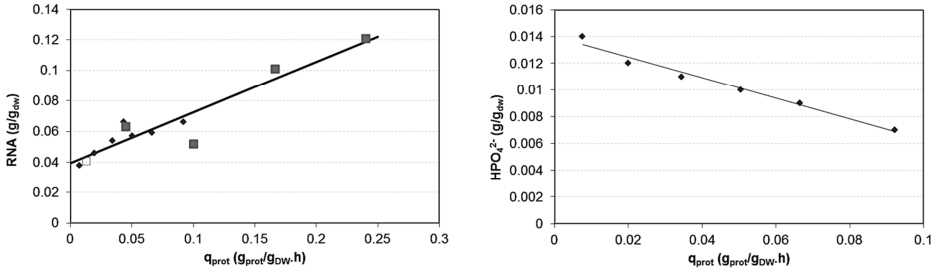

Figure 0.18: *Correlation between protein production rate (q_{prot}) and the RNA (left plot) and HPO_4^{2-} amounts in the cell (right plot). The black line indicates the regression obtained by considering the data from de Lange et al. (2001) (◆) and Nissen et al. (1996) (■).*

By having the RNA levels described as a function of the protein production rate and having set that the DNA and lipid contents to be constant, it was possible to calculate the total protein content from the N balance, using the nitrogen content in the biomolecules (N_i) according to the values presented in **Table 5.8** and the N_{biom} obtained from the elemental composition:

$$\Pr ot.N_{prot} = Biomass.N_{biom} - RNA.N_{RNA} - DNA.N_{DNA} - Lipid.N_{lipid} \quad (5.17)$$

The total carbohydrate content (*Carb*) can be calculated in a similar way from the carbon balance:

$$Carb.C_{carb} = Biomass.C_{biom} - \Pr ot.C_{prot} - RNA.C_{RNA} - DNA.C_{DNA} - Lipid.C_{lipid} \quad (5.18)$$

These mass balances where included in a reconciliation routine where, by using the elemental composition measurements as an input, the amount of carbohydrate, protein, RNA and phosphate could be calculated as a function of growth rate.

5.2 Details of the kinetic model

List of abbreviations used

Abbreviation	Name	Molecular Formula
Intracellular metabolites		
ADP	ADP	$C_{10}H_{12}N_5O_{10}P_2^{-3}$
AMP	AMP	$C_{10}H_{12}N_5O_7P^{-2}$
ATP	ATP	$C_{10}H_{12}N_5O_{13}P_3^{-4}$
DHAP	dihydroxyacetone-phosphate	$C_3H_5O_6P^{-2}$
F16P	fructose1.6-bisphosphate	$C_6H_{10}O_{12}P_2^{-4}$
F6P	fructose6-phosphate	$C_6H_{11}O_9P^{-2}$
G6P	glucose6-phosphate	$C_6H_{11}O_9P^{-2}$
GAP	glyceraldehyde 3-phosphate	$C_3H_5O_6P^{-2}$
GLYC	glycerol	$C_3H_8O_3$
H	hydrogen	H^+
NAD	NAD	
NADH	NADH	
P_i	phosphate	PHO_4^{-2}
PEP	phosphoenol-pyruvate	$C_3H_2O_6P^{-3}$
P13G	1,3-phosphoglycerate	$C_3H_4O_{10}P_2^{-4}$
P2G	2-phosphoglycerate	$C_3H_4O_7P^{-3}$
P3G	3-phosphoglycerate	$C_3H_4O_7P^{-3}$
PYR	pyruvate	$C_3H_3O_3^{-1}$
T6P	Trehalose-6-phosphate	$C_{12}H_{21}O_{14}P^{-2}$
Extracellular Metabolites		
X	biomass	(growth rate dependent)
ACTALex	acetaldehyde	C_2H_4O
ACTex	acetate	$C_2H_3O_2^{-1}$
CO_2	carbon dioxide	CO_2
ETOHex	ETOH	C_2H_6O
GLUCex	glucose	$C_6H_{12}O_6$
GLYCex	glycerol	$C_3H_8O_3$
LACex	lactate	$C_3H_5O_3^{-1}$
PYRex	pyruvate	$C_3H_3O_3^{-1}$
SUCex	succinate	$C_4H_4O_4^{-2}$

List of reactions described by the kinetic model

Code	Enzyme	EC	Reaction
Glycolysis			
HK	hexokinase	2.7.1.1	1 ATP + 1 GLUC → 1 ADP + 1 G6P + 1 H^+
PGI	G6P isomerase	5.3.1.9	1 G6P ↔ 1 F6P
PFK	phophofructokinase	2.7.1.11	1 ATP + 1 F6P → 1 ADP + 1 F16P + 1 H^+
FBA	fructose biphophate aldolase	4.1.2.13	1 F16P ↔ 1 DHAP + 1 GAP
TPI	triose phosphate isomerase	5.3.1.1	1 DHAP ↔ 1 GAP
TDH	GAP dehydrogenase	1.2.1.12	1 GAP + 1 NAD^+ + 1 P_i ↔ 1 13PG + 1 H^+ + 1 NADH
PGK	phosphoglycerate kinase	2.7.2.3	1 13PG + 1 ADP ↔ 1 3PG + 1 ATP
GPM	phophoglycerate mutase	5.4.2.1	1 3PG ↔ 1 2PG
ENO	enolase	4.2.1.11	1 2PG ↔ 1 H_2O + 1 PEP
PYK	pyruvate kinase	2.7.1.40	1 ADP + 1 H^+ + 1 PEP → 1 ATP + 1 PYR
Pentose phosphate pathway			
ZWF	G6P dehydrogenase	1.1.1.49	1 G6P + 1 $NADP^+$ + H_2O→ 1 6PG + 1 H^+ + 1 NADPH
TKL1	transketolase 1	2.2.1.1	1 RIB5P + 1 XYL5P ↔ 1 GAP + 1 SED7P
TAL	transaldolase	2.2.1.2	1 GAP + 1 SED7P ↔ 1 E4P + 1 F6P
TKL2	transketolase 2	2.2.1.1	1 E4P + 1 XYL5P ↔ 1 F6P + 1 GAP
Pyruvate branchpoint			
PYC	pyruvate carboxylase	6.4.1.1	1 ATP + 1 CO_2 + 1 H_2O + 1 PYR → 1 ADP + 2 H^+ + 1 OXACT + 1 P_i
PDC	pyruvate decarboxylase	4.1.1.1	1 H^+ + 1 PYR → 1 ACTAL + 1 CO_2
PDH	pyruvate dehydrogenase		1 CoA + 1 NAD^+ + 1 PYR → 1 AcCoA + 1 CO_2 + 1 NADH
Glycerol metabolism			
GDP	glycerol dehydrogenase	1.1.1.8	0.5 F16P + 1 H^+ + 1 NADH → 1 GOH3P + 1 NAD^+
Transport			
q_S	Glucose transporter		GLUCex → GLUC
GLYCt	Glycerol transporter		GLYC ↔ GLYCex

ETOHt	Ethanol transporter	$ETOH \leftrightarrow ETOHex$
ACTt	Acetate transporter	$ACT + H^+ \rightarrow ACTex + H^+_{ext}$
SUCt	Succinate transport	$SUC + 2\ H^+ \rightarrow SUCex + 2\ H^+_{ex}$
PYRt	Pyruvate transporter	$PYR + H^+ \rightarrow PYRext + H^+_{ex}$
CO_2t	CO_2 diffusion	$CO_2 \rightarrow CO_2ex$

Biomass and Energy

	Biomass formation	(see next section)
v_{ATP}	ATP used for maintenance	$ATP + H^+ \rightarrow ADP + P_i + H^+_{ext}$
ADK	Adenylate kinase	$AMP + ATP \leftrightarrow 2\ ADP$

Stoichiometry of Biomass Formation

The following equations describe the functions used to calculate the coefficients of the biomass reaction (BR_i) as a function of growth rate. They were obtained by fitting third order polynomials to the coefficients estimated when lumping the full stoichiometric model (see page 134).

$$BR_{G6P} = 5.93x10^{-09}.\mu^3 - 3.14x10^{-06}.\mu^2 + 5.80x10^{-04}.\mu - 8.18x10^{-02};$$

$$BR_{GAP} = 4.86x10^{-11}.\mu^3 - 2.59x10^{-08}.\mu^2 + 4.61x10^{-06}.\mu + 4.93x10^{-04};$$

$$BR_{P3G} = -6.88x10^{-10}.\mu^3 + 3.66x10^{-07}.\mu^2 - 7.91x10^{-05}.\mu - 1.34x10^{-02};$$

$$BR_{PEP} = -9.54x10^{-10}.\mu^3 + 5.07x10^{-07}.\mu^2 - 9.04x10^{-05}.\mu - 9.67x10^{-03};$$

$$BR_{PYR} = -3.42x10^{-09}.\mu^3 + 1.82x10^{-06}.\mu^2 - 3.24x10^{-04}.\mu - 3.47x10^{-02};$$

$$BR_{ATP} = -3.36x10^{-08}.\mu^3 + 1.79x10^{-05}.\mu^2 - 3.28x10^{-03}.\mu - 5.33x10^{-01};$$

$$BR_{ADP} = - BR_{ATP};$$

$$BR_{NAD} = -2.56x10^{-09}.\mu^3 + 1.36x10^{-06}.\mu^2 - 2.66x10^{-04}.\mu - 3.48x10^{-02};$$

$$BR_{NADH} = - BR_{NAD};$$

$$BR_{CO2} = 2.87x10^{-09}.\mu^3 - 1.53x10^{-06}.\mu^2 + 2.65x10^{-04}.\mu + 2.82x10^{-02};$$

Boundary reactions

The fluxes through the model boundaries were calculated from the equations described below. They were obtained by fitting different functions to the boundary fluxes obtained from metabolic flux analysis.

$v_{PYRt} = 0.000022\ q_s^2 - 0.0039\ q_s + 0.246;$

$v_{PYC} = 4.95\ x10^{-2}\ q_s - 1.1;$

$v_{ACS} = 0.0202\ q_s - 0.408;$

$v_{GDP} = 2.31\ x10^{-6}\ q_s^3 - 1.13\ x10^{-3}\ q_s^2 + 0.0298\ q_s - 8.65;$

$v_{TKL1} = 2.23\ x10^{-2}\ q_s – 0.343;$

$v_{TKL2} = 0.017\ q_s - 0.215;$

$v_{TAL} = v_{TKL1};$

$v_{G6PDH} = 0.0686\ q_s - 1.19;$

$v_{LACt} = 0.0000361\ q_s^2 + 0.00581\ q_s - 0.0711;$

$v_{PDH} = 0.0252\ q_s - 0.61;$

$v_{PDC} = 1.55\ q_s + 13.4;$

6. Conclusions and Outlook

New insights gained from this research

Although temperature is a crucial parameter for the growth of organisms, not much is known on how they have evolved to cope with suboptimal and dynamic temperature conditions, as these occur in their natural habitats. This is particularly relevant for poikilothermic organisms (such as microorganisms) since their internal temperature is directly dependent on the temperature of their environment. This is valid either in their natural habitat or in an artificial environment such as industrial fermentations. Changes in temperature settings might also lead to alterations of other parameters, such as growth rate or residual substrate concentration. These are likely to cause modifications at different omics levels (metabolomics, fluxomics, proteomics or transcriptomics) increasing the complexity of the results obtained. Therefore, to fully understand how temperature influences the metabolism of microorganisms, it is important to incorporate data from different experimental conditions and regulatory levels in a comprehensive way.

This thesis presents a fruitful effort on understanding the mechanisms used by the yeast *Saccharomyces cerevisiae* growing anaerobically on glucose to regulate the central carbon metabolism in the temperature range between 12 and 30 °C. This temperature range is relevant in industrial processes, such as beer fermentation, and during diurnal temperature profiles in natural habitats. Meaningful conclusions could be drawn by applying a

Systems Biology approach, where data on metabolite levels, *in vitro* enzyme activities and fluxes from different experimental conditions were used to validate *in silico* model predictions. By studying different temperatures in both glucose-excess and glucose-limiting conditions it was possible to avoid context dependent conclusions on the mechanisms used by *S. cerevisiae* to respond to temperature changes in the suboptimal range. Another important feature of this study is the use of fast dynamic temperature conditions (minutes to hours) instead of constant ones. This approach has shown to be crucial to differentiate between the impact of suboptimal temperatures as such from the effect of growth rate or extracellular glucose concentration on cellular metabolism. Also it allowed obtaining a dataset with large fold change in both rates and metabolite concentrations from a limited number of experiments.

Although *in vivo* enzymatic activities are strongly temperature dependent, it appears that flux-regulation mechanisms in yeast (either metabolic or hierarchical) are more sensitive to changes in residual substrate concentration than to temperature, within the studied range of 12 to 30 °C. Even though the growth rate can vary up to six fold due to the lower glycolytic capacity at 12 °C compared to 30 °C, this range of temperatures is not likely to require activation of temperature-specific mechanisms to regulate yeast glycolysis, such as changes in enzyme levels or expression of different isoenzymes. The yields on glucose of the most significant fermentation products (CO_2, ethanol, biomass, glycerol, acetate, lactate, succinate and pyruvate) were not significantly changed in the temperature range between 12 and 30 °C. More interestingly, it could be demonstrated *in vivo* that changes in cultivation temperature resulted in changes of the catalytic activities of the glycolytic enzymes that were identical for each enzyme. This identical temperature dependency of the enzymes of a pathway results in minimization of changes in the intracellular metabolite level, thus maintaining metabolite homeostasis under dynamic temperature conditions.

Relevance of these results in environmental and biotechnological contexts

The minor changes in enzyme levels observed for the range of growth rates studied (0.026 to 0.27 h^{-1}) together with the minimal alterations of metabolite levels upon temperature perturbations in the mild suboptimal range (12 – 30 °C), highlight the robustness of *Saccharomyces cerevisiae*. This

means that this yeast is able to sustain perturbations in its environment, such as changes in substrate amount and temperature, without requiring energy-costly cycles of enzyme synthesis and breakdown. This feature is probably an evolutionary consequence of the variety of environmental conditions *S. cerevisiae* needs to cope with in its natural habitat, which includes broad diurnal temperature ranges and large changes in substrate concentration.

Robustness is a very desirable attribute of industrial strains. Contrary to what happens in lab-scale conditions, it is very hard to maintain a homogeneous environment in large-scale fermentors. Very often, substrate concentration gradients are formed due to poor mixing efficiency, as well as temperature gradients, especially when there are external-loop cooling systems. The use of robust strains helps minimizing the impact of such heterogeneous fermentation conditions on the production of the desired compound. The research presented in this thesis suggests that suboptimal temperature gradients in large-scale fermentors are unlikely to have an impact on the production yields (Schmid *et al.*, 2009).

On the other hand, the observed robustness upon temperature perturbations can be seen as a hurdle for strain improvement programs. There was no evidence for different rate-controlling steps at different suboptimal temperatures, meaning that it is unlikely that metabolic engineering strategies targeting one single enzyme would provide strains for which the growth rate is less sensitive to temperature changes compared to the parental one. Also, in light of the near absence of hierarchical regulation between 12 and 30 °C steady-state chemostats, one might argue if evolutionary engineering strategies (such as performing fermentations for a high number of generations at low temperatures) will lead to evolved strains which can better cope to low temperatures or simply with higher affinity for the substrate. Evolutionary engineering strategies need to be designed according to the specific target of the strain improvement program. For instance, to aim at strains with lower optimum growth temperature (i.e. more psychrophilic) might require a different experimental setup than when targeting for strains able to maintain high growth rates for a broader range of temperatures.

Remarks on experimental setups used to study the impact of temperature on metabolic networks

Chemostat cultivations operated at the same dilution rate are very often chosen as a way to avoid growth-rate dependent responses when studying temperature impact on metabolism (see, for example, Tai *et al.* (2007b)). This approach can be misleading since, as shown by the results of this thesis, it is the residual substrate concentration and not fluxes that mostly determine metabolic response upon temperature changes. By setting the same growth rate at different temperatures, the residual substrate concentration is known to adjust to compensate for the temperature-induced changes in catalytic activity of the enzymes. So, to study the impact of temperature on the physiology and metabolism of cells under glucose-limited conditions, it would be wiser to compare chemostats with the same extracellular glucose concentration. For instance, as shown in Chapter 5, chemostat cultivations carried out at 12 °C and dilution rate of 0.03 h^{-1} should be compared to cultivations at 30 °C and 0.2 h^{-1}. The residual glucose concentration, intracellular metabolite levels and enzyme amounts are very comparable between these two conditions, making them the best settings to look for temperature specific responses in other metabolic pathways.

The observation that temperature sensitivities of the different glycolytic enzymes under *in vivo* conditions are the same raises more concerns regarding the reliability of *in vitro* enzyme activity measurements to understand *in vivo* processes. *In vitro* studies have reported different temperature sensitivities for the glycolytic enzymes in *S. cerevisiae* (Tai *et al.*, 2007a), contradicting the conclusions from this thesis. It is interesting to point out that the enzymes that have shown higher temperature sensitivities are the ones where coupling enzymes from animal cells were used in the analytical protocol. As discussed in the introduction section, animal cells have evolved in an environment where temperature is conserved in a very narrow range (the internal body temperature). It is therefore possible that, although used in excess amounts under standard assay conditions (30 °C), the activity losses of the coupling enzymes at lower temperatures could be more severe than for yeast enzymes, interfering with the outcome of *in vitro* enzyme activity assays. The results from this thesis suggest that the development of *in vivo* kinetic models can provide more reliable information concerning changes in the specific catalytic activity of the enzymes than *in vitro* assays done to cell extracts.

Nonetheless, at this moment it is still not possible to identify *in vivo* if the changes in enzyme activities are a consequence exclusively from the temperature impact on the catalytic activity, or if other compensation mechanisms, such as reversible phosphorylation or changes in intracellular pH, can also be playing a role. A nice alternative to test this could rely on *in vitro* glycolysis systems where multi-enzyme networks can be analyzed in real-time (Bujara *et al.*, 2011). The impact of changes in enzyme activities can be determined by measuring the changes in metabolite concentrations using mass spectrometry methods. This not only avoids the use of coupling enzymes but also the experimental conditions will be the same for all enzymes, better mimicking the *in vivo* situation.

Prospects on temperature studies under settings different from the ones applied in this thesis

This research focused on the anaerobic central carbon metabolism of *S. cerevisae* in the mild-hypothermic range (12 to 30 °C). However, this scope can be considered rather narrow when compared with the span of temperatures in natural environments and the different organisms that it can affect. It seems therefore appropriate to consider contributions this thesis can give to study the temperature impact on other biological systems or other growth conditions via other experimental setups.

Temperature impact on metabolic pathways other than glycolysis

Although no adaptation mechanism of central carbon metabolism could be pointed out as being a specific response to temperature dynamics, this does not exclude that enzymes from other metabolic pathways might respond differently to temperature changes. An example is glycogen metabolism since it is still not clear why concentrations in steady-state 12 °C chemostats (high residual glucose concentration) are higher than at 30 °C, while during the dynamic temperature conditions the glycogen levels seem to decrease with increasing extracellular substrate concentration. Nitrogen-limited cultivations could help understanding if changes in glycogen levels are a temperature-specific response since, under these conditions, the storage carbohydrate content is lower compared to carbon-limited cultivations.

It would also be very interesting to extend the study to anabolic pathways and not restrain it to catabolic ones such as glycolysis. The results from this

thesis do not exclude the possibility of changes in biomass composition at lower temperatures, which would require specific regulation mechanisms of biosynthetic pathways (e.g. lipid synthesis). The general character of the theoretical model developed in Chapter 4 allows it to be directly applied to study other pathways and to set the fundaments for experimental design in settings where hierarchical regulation may play a more relevant role.

Impact of more extreme temperature conditions on the metabolism of *S. cerevisiae*

The findings of this research are restricted to mild suboptimal temperatures. However, many industrial processes require temperatures higher than the optimal growth temperature. Some studies are available on the impact of supraoptimal temperatures on growth and metabolic response of *S. cerevisiae* (Postmus *et al.*, 2008; Postmus *et al.*, 2012). Nonetheless, they use experimental approaches similar to the ones described for cold studies, with all the disadvantages already discussed in the introduction chapter of this thesis. Extension of temperature studies to more extreme conditions could be achieved by first quantifying the temperature impact on growth rate for the entire span of temperatures where growth can occur. This can be done by using, for instance, the extended empirical model of Ratkowsky *et al.* (1983). Having such a relation between the growth rate and temperature would allow simulating the kinetic model developed within this thesis for the entire range of temperatures and compare the results to experimental observations. Nonetheless, as mentioned before, high temperatures can cause enzyme denaturation, imposing more complex regulation mechanisms of cell metabolism. Factors such as cell viability, protein degradation rates and RNA stability will very likely need to be taken into account when studying supraoptimal temperatures and heat-shock responses.

Temperature impact on other organisms (poikilotherms or not)

One big question raised by this thesis is if the striking observation of similar temperature-dependencies of glycolytic enzymes can be extended to other organisms or is merely an intrinsic property of yeast cells. It has been reported that there are large differences in responses to temperature changes amongst different organisms. For instance, it is known that mammals use reversible phosphorylation as a way to respond to

temperature shifts (Storey, 1997) and that affinities and inhibition constants of enzymes from animal cells decrease with decreasing temperature (Macdonald and Storey, 2005) to compensate for the lower maximal rate at lower temperature. However, in these situations, a decrease in temperature also causes a drop in the tissue's pH. Although external pH was set to be constant during all temperature perturbations carried out during this research, it cannot be guaranteed that the intracellular pH was constant. Therefore, it cannot be excluded that intracellular pH can be used by yeast to compensate the temperature impact on the catalytic activity.

Nonetheless, studies on the composition of proteins from extremophiles have shown that they are very similar to the ones from mesophiles (Arnold *et al.*, 2001). This observation, together with the similarity of growth-rate profiles with temperature for most unicellular organisms, indicates that identical temperature sensitivities of the glycolytic enzymes in mild hypothermic ranges can be a conserved characteristic between organisms. If proven to be the case, this can beautifully illustrate the principle of unity in biochemistry for all organisms, as first described by Kluyver and Donker (1961).

7. References

Abbott, D. A., Suir, E., Duong, G.-H., De Hulster, E., Pronk, J. T. and Van Maris, A. J. A. (2009). Catalase overexpression reduces lactic acid-induced oxidative stress in *Saccharomyces cerevisiae*. *Appl Environ Microbiol* **75**, 2320-2325.

Al-Fageeh, M. B. and Smales, C. M. (2006). Control and regulation of the cellular responses to cold shock: the responses in yeast and mammalian systems. *Biochem J Rev* **397**, 247-259.

Alberty, R. A. (2003). *Thermodynamics of Biochemical Reactions*, John Wiley & Sons, New Jersey, USA.

Arnold, F. H., Wintrode, P. L., Miyazaki, K. and Gershenson, A. (2001). How enzymes adapt: lessons from directed evolution. *Trends Biochem Sci* **26**, 100-106.

Baensch, J., Gysler, C. and Niederberger, P. (1998). Low-temperature inactive industrial baker's yeast and process for preparing same. Patent US5776526, issued July 7, 1998.

Beltran, G., Novo, M., Guillamon, J. M., Mas, A. and Rozes, N. (2008). Effect of fermentation temperature and culture media on the yeast lipid composition and wine volatile compounds. *Int J Food Microbiol* **121**, 169-177.

Bernaerts, K., Servaes, R. D., Kooyman, S., Versyck, K. J. and Van Impe, J. F. (2002). Optimal temperature input design for estimation of the square root model parameters: parameter accuracy and model validity restrictions. *Int J Food Microbiol* **73**, 145-157.

Bloomfield, D. K. and Bloch, K. (1960). The formation of delta 9-unsaturated fatty acids. *J Biol Chem* **235**, 337-45.

Boender, L. G., De Hulster, E. A., Van Maris, A. J., Daran-Lapujade, P. A. and Pronk, J. T. (2009). Quantitative physiology of *Saccharomyces cerevisiae* at near-zero specific growth rates. *Appl Environ Microbiol* **75**, 5607-5614.

Boulton, R. (1980). The prediction of fermentation behavior by a kinetic model. *American Journal of Enology and Viticulture* **31**, 40-45.

Brown, C. M. and Rose, A. H. (1969). Effects of temperature on composition and cell volume of *Candida utilis*. *J Bacteriol* **97**, 261-270.

Bruggeman, F. J. and Westerhoff, H. V. (2007). The nature of systems biology. *Trends Microbiol* **15**, 45-50.

Bujara, M., Schumperli, M., Pellaux, R., Heinemann, M. and Panke, S. (2011). Optimization of a blueprint for *in vitro* glycolysis by metabolic real-time analysis. *Nat Chem Biol* **7**, 271-7.

Canelas, A., Ras, C., Ten Pierick, A., Van Dam, J., Heijnen, J. and Van Gulik, W. (2008). Leakage-free rapid quenching technique for yeast metabolomics. *Metabolomics* **4**, 226-239.

Canelas, A. B., Ras, C., Ten Pierick, A., Van Gulik, W. M. and Heijnen, J. J. (2011). An *in vivo* data-driven framework for classification and quantification of enzyme kinetics and determination of apparent thermodynamic data. *Metab Eng* **13**, 294-306.

Chaui-Berlinck, J. G., Navas, C. A., Monteiro, L. H. and Bicudo, J. E. (2004). Temperature effects on a whole metabolic reaction cannot be inferred from its components. *Proc Biol Sci* **271**, 1415-1419.

Cipollina, C., Ten, P. A., Canelas, A. B., Seifar, R. M., Van Maris, A. J., Van Dam, J. C. and Heijnen, J. J. (2009). A comprehensive method for the quantification of the non-oxidative pentose phosphate pathway intermediates in *Saccharomyces cerevisiae* by GC-IDMS. *J Chromatogr B Analyt Technol Biomed Life Sci* **877**, 3231-3236.

Connors, K. (1990). Introduction to chemical kinetics. In *Chemical Kinetics: the study of reaction rates in solution* (Connors, K., ed.). VCH Publishers, New York, USA.

Cruz, A. L. B., Verbon, A. J., Geurink, L. J., Verheijen, P. J. T., Heijnen, J. J. and Van Gulik, W. M. (2012). Use of sequential batch fermentations to characterize the impact of mild hypothermic temperatures on the anaerobic stoichiometry and kinetics of *Saccharomyces cerevisiae*. *Biotechnol Bioeng* **109**, 1735-1744.

Daran-Lapujade, P., Jansen, M. L., Daran, J. M., Van Gulik, W., De Winde, J. H. and Pronk, J. T. (2004). Role of transcriptional regulation in controlling fluxes in central carbon metabolism of *Saccharomyces cerevisiae*. A chemostat culture study. *J Biol Chem* **279**, 9125-9138.

De Jong-Gubbels, P., Van Rolleghem, P., Heijnen, S., Vandijken, J. P. and Pronk, J. T. (1995). Regulation of carbon metabolism in chemostat cultures of *Saccharomyces cerevisiae* grown on mixtures of glucose and ethanol. *Yeast* **11**, 407-418.

De Jonge, L. P., Buijs, N. A. A., Ten Pierick, A., Deshmukh, A., Zhao, Z., Kiel, J. A. K. W., Heijnen, J. J. and Van Gulik, W. M. (2011). Scale-down of penicillin production in *Penicillium chrysogenum*. *Biotechnology Journal* **6**, 944-958.

Den Besten, H. M., Ingham, C. J., V., V. H., Beerthuyzen, M. M., Zwietering, M. H. and Abee, T. (2007). Quantitative analysis of population heterogeneity of the adaptive salt stress response and growth capacity of *Bacillus cereus* ATCC 14579. *Appl Environ Microbiol* **73**, 4797-4804.

Diderich, J. A., Teusink, B., Valkier, J., Anjos, J., Spencer-Martins, I., Van Dam, K. and Walsh, M. C. (1999). Strategies to determine the extent of control exerted by glucose transport on glycolytic flux in the yeast *Saccharomyces bayanus*. *Microbiology* **145**, 3447-3454.

Douma, R. D., De Jonge, L. P., Jonker, C. T. H., Seifar, R. M., Heijnen, J. J. and Van Gulik, W. M. (2010). Intracellular metabolite determination in the presence of extracellular abundance: Application to the penicillin biosynthesis pathway in *Penicillium chrysogenum*. *Biotechnol Bioeng* **107**, 105-115.

Entian, K.-D. and Kötter, P. (2007). Yeast genetic strain and plasmid collections. In *Yeast Gene Analysis* (Stansfield, I. & Stark, M. J. R., eds.), pp. 629-666. Academic Press Ltd., San Diego.

Fazio, A., Jewett, M., Daran-Lapujade, P., Mustacchi, R., Usaite, R., Pronk, J., Workman, C. and Nielsen, J. (2008). Transcription factor control of growth rate dependent genes in *Saccharomyces cerevisiae*: a three factor design. *BMC Genomics* **9**.

Feller, G. and Gerday, C. (1997). Psychrophilic enzymes: molecular basis of cold adaptation. *Cell Mol Life Sci* **53**, 830-41.

Feller, G. and Gerday, C. (2003). Psychrophilic enzymes: hot topics in cold adaptation. *Nat Rev Microbiol* **1**, 200-208.

Feller, G. (2010). Protein stability and enzyme activity at extreme biological temperatures. *Journal of Physics: Condensed Matter* **22**, 323101.

Fendt, S. M., Buescher, J. M., Rudroff, F., Picotti, P., Zamboni, N. and Sauer, U. (2010). Tradeoff between enzyme and metabolite efficiency maintains metabolic homeostasis upon perturbations in enzyme capacity. *Mol Syst Biol* **6**.

François, J. M., Walther, T. and Parrou, J. L. (2012). Genetics and regulation of glycogen and trehalose metabolism in *Saccharomyces cerevisiae*. In *Microbial Stress Tolerance for Biofuels* (Liu, Z. L., ed.), Vol. 22, pp. 29-55. Springer Berlin Heidelberg.

Gancedo, J. M. (2008). The early steps of glucose signalling in yeast. *FEMS Microbiol Rev* **32**, 673-704.

Gonçalves, P., Valerio, E., Correia, C., de Almeida, J. M. and Sampaio, J. P. (2011). Evidence for divergent evolution of growth temperature preference in sympatric *Saccharomyces* species. *PLoS One* **6**, e20739.

Gysler, C., Hottinger, H. and Niederberger, P. (1996). Baker's yeast. Patent EP0487878, issued Mar 13, 1996.

Haselbeck, R. J. and McAlister-Henn, L. (1993). Function and expression of yeast mitochondrial NAD- and NADP-specific isocitrate dehydrogenases. *J Biol Chem* **268**, 12116-22.

Hatakeyama, T. S. and Kaneko, K. (2012). Generic temperature compensation of biological clocks by autonomous regulation of catalyst concentration. *Proc Natl Acad Sci U S A* **109**, 8109-14.

Hazel, J. R. and Prosser, C. L. (1974). Molecular mechanisms of temperature compensation in poikilotherms. *Physiol Rev* **54**, 620-677.

Heinemann, M. and Sauer, U. (2010). Systems biology of microbial metabolism. *Curr Opin Microbiol* **13**, 337-343.

Helbig, A., Daran-Lapujade, P., Van Maris , A., Hulster, E. D., Ridder, D. D., Pronk, J., Heck, A. and Slijper, M. (2011). The diversity of protein turnover and abundance under nitrogen-limited steady-state conditions in *Saccharomyces cerevisiae*. *Molecular Biosystems* **7**, 3316-3326.

Hess, B. and Brand, K. (1965). Enzymes and metabolite profiles. In *Control of energy metabolism* (Chance, B., Estabrook, R. K. & Williamson, J. R., eds.). Academic Press, New York, USA.

Hohmann, S. and Mager, W. H. (2003). Yeast stress response. In *Topics in current genetics* (Hohmann, S., ed.), Vol. 1. Springer, Berlin (Germany).

Homma, T., Iwahashi, H. and Komatsu, Y. (2003). Yeast gene expression during growth at low temperature. *Cryobiology* **46**, 230-237.

Jansen, M. L. A., Diderich, J. A., Mashego, M., Hassane, A., De Winde, J. H., Daran-Lapujade, P. and Pronk, J. T. (2005). Prolonged selection in aerobic, glucose-limited chemostat cultures of *Saccharomyces cerevisiae* causes a partial loss of glycolytic capacity. *Microbiology* **151**, 1657-1669.

Kawasaki, H., Kyogoku, Y. and Ouchi, K. (2000). Baking process. Patent issued Dec 27, 2000.

Kishimoto, M. (1994). Fermentation characteristics of hybrids between the cryophilic wine yeast *Saccharomyces bayanus* and the mesophilic wine yeast *Saccharomyces cerevisiae*. *J Ferment Bioeng* **77**, 432-435.

Kluyver, A. J. and Donker, H. J. (1961). Unity and diversity in the metabolism of micro-organisms. In *Milestones in microbiology 1546 to 1940* (Brock, T. D., ed.), pp. 247-263. Prentice-Hall.

Kovarova, K., Zehnder, A. J. and Egli, T. (1996). Temperature-dependent growth kinetics of *Escherichia coli* ML 30 in glucose-limited continuous culture. *J Bacteriol* **178**, 4530-4539.

Lange, H. C., Eman, M., Van, Z. G., Visser, D., Van Dam, J. C., Frank, J., De Mattos, M. J. and Heijnen, J. J. (2001). Improved rapid sampling for *in vivo*

kinetics of intracellular metabolites in *Saccharomyces cerevisiae*. *Biotechnol Bioeng* **75**, 406-415.

Lange, H. C. and Heijnen, J. J. (2001). Statistical reconciliation of the elemental and molecular biomass composition of *Saccharomyces cerevisiae*. *Biotechnol Bioeng* **75**, 334-344.

Larsson, C., Nilsson, A., Blomberg, A. and Gustafsson, L. (1997). Glycolytic flux is conditionally correlated with ATP concentration in *Saccharomyces cerevisiae*: a chemostat study under carbon- or nitrogen- limiting conditions. *J Bacteriol* **179**, 7243-7250.

Libkind, D., Hittinger, C. T., Valerio, E., Goncalves, C., Dover, J., Johnston, M., Goncalves, P. and Sampaio, J. P. (2011). Microbe domestication and the identification of the wild genetic stock of lager-brewing yeast. *Proceedings of the National Academy of Sciences of the United States of America* **108**, 14539-14544.

Lowry, O. H., Rosebrough, N. J., Farr, A. L. and Randall, R. J. (1951). Protein measurement with the folin phenol reagent. *J Biol Chem* **193**, 265-275.

Macdonald, J. A. and Storey, K. B. (2005). Temperature and phosphate effects on allosteric phenomena of phosphofructokinase from a hibernating ground squirrel (*Spermophilus lateralis*). *FEBS J* **272**, 120-128.

Maier, A., Volker, B., Boles, E. and Fuhrmann, G. F. (2002). Characterisation of glucose transport in *Saccharomyces cerevisiae* with plasma membrane vesicles (countertransport) and intact cells (initial uptake) with single Hxt1, Hxt2, Hxt3, Hxt4, Hxt6, Hxt7 or Gal2 transporters. *FEMS Yeast Res* **2**, 539-50.

Mashego, M. R., WM, V. G., JL, V. and JJ, H. (2003). Critical evaluation of sampling techniques for residual glucose determination in carbon-limited chemostat culture of *Saccharomyces cerevisiae*. *Biotechnol Bioeng* **83**, 395-399.

Mashego, M. R., Jansen, M. L., Vinke, J. L., Van Gulik, W. M. and Heijnen, J. J. (2005). Changes in the metabolome of *Saccharomyces cerevisiae* associated with evolution in aerobic glucose-limited chemostats. *FEMS Yeast Res* **5**, 419-430.

Matsuzawa, T. and Ishiguro, I. (1980). Delta 1-Pyrroline-5-carboxylate reductase from Baker's yeast. Purification, properties and its application in the assays of L-delta 1-pyrroline-5-carboxylate and L-ornithine in tissue. *Biochim Biophys Acta* **613**, 318-23.

Murata, Y., Homma, T., Kitagawa, E., Momose, Y., Sato, M. S., Odani, M., Shimizu, H., Hasegawa-Mizusawa, M., Matsumoto, R., Mizukami, S., Fujita, K., Parveen, M., Komatsu, Y. and Iwahashi, H. (2006). Genome-wide expression analysis of yeast response during exposure to 4 ºC. *Extremophiles* **10**, 117-128.

Nijkamp, J., Van den Broek, M., Datema, E., De Kok, S., Bosman, L., Luttik, M., Daran-Lapujade, P., Vongsangnak, W., Nielsen, J., Heijne, W., Klaassen, P., Paddon, C., Platt, D., Kötter, P., Van Ham, R., Reinders, M., Pronk, J., Ridder, D. and Daran, J.-M. (2012). De novo sequencing, assembly and analysis of the genome of the laboratory strain *Saccharomyces cerevisiae* CEN.PK113-7D, a model for modern industrial biotechnology. *Microbial Cell Factories* **11**, 36.

Nikerel, E. (2009). Managing complexity of cellular systems: theoretical tools for modeling of metabolic reaction networks, TU Delft.

Nissen, T. L., Schulze, U., Nielsen, J. and Villadsen, J. (1997). Flux distributions in anaerobic, glucose-limited continuous cultures of *Saccharomyces cerevisiae*. *Microbiology* **143**, 203-218.

Oldiges, M. and Takors, R. (2005). Applying metabolic profiling techniques for stimulus-response experiments: chances and pitfalls. In *Technology Transfer in Biotechnology* (Kragl, U., ed.), Vol. 92, pp. 173-196. Springer Berlin Heidelberg.

Oliveira, A. P., Ludwig, C., Picotti, P., Kogadeeva, M., Aebersold, R. and Sauer, U. (2012). Regulation of yeast central metabolism by enzyme phosphorylation. *Mol Syst Biol* **8**, 623.

Panadero, J., Pallotti, C., Rodriguez-Vargas, S., Randez-Gil, F. and Prieto, J. A. (2006). A downshift in temperature activates the high osmolarity glycerol (HOG) pathway, which determines freeze tolerance in *Saccharomyces cerevisiae*. *J Biol Chem* **281**, 4638-45.

Parrou, J. L. and Francois, J. (1997). A simplified procedure for a rapid and reliable assay of both glycogen and trehalose in whole yeast cells. *Anal Biochem* **248**, 186-188.

Pizarro, F. J., Jewett, M. C., Nielsen, J. and Agosin, E. (2008). Growth temperature exerts differential physiological and transcriptional responses in laboratory and wine strains of *Saccharomyces cerevisiae*. *Appl Environ Microbiol* **74**, 6358-6368.

Postma, E., Scheffers, W. A. and Van Dijken, J. P. (1989). Kinetics of growth and glucose transport in glucose-limited chemostat cultures of *Saccharomyces cerevisiae* CBS 8066. *Yeast* **5**, 159-165.

Postmus, J., Canelas, A. B., Bouwman, J., Bakker, B. M., van Gulik, W., de Mattos, M. J. T., Brul, S. and Smits, G. J. (2008). Quantitative Analysis of the High Temperature-induced Glycolytic Flux Increase in Saccharomyces cerevisiae Reveals Dominant Metabolic Regulation. *Journal of Biological Chemistry* **283**, 23524-23532.

Postmus, J., Aardema, R., De Koning, L. J., De Koster, C. G., Brul, S. and Smits, G. J. (2012). Isoenzyme expression changes in response to high temperature determine the metabolic regulation of increased glycolytic flux in yeast. *FEMS Yeast Res* **12**, 571-81.

Ratkowsky, D. A., Olley, J., McMeekin, T. A. and Ball, A. (1982). Relationship between temperature and growth rate of bacterial cultures. *J Bacteriol* **149**, 1-5.

Ratkowsky, D. A., Lowry, R. K., McMeekin, T. A., Stokes, A. N. and Chandler, R. E. (1983). Model for bacterial culture growth rate throughout the entire biokinetic temperature range. *J Bacteriol* **154**, 1222-1226.

Raymond, R. K., Kastanos, E. K. and Appling, D. R. (1999). Saccharomyces cerevisiae expresses two genes encoding isozymes of methylenetetrahydrofolate reductase. *Arch Biochem Biophys* **372**, 300-8.

Redon, M., Guillamon, J. M., Mas, A. and Rozes, N. (2011). Effect of growth temperature on yeast lipid composition and alcoholic fermentation at low temperature. *Eur Food Res Technol* **232**, 517-527.

Rizzi, M., Baltes, M., Theobald, U. and Reuss, M. (1997). *In vivo* analysis of metabolic dynamics in *Saccharomyces cerevisiae*: II. Mathematical model. *Biotechnol Bioeng* **55**, 592-608.

Ruoff, P., Zakhartsev, M. and Westerhoff, H. V. (2007). Temperature compensation through systems biology. *FEBS J* **274**, 940-50.

Russell, N. J., Harrisson, P., Johnston, I. A., Jaenicke, R., Zuber, M., Franks, F. and Wynn-Williams, D. (1990). Cold adaptation of microorganisms [and discussion]. *Philosophical Transactions of the Royal Society of London B Biological Sciences* **326**, 595-611.

Sahara, T., Goda, T. and Ohgiya, S. (2002). Comprehensive expression analysis of time-dependent genetic responses in yeast cells to low temperature. *J Biol Chem* **277**, 50015-50021.

Salvado, Z., Arroyo-Lopez, F. N., Guillamon, J. M., Salazar, G., Querol, A. and Barrio, E. (2011). Temperature adaptation markedly determines evolution within the genus *Saccharomyces*. *Appl Environ Microbiol* **77**, 2292-2302.

Sauer, U. (2001). Evolutionary engineering of industrially important microbial phenotypes. *Adv Biochem Eng Biotechnol* **73**, 129-169.

Schaaff, I., Heinisch, J. and Zimmermann, F. K. (1989). Overproduction of glycolytic enzymes in yeast. *Yeast* **5**, 285-290.

Schade, B., Jansen, G., Whiteway, M., Entian, K. D. and Thomas, D. Y. (2004). Cold adaptation in budding yeast. *Molecular Biology of the Cell* **15**, 5492-5502.

Schmid, F., Schadt, J., Jiranek, V. and Block, D. E. (2009). Formation of temperature gradients in large- and small-scale red wine fermentations during cap management. *Australian Journal of Grape and Wine Research* **15**, 249-255.

Scott, J. and Hall, R. (1970). Brewery process. Patent GB1204160, issued Sep 3, 1970.

Seifar, R. M., Ras, C., Van Dam, J. C., Van Gulik, W. M., Heijnen, J. J. and Van Winden, W. A. (2009). Simultaneous quantification of free nucleotides in complex biological samples using ion pair reversed phase liquid chromatography isotope dilution tandem mass spectrometry. *Anal Biochem* **388**, 213-219.

Shaw, M. K. (1967). Effect of abrupt temperature shift on the growth of mesophilic and psychrophilic yeasts. *J Bacteriol* **93**, 1332-1336.

Storey, K. B. (1997). Metabolic regulation in mammalian hibernation: enzyme and protein adaptations. *Comp Biochem Physiol A Physiol* **118**, 1115-24.

Suutari, M. and Laakso, S. (1994). Microbial fatty acids and thermal adaptation. *Crit Rev Microbiol* **20**, 285-328.

Tai, S. L., Daran-Lapujade, P., Luttik, M. A. H., Walsh, M. C., Diderich, J. A., Krijger, G. C., Van Gulik, W. M., Pronk, J. T. and Daran, J. M. (2007a). Control of the glycolytic flux in *Saccharomyces cerevisiae* grown at low temperature: a multi-level analysis in anaerobic chemostat cultures. *J Biol Chem* **282**, 10243-10251.

Tai, S. L., Daran-Lapujade, P., Walsh, M. C., Pronk, J. T. and Daran, J. M. (2007b). Acclimation of *Saccharomyces cerevisiae* to low temperature: a chemostat-based transcriptome analysis. *Molecular Biology of the Cell* **18**, 5100-5112.

Taymaz-Nikerel, H., Van Gulik, W. M. and Heijnen, J. J. (2011). *Escherichia coli* responds with a rapid and large change in growth rate upon a shift from glucose-limited to glucose-excess conditions. *Metab Eng* **13**, 307-18.

Ter Kuile, B. H. and Westerhoff, H. V. (2001). Transcriptome meets metabolome: hierarchical and metabolic regulation of the glycolytic pathway. *FEBS Lett* **500**, 169-171.

Teusink, B., Passarge, J., Reijenga, C. A., Esgalhado, E., Van der Weijden, C. C., Schepper, M., Walsh, M. C., Bakker, B. M., Van Dam, K., Westerhoff, H. V. and Snoep, J. L. (2000). Can yeast glycolysis be understood in terms of *in vitro* kinetics of the constituent enzymes? Testing biochemistry. *Eur J Biochem* **267**, 5313-5329.

Theobald, U., Mailinger, W., Baltes, M., Rizzi, M. and Reuss, M. (1997). *In vivo* analysis of metabolic dynamics in *Saccharomyces cerevisiae* : I. Experimental observations. *Biotechnol Bioeng* **55**, 305-316.

Thieringer, H. A., Jones, P. G. and Inouye, M. (1998). Cold shock and adaptation. *Bioessays* **20**, 49-57.

Van Dam, J. C., Eman, M. R., Frank, J., Lange, H. C., Van Dedem, G. W. K. and Heijnen, S. J. (2002). Analysis of glycolytic intermediates in *Saccharomyces cerevisiae* using anion exchange chromatography and electrospray ionization with tandem mass spectrometric detection. *Anal Chim Acta* **460**, 209-218.

Van den Brink, J., Canelas, A. B., Van Gulik, W. M., Pronk, J. T., Heijnen, J. J., De Winde, J. H. and Daran-Lapujade, P. (2008). Dynamics of glycolytic regulation during adaptation of *Saccharomyces cerevisiae* to fermentative metabolism. *Appl Environ Microbiol* **74**, 5710-5723.

Van Derlinden, E., Bernaerts, K. and Van Impe, J. F. (2008). Dynamics of *Escherichia coli* at elevated temperatures: effect of temperature history and medium. *J Appl Microbiol* **104**, 438-453.

Van Eunen, K. (2010). Regulation by protein degradation: measuring protein turnover rates in standardized cultures. In *The multifarious and dynamic regulation of the living cell* (Van Eunen, K., ed.), pp. 129-157. Vrije Universiteit Amsterdam, Amsterdam (The Netherlands).

Van Eunen, K., Bouwman, J., Daran-Lapujade, P., Postmus, J., Canelas, A. B., Mensonides, F. I. C., Orij, R., Tuzun, I., Van den Brink, J., Smits, G. J., Van Gulik, W. M., Brul, S., Heijnen, J. J., De Winde, J. H., Teixeira de Mattos, M. J., Kettner, C., Nielsen, J., Westerhoff, H. V. and Bakker, B. M. (2010). Measuring enzyme activities under standardized *in vivo*-like conditions for systems biology. *FEBS J* **277**, 749-760.

Van Eunen, K., Kiewiet, J. A., Westerhoff, H. V. and Bakker, B. M. (2012). Testing biochemistry revisited: how *in vivo* metabolism can be understood from *in vitro* enzyme kinetics. *PLoS Comput Biol* **8**, e1002483.

Van Gulik, W., Van Winden, W. A. and Heijnen, J. J. (2003). Flux analysis: modeling and engineering solutions. In *Handbook of Industrial Cell Culture: Mammalian, Microbial, and Plant Cells* (Vinci, V. A. & Parekh, S. R., eds.), pp. 349-392. Humana Press Inc., New Jersey, USA.

Van Gulik, W. M. and Heijnen, J. J. (1995). A metabolic network stoichiometry analysis of microbial growth and product formation. *Biotechnol Bioeng* **48**, 681-698.

Van Hoek, P., Van Dijken, J. P. and Pronk, J. T. (2000). Regulation of fermentative capacity and levels of glycolytic enzymes in chemostat cultures of *Saccharomyces cerevisiae*. *Enzyme Microb Technol* **26**, 724-736.

Verduyn, C., Postma, E., Scheffers, W. A. and Van Dijken, J. P. (1990). Physiology of *Saccharomyces cerevisiae* in anaerobic glucose-limited chemostat cultures. *J Gen Microbiol* **136**, 395-403.

Verheijen, P. (2009). Data reconciliation and error detection. In *The metabolic pathway engineering handbook: Fundamentals* (Van Gulik, W., ed.). CRC Press, Boca Raton, Florida (USA).

Visser, D., Van der Heijden, R., Mauch, K., Reuss, M. and Heijnen, S. (2000). Tendency modeling: a new approach to obtain simplified kinetic models of metabolism applied to *Saccharomyces cerevisiae*. *Metab Eng* **2**, 252-275.

Walker, G. M. (1998). *Yeast Physiology and Biotechnology*, Wiley, West Sussex (England).

Westerhoff, H. V., Winder, C., Messiha, H., Simeonidis, E., Adamczyk, M., Verma, M., Bruggeman, F. J. and Dunn, W. (2009). Systems biology: the elements and principles of life. *FEBS Lett* **583**, 3882-3890.

Wilderer, P. A., Irvine, R. L., Horonszy, M. C., Robert, L. I. and Mervyn, C. G. (2001). General overview of SBR application. In *Sequencing batch reactor technology*. IWA Publishing.

Woods, H. A. (2003). Temperature and the chemical composition of poikilothermic organisms. *Funct Ecol* **17**, 237-245.

Wu, L., Mashego, M. R., Van Dam, J. C., Proell, A. M., Vinke, J. L., Ras, C., Van Winden, W. A., Van Gulik, W. M. and Heijnen, J. J. (2005). Quantitative analysis of the microbial metabolome by isotope dilution mass spectrometry using uniformly ^{13}C-labeled cell extracts as internal standards. *Anal Biochem* **336**, 164-171.

Curriculum vitae

Ana Luísa Braga da Cruz was born on the 10th May 1983 in S. Julião do Tojal (Portugal). In 2001, after finishing her secondary studies in Colégio do Sagrado Coração de Maria (Lisbon, Portugal), she went to Instituto Superior Técnico (Lisbon, Portugal) to graduate as BSc and MSc in Biotechnological Engineering. Part of her Master studies were carried out in DSM Food Specialities (Delft, The Netherlands) where she became acquainted with research performed in an industrial setting.

After completion of the Master Degree (2007) she returned to Portugal to work as a researcher in a joint project from IBET Pilot Plant (Oeiras, Portugal) and REQUIMTE/CQFB, Universidade Nova de Lisboa (Monte da Caparica, Portugal).

In 2008 she decided to return to the Netherlands to carry out a PhD in the Cell Systems Engineering group (former Bioprocess Technology Group) from the Biotechnology Department of the Technical University of Delft.

List of Publications

Articles

Cruz ALB, Verbon AJ, Geurink LJ, Verheijen PJT, Heijnen JJ, Van Gulik WM (2012). Use of sequential batch fermentations to characterize the impact of mild hypothermic temperatures on the anaerobic stoichiometry and kinetics of *Saccharomyces cerevisiae*. *Biotech Bioeng* **109**(7), 1735-1744

Cruz ALB, Hebly M, Wahl A, Pronk J, Heijnen JJ, Daran-Lapujade P, Van Gulik WM (2012). Similar temperature-dependencies of glycolytic enzymes: an evolutionary adaptation to temperature dynamics? *BMC Syst Biol* **6**(151)

Cruz ALB, Lo Conte R, Wahl A, Heijnen JJ, Van Gulik WM (2012). Modeling the macroscopic behavior during temperature shifts allows discriminating temperature from substrate dependencies of yeast metabolism. (*Manuscript under preparation*)

Seresht AK, Cruz ALB, De Hulster E, Hebly M, Palmqvist EA, Van Gulik WM, Daran JM, Pronk J, Olsson L (2013). Long-term adaptation of *Saccharomyces cerevisiae* to the burden of recombinant insulin production. *Biotech Bioeng* (*Published ahead of print*)

Van Dam JC, Ras C, Ten Pierick A, Cruz ALB, Zeng Z, Heijnen JJ, Seifar RM (2012). Application of isotope dilution mass spectrometry in quantitative metabolite analysis. (*Submitted for publication*)

Bekers K, Cruz ALB, Verheijen PJT, Wahl A, Heijnen JJ, Van Gulik WM (2012). Unified *in vivo* kinetic model of aerobic and anaerobic yeast glycolysis. (*Manuscript under preparation*)

Patents

Reis MA, Oliveira RM, Freitas MF, Chagas BF, Cruz ALB, Cunha AE, Clemente JJ (2010) Process for the co-production of chitin, its derivatives and polymers containing glucose, mannose and/or galactose, by the fermentation of the yeast *Pichia pastoris,* International publication number WO 2010/013174 A3, published on the 4th February 2010.

Oral Presentations

Cruz ALB, Bekers K, Verheijen PJT, Wahl A, Heijnen JJ, Van Gulik WM. Unified kinetic model of aerobic and anaerobic yeast glycolysis. *5th Kluyver Centre Programme Meeting Day,* Wageningen, The Netherlands, September 20, 2012.

Cruz ALB, Hebly M, Wahl SA, Daran-Lapujade P, Pronk JT, Heijnen JJ, Van Gulik WM. Regulation of glycolytic flux in *Saccharomyces cerevisiae* exposed to temperature changes. *Yeasterday*, Groningen, The Netherlands, May 17, 2012.

Cruz ALB, Wahl SA, Haverkorn D, Heijnen JJ, Van Gulik WM. Regulation of glycolytic flux in *Saccharomyces cerevisiae* exposed to low temperature. *The 8th Kluyver Centre Symposium*, Noordwijkerhout, The Netherlands, January 2011.

Cruz ALB, Wahl SA, Heijnen JJ, Van Gulik WM. Temperature Dependency of Yeast Central Metabolism: Experimental findings and modeling approaches. *NCSB Symposium*, Soesterberg, The Netherlands, October 21-22, 2010.

Cruz ALB, Wahl SA, Gulik W, Heijnen JJ. Regulation of glycolytic flux in *S. cerevisiae. 3rd Kluyver Centre Programme Meeting Day,* Wageningen, The Netherlands, September 23, 2010.

Poster Presentations

Cruz ALB, Hebly M, Wahl SA, Pronk JT, Heijnen JJ, Daran-Lapujade P, Van Gulik WM. Regulation of glycolytic flux in *Saccharomyces cerevisiae* exposed to temperature changes. *Metabolic Engineering IX,* Biarritz, France, June 3-7, 2012

Bekers KM, Cruz ALB, Verheijen PJT, Wahl A, Heijnen JJ, Van Gulik WM. Simplicity makes sense: A (straight) forward approach to modeling anaerobic yeast metabolism. *Metabolic Engineering IX,* Biarritz, France, June 3-7, 2012

Cruz ALB, Wahl SA, Heijnen JJ, Van Gulik WM. Temperature Dependency of Yeast Central Metabolism. *International Conference on Systems Biology*, Heidelberg, Germany, August 28 – September 1, 2011.

Cruz ALB, Verbon A, Geurink L, Wahl SA, Van Gulik WM, Heijnen JJ. Sequential batch reactors for temperature-dependent kinetic studies. *Metabolic Engineering VIII*, Jeju, South Korea, June 13-18, 2010.

Cruz ALB, Verbon A, Geurink L, Wahl SA, Van Gulik WM, Heijnen JJ. Sequential batch reactors for temperature-dependent kinetic studies. *4th Conference on Physiology of Yeast and Filamentous Fungi*, Rotterdam, The Netherlands, June 1-4, 2010.

Acknowledgments

When I finished my MSc, and especially after doing an internship at DSM, I knew that research was “the” job for me. The hobby that we are lucky to do every day. But, maybe because of some lack of ambition or simply not enough confidence, I did not feel that doing a PhD was the path to follow. Therefore, my first acknowledgments need to go to the people that thankfully were there to open my eyes. Philippe Gaudin and Rui Oliveira, the support you gave me was crucial to believe I could stand out by myself. You made me see I could use a PhD as the perfect opportunity to explore my capacities that were for so long hindered below heavy textbooks and final exams.

Once the decision of doing the PhD was made, it was somewhat easy to choose the group. Modeling was calling for me for quite some time. I had to check for myself what I heard through the grapevine: that Prof. Sef Heijnen was an extremely demanding promotor and with a genius hard to keep up. My family usually says I never take the easiest road and thermodynamics was one of my worse courses in university. So, why not? I can now say that what I heard through the grapevine was true. But more should be said on how he uses his challenging character and genius in our favor. I can easily get bored with a topic, but I am absolutely sure that I would be glad to keep working on impact of low temperature on *S. cerevisiae* for the rest of my life if Sef would keep being my boss.

But my daily supervisor, the person to whom I ran to before starting to knock my head on the wall, was Walter. It would be easy to list the reasons why you were such a good supervisor. But the one I really want to stress and deeply thank you is the gesture of putting the interests of your students in front of your own, regardless of consequences. I don’t know many people who would do it and I genuinely admire you for that.

Aljoscha, I must confess that coming directly from “hierarchical” Portugal it was initially difficult from me to join, and not separate, the supervisor from the friend to whom I can go to concerts, poker nights and football matches. I’m really happy I learned how to do it with you ☺

Peter Verheijen, you are for me a young man with the wisdom of a patriarch. Thank you for being my voice of reason in so many moments, serious and less serious.

Sef, Walter, Aljoscha and Peter: really thank you for the scientist you made out of me. A scientist that knows when to be stubborn but does recognize when there is a person sitting on the other side of the table.

There is always a group of people that actually make it a bit unfair that the thesis only has the name of one person below the title. Lars Geurink, Edwin van der Pol, Annelie Verbon, Diederik Haverkorn, Roberta Lo Conte, Christiaan van der Hoek and David Casper: some of the work in this thesis would not be here if it wasn't for you. But, above all, to supervise you might have been the most fun and rewarding part of my PhD. Thank you for that.

And then there is the people within the group without which nobody would ever finish a PhD. Jan van Dam, Angela ten Pierick, Cor Ras, Zen Zhen, Reza Seifar, Patricia van Dam, Rob Kerste and Dirk Geerts: your technical assistance was crucial, but your capacity to go the extra mile is the memory I will cherish the most.

Jenifer, it is easy to sometimes overlook the work that is done behind the scenes, but everybody in BPT (sorry, CSE) knows how important you are for the group. Your efficiency is inspiring and makes it so much lighter for us to do our everyday tasks.

Of course also a big thank you to all the BPTers I had the opportunity to come across. Emrah, André, Hilal, Rutger, Lodewijk, Zheng, Elaheh, Amit, Rob, Camilo, Hugo, Jinrui, Sergio and Domenico: science is always best when we have people to do it with us. I didn't need to ask your help to do pulse experiments (what a gap in my portfolio) but you were always there when I needed, with the right advices and feedback.

A very dear word of appreciation goes to Pascale Daran-Lapujade, Erik de Hulster, Marijke Luttik and Huong Duong. It is really comforting to obtain such unconditional help from people outside our group. Also thank you to Prof. Jack Pronk. When I really needed it, the door was always open.

I had great opportunities to take my head out of the sand that can be our PhD topic. Ali, I really loved working with you and I can't thank you enough for pulling me to your project. Anisha, Karen, Ruchir, Milan, Margriet, Karen and Johan: YISB is a great initiative and I only regret we could not have started it sooner. It was great working with you and I can't wait to collaborate with you again.

I also really need to give a thank you note to Prof. Bas Teusink, Prof. Matthias Heinemann and Prof. Matthias Reuss. Not only because the work

carried out in your groups really helped my own research, but also because it is so inspiring to have contact with Professors that still exhale such pure passion for Science. To meet you sure made my decision between academia and industry a lot harder.

I want also to thank the people that (hopefully) will make it possible for me to close this chapter of my career. Prof. Teixeira de Mattos, Prof. Martins dos Santos and Dr. Hayco Bloemen, thank you for participating in my defense and to challenge me one more time in topics that were so dear for me to work on.

My friends: it can be strange for some of you to have your names here when there might be such a thin connection with your role on my PhD thesis. Well, I will always use any excuse I can get just to thank you for being my friends or simply for pulling me out of work. Barbara, Francesco, Arturo, André, Fanni, Emrah, Hilal, Asya, Tânia, Mathieu, Aljoscha, Victor, Rutger, Carla, Alexander, Anouk, Filipa Mendes, Elaheh, Irina, Lucie, Filipa Baptista, Joana Ip, Joana Lobo and Alfredo. I need from this group to make two special acknowledgments. Tânia and Barbara: you are family to me.

Kaat and Marit, to classify you is even harder. We worked together, had fun together, grew up together. I ask you to be my *paranymphs* because your strength, commitment and geniality complete me. I really admire you girls.

And in the end I leave some words to the people that I don't know if I should acknowledge or apologize. Pai, mãe, Marta and the rest of my big-tight family: it is still hurtful to think how this book took me away from you. I really miss you.

Ricardo, there would be no Luísa without you. Ana would also have made it, but she would never be as happy and strong as Luísa is. I love you.

I always felt very lucky that I did not have a moment where I felt lost during my PhD. After reading all the names above, I know it couldn't had gone any other way. Thank you all.